The Dissertation Committee for Racheal Dawn Lute Certifies that this is the approved version of the following dissertation:

DURABILITY OF CALCIUM-ALUMINATE BASED BINDERS FOR RAPID REPAIR APPLICATIONS

Committee:

Kevin J. Folliard, Supervisor

Michael D.A. Thomas

David W. Fowler

Maria C.G. Juenger

Harovel G. Wheat

DURABILITY OF CALCIUM-ALUMINATE BASED BINDERS FOR RAPID REPAIR APPLICATIONS

by

Racheal Dawn Lute, B.S.Arch.E.; M.S.E.

Dissertation

Presented to the Faculty of the Graduate School of

The University of Texas at Austin

in Partial Fulfillment

of the Requirements

for the Degree of

Doctor of Philosophy

The University of Texas at Austin

May 2016

Dedication

To my parents, your resilience and humor are daily sources of inspiration.

Acknowledgements

I would first like to thank my soon-to-be husband, Lucas Anderson, for moving back to Austin with me so I could pursue this Ph.D. It has been quite an adventure and your motivation and emotional support have been invaluable. I'm looking forward to new adventures with you in this next chapter of our lives. I would also like to thank my parents, Rich and Lori, my brother, Scott, and Johanna and James. You have to be the silliest bunch of people I know, and no one can make me laugh like you guys. I'm so glad we're all together again. Thanks so much for your support and the many laughs!

Thank you my friends and colleagues, old and new, at the lab. Thano Drimalas, you were a great mentor to me as an undergraduate and have continued to be so as I've gone through both graduate degrees. More than that you've been a great friend! Fred Aguayo, thanks for the advice, laughs, and coffee runs over the last three years. I'm so glad we were able to finish at the same time as it's been so nice to have you to commiserate with. I can't wait to see what you achieve at Texas State. I know you'll be great! Thanks also to those who volunteered their man power to this project. Mitchell Dornak and Anthony Garcia, thanks for helping me remember how to mix concrete. Thanks also to Victoria Ibarra, Jessica Milligan, and Zia Lyle. This work could not have been possible without your assistance as undergraduate researchers.

I would like to express my sincere appreciation for Sherian Williams. Thanks so much for keeping us all in line and taking care of our lab needs. Few things would be accomplished at the lab if it weren't for you. I've got a big box of donuts ready and waiting for you! Also, thank you to Mike Rung for helping me with so many computer issues! I really appreciate all your help.

Thank you to Kerneos for funding this research. More specifically thank you to Charles Alt and Herve Fryda for sharing your knowledge and advice as I worked through this project. Next, thank you to my friends in the Scientific Network: Ted Moffatt, Matt Adams, Anthony Bentivegna, Mike Thomas, and of course, Jason Ideker. We must be the luckiest bunch of researchers! It has been such a great experience to be able to learn and travel with you all. Jason, thanks for being such a great friend and mentor over the last 12 years, if you can believe it's been that long! I'll meet you at the minibar. Thank you also to Karen Scrivener for allowing me to spend two months at EPFL, and to Julien Bizzozero and Simon Nuytten for your help while I was there. My experience in Switzerland helped me to grow so much as a researcher and as a person and I will forever be thankful for that.

I would also like to thank Maria Juenger, David Fowler, and Harovel Wheat for agreeing to be on my committee. I truly value your expertise and advice. An extra special thanks to Maria for being an adviser on both my master's and doctoral degrees.

Last, but not least, so many thanks to my advisor, Kevin Folliard. Your enthusiasm for concrete is unparalleled and has compelled so many of us to follow in your footsteps. Thank you for allowing me to return to work on this project. I have learned so much, traveled to fantastic places, and met the most amazing people. I will forever be grateful to you for that.

DURABILITY OF CALCIUM-ALUMINATE BASED BINDERS FOR RAPID REPAIR APPLICATIONS

Racheal Dawn Lute, Ph.D.

The University of Texas at Austin, 2016

Supervisor: Kevin J. Folliard

Within the last few decades, the amount of vehicle miles traveled within the US has increased approximately 40% with the construction of new roads only increasing 4% during this same time period. This dramatic increase in traffic on existing infrastructure has led to the rapid decline of the condition our nation's roads resulting in the increased need for maintenance and repair. Rapid hardening repair materials are in high demand for these applications as they allow for minimal traffic delays and road closures. Calcium aluminate cement (CAC) is a rapid hardening binder that is used for specialty applications where high early strength and increased durability are desired. In recent years, blended cement systems incorporating both CAC and calcium sulfate (C$) with portland cement (PC) have been developed to utilize the rapid hardening characteristics of CAC but at a reduced cost. While the durability of CAC is well researched and documented, the durability of these new blended systems is not yet fully understood. The focus of this research was to evaluate the performance and long term durability of various blended systems which utilize CAC or calcium sulfoaluminate cement (CSA) to attain rapid hardening. More specifically, these systems were evaluated to determine their resistance

to common modes of concrete deterioration such as alkali-silica reaction, external sulfate attack, delayed ettringite formation, carbonation, and corrosion in marine environments through in-situ lab methods and large scale outdoor exposure.

The results of the testing conducted related to alkali-silica reaction, external sulfate attack, and delayed ettringite formation identified the potential for large levels of expansion in blended systems of PC:CAC:C$ and PC:CSA. Details regarding each mode of deterioration and mechanisms of expansion are discussed.

Table of Contents

List of Tables

List of Figures

Glossary

CEMENT CHEMISTRY NOTATION

A: Al_2O_3

C: CaO

S: SiO_2

F: Fe_2O_3

$: SO_3

H: H_2O

ABBREVIATIONS

AFA	Activated Fly Ash
CAC	Calcium Aluminate Cement
CH	Calcium Hydroxide
C-S-H	Calcium Silicate Hydrate
CSA	Calcium Sulfoaluminate Cement
OPC	Ordinary Portland Cement
PC	Portland Cement
EDS	Energy Dispersive Spectroscopy
SEM	Scanning Electron Microscopy
XRD	X-Ray Diffraction
TEXMEX	Texas Marine Exposure Site

Chapter 1: Introduction

1.1 Research Scope and Objectives

Calcium-aluminate cements (CAC) have been utilized for their rapid hardening abilities and purported chemical and sulfate resistance since the early 1900's. However, the high cost of raw materials necessary for the production of CACs limits their use to specific, niche applications. In recent years, producers have begun to blend CACs with calcium sulfate (C$) and portland cement (PC) in an attempt to employ the rapid hardening abilities of CACs but at a reduced cost. Despite the significant amount of research conducted and information available on CACs, very little data is available on the long term performance and durability of calcium-aluminate based blends.

The objectives of the research presented herein were aimed at examining the durability of these blended systems and to add to the knowledge base of CAC-based materials. More specifically, the objectives were as follows:

- To examine the durability of blended systems of CAC, C$ and PC in terms of potential for alkali-silica reaction (ASR), external sulfate attack, delayed ettringite formation, carbonation, as well as performance in a marine environment
- To evaluate the durability of other systems with rapid hardening abilities such as calcium sulfoaluminate (CSA) cements, CSA-PC blends, and others for comparison
- To employ lab methods and outdoor exposure to provide long term performance data for calcium aluminate based binders

- To characterize the microstructural development of calcium aluminate based binders and other comparable binders experiencing common modes of concrete deterioration such as alkali-silica reaction (ASR), external sulfate attack, delayed ettringite formation, carbonation, as well as performance in a marine environment

1.2 SCIENTIFIC NETWORK

The research conducted under this project was funded by Kerneos Aluminate Technologies in conjunction with a larger Scientific Network of research universities. Kerneos, formerly LaFarge Aluminates, established the Scientific Network in 2004 in an effort to expand the fundamental knowledge of calcium aluminate cements through scholarly research. During the past 12 years, several doctoral candidates from various universities have aided in this international endeavor. Dr. Karen Scrivener at Ecole Polytechnique Federale de Lausanne (EPFL) directed research efforts focused on characterizing the microstructural development of CAC based systems. The research led by Dr. Michael Thomas at University of New Brunswick focused on evaluating the durability of CAC and later CAC-based blends used for repair applications. Dr. Jason Ideker began his relationship with the Scientific Network as a Ph.D Candidate at The University of Texas where his work focused on early-age volume change of CAC-based systems. Later, he led efforts at Oregon State University on the development of American Society for Testing and Materials (ASTM) standards related to determining converted strength of CAC. The work described in this dissertation is the third project within the Scientific Network to be led by Dr. Kevin Folliard at The University of Texas. The focus of this research is to evaluate the durability and long-term performance of new a CAC based ternary blend and other ettringite based binders, while previous work focused on

characterization of hydration and early-age properties of CAC based systems. This dissertation marks the end of the Scientific Network for the time being; however, our modern world continues to demand innovation of construction materials and therefore a need for future research.

1.3 ORGANIZATION OF DISSERTATION

This dissertation was written using a manuscript format in which each individual chapter is intended to be a self-contained manuscript to be submitted for journal publication. Some redundancy between chapters, particularly in reference to description of material properties, is a consequence of this format. All of the research detailed here was focused on examining the durability and long-term performance of blended systems of portland cement with calcium aluminate cement and calcium sulfate. Other binders were also evaluated for comparison purposes. The outline of the dissertation is as follows:

Chapter 1 serves as an introduction to the dissertation. Information regarding the background of the Kerneos Scientific Network as well as the research scope and goals of the work presented here are provided. This chapter also includes a brief review of the characteristics, history of use, and performance of the materials used throughout this study.

Chapter 2 details the evaluation of alkali-silica reaction (ASR) in calcium aluminate-based binders. The potential for ASR in various alternative binders was examined using standardized test methods and large-scale outdoor exposure. The performance of a newly developed blended system consisting of portland cement, calcium aluminate cement and calcium sulfate was of greatest interest. The ability of current test methods to effectively characterize the potential for ASR in alternative binders was also investigated.

Chapter 3 investigates the performance of calcium aluminate based binders exposed to sulfate environments. Paste, mortar and concrete specimens were exposed to various concentrations of sodium sulfate in a laboratory setting using commonly used standard methods. Concrete specimens were also exposed to sulfate solutions in an outdoor exposure site developed to mimic real world performance. X-ray diffraction was used to characterize the microstructural development of the binders exposed to external sulfates to elucidate the cause of high levels of expansion in certain binders.

Chapter 4 examines the potential for delayed ettringite formation (DEF) in ettringite based binders. The binder systems discussed throughout this dissertation rely on the formation of ettringite for high early strength. Concrete prisms and large-scale concrete exposure blocks were heat cured in an attempt to trigger DEF. The temperature threshold necessary to trigger DEF in ettringite based binders was also examined. After recording significant levels of expansion in concrete specimens, x-ray diffraction was used to characterize the microstructural development of heat cured paste samples

Chapter 5 presents research focused on the carbonation resistance of calcium aluminate based blends and other ettringite based binders. The depth of carbonation was evaluated in concrete prisms exposed to natural carbonation in an outdoor exposure site over a two year period.

Chapter 6 details the development of the newly established Texas Marine Exposure Site (TEXMEX) and provides preliminary results of the corrosion resistance of ettringite based binders in a marine environment.

Chapter 7 closes this dissertation with a review of general conclusions from each chapter and provides recommendations for future research.

1.4 Review of Materials

This section is intended to provide a review of the properties, characteristics and performance of the materials used in this study. More extensive literature reviews on the early age properties and microstructural development of CAC based binders were conducted under previous research projects by Ideker (2008), Gosselin (2009), Bentivegna (2012), Adams (2015), and Moffatt (2016).

1.4.1 Calcium Aluminate Cement

1.4.1.1 History of CAC

It was realized in the mid-1800's that alumina-rich calcium aluminates had excellent cementing properties; however, later research and the development of modern calcium aluminate cements is largely credited to Jules Bied. His work at the laboratories of the J. & A. Pavin de LaFarge company in Le Teil, France was prompted by issues with the rapid deterioration of mortar and concrete is sulfate (gypsum) rich soils. This led to the patenting of a manufacturing process for calcium aluminate cements in 1908. These cements were purported to have excellent sulfate resistance and also the ability to harden much more rapidly than portland cements. After a few modifications to the manufacturing process and several years of trials by the LaFarge company and the French government, the cement was put on the market in 1918 and sold under the name Ciment Fondu LaFarge (Capmas & Scrivener, 1998).

Ciment Fondu was utilized throughout Europe for its raid hardening ability during World War I and World War II for rapid replacement of gun emplacements and other necessary repairs. However, in the 1930's poor performance of concrete with high water/cement ratios after conversion were recognized. The continued use of high water/cement ratios led to subsequent failures which led to the French government placing

severe restrictions on the use of CAC in the public sector in 1943 (Capmas & Scrivener, 1998). By the 1960's, other failures across Europe led to the discontinuation of the use of CACs in Germany. Meanwhile, extensive research and long-term testing conducted in France indicated that good quality concrete could be produced that would retain adequate strength after conversion by maintaining water/cement rations below 0.40 and cement contents above 400 kg/m^3. This led to the removal of the previous restrictions on CAC in France with the recommendation that a maximum water/cement ratio of 0.4 and minimum cement content of 400 kg/m^3 (674 lb/yd^3) be enforced (Capmas & Scrivener, 1998).

An extensive market for CAC in prestressed concrete developed in the 1950's and 1960's in the UK. Early codes of practice clearly show that the effects of conversion on strength were well known; however, this led to language aimed at limiting or preventing conversion, which is now known to be impossible. Although a maximum water/cement ratio of 0.4 was specified this would have been difficult to achieve with a minimum cement content of 400 kg/m^3 due to high aggregate/cement ratios used at the time. Often a water/cement ratio of 0.5 or higher would have been necessary to achieve placement. In 1973, two CAC concrete structures collapsed: the Camden School for Girls (built 1955) and the Bennett Building of the University of Leicester (built 1965). Although, strength loss was noted in both cases, it was determined to be of minor consequence to the failures. Instead, a major cause of failure was inadequate support nibs to the roof beams. An additional collapse of roof beams over a swimming pool at the Sir John Cass School in Stepney in 1974 was attributed principally to strength loss resulting from conversion, further aggravated by sulfate attack. There was also evidence that the concrete did not meet code requirements due to the use of a high water/cement ratio. These events led to changes in the UK Building Regulation effectively preventing the use of CACs in buildings (Capmas & Scrivener, 1998).

In over 100 years of use, well-made good quality CAC concrete has shown to have good performance. However, it seems CAC is more sensitive to misuse that portland cement increasing the importance of good construction practices and design based on converted strengths.

1.4.1.2 Hydration and Conversion of CAC

The hydration of CAC is much more rapid than PC due to the absence of diffusion barriers. This allows for the rapid dissolution of calcium and aluminate ions and subsequent formation of calcium aluminate hydrates as part of a massive precipitation process which rapidly fills in voids and leads to quick and efficient hardening and strength development. This rapid and efficient hardening results in compressive strengths around 28 to 35 MPa (4,000 to 5,000 psi) in four hours.

Unlike portland cement systems which experience continual strength gain over time, CAC systems inevitably experience strength loss over time due to "conversion". During the hydration of CAC at ambient temperatures, metastable hydrates (CAH_{10} and C_2AH_8) are formed; however, with time or an increase in temperature these metastable hydrates will convert to C_3AH_6 and AH_3 which are more thermodynamically stable hydrates. Scrivener and Capmas (Capmas & Scrivener, 1998) summarized the main hydration and conversion reactions for CAC, as shown in equations 1.1 - 1.5 below:

$$CA + 10H \rightarrow CAH_{10} \quad (1.1)$$

$$2CA + 11H \rightarrow C_2AH_8 + AH_3 \quad (1.2)$$

$$3CA + 12H \rightarrow C_3AH_6 + 2\ AH_3 \quad (1.3)$$

$$2CAH_{10} \rightarrow C_2AH_8 + AH_3 + 9\ H^* \quad (1.4)$$

$$3C_2AH_8 \rightarrow 2\ C_3AH_6 + AH_3 + 9\ H^* \quad (1.5)$$

* Conversion reactions

Conversion also causes an increase in porosity which can lead to significant strength loss. During conversion some water is released as the meta-stable hydrates convert to stable hydrates. This water is subsequently recombined to form additional hydration products, resulting in a slight increase in strength. The typical strength development of a CAC mixture that has undergone conversion is depicted in Figure 1.1.

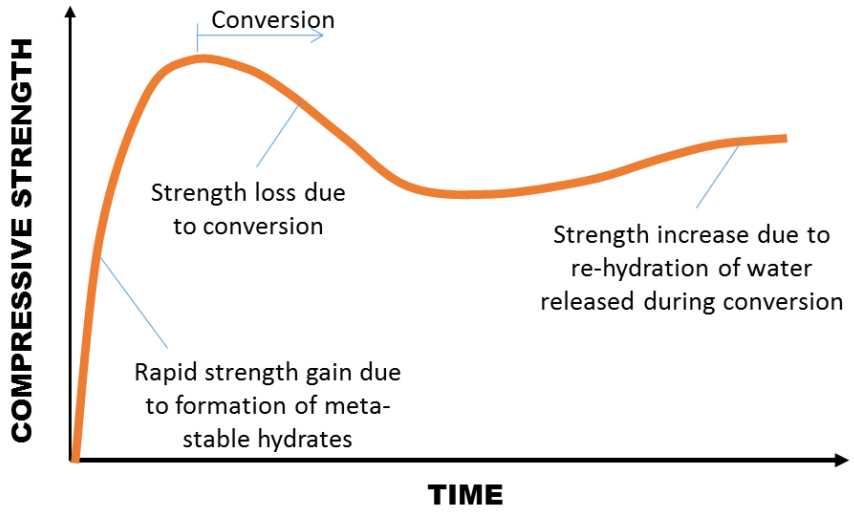

Figure 1.1: Plot showing typical strength development curve for CAC

1.4.1.3 Applications of CAC Concrete

Some applications and benefits of CAC that have been realized since its invention include (Scrivener, 2001):

- Rapid hardening with setting times similar to those of Portland cement

- Resistance to attack by acids and some other chemicals aggressive to Portland cement
- Ability to withstand repeated heating to high temperatures
- Ability to withstand low temperatures in placing and use
- Resistance to abrasion and impact with appropriate aggregates
- In mixtures containing Portland cement, calcium sulfate or both, the ability to form ettringite which can lead to controllable setting and hardening, shrinkage compensation and combination of free water.

Due to their high cost, CACs are not typically used in applications where portland cement concretes perform well. They are, however, used in specialized applications which harness the benefits of the properties listed above. For instance, the use of CAC for rapid repair and construction applications has gained in popularity in recent years, especially for pavement and runway repairs. Also, the increased abrasion resistance of CAC concretes makes them very suitable for highly abrasive environments including the spillway of dams, sections of roadway subjected to heavy wear, and industrial floors (Bentivegna, 2012).

1.4.1.4 Durability of CAC

Alkali-Silica Reactivity

ASR is triggered by long-term exposure to the internal pore water in concrete, and this reaction can occur as long as the pH is above about 13.2. In the case of CAC concrete, the lower pore solution pH provides protection against ASR as silica exhibits very limited solubility in the CAC pore solution (with pH values on the order of 12.2 to 12.4). It is possible that external alkalies, in the form of NaCl-based deicing salts or seawater, could

permeate into CAC concrete and potentially increase the pore solution pH, thereby triggering ASR (Ideker, 2008). Little research has been conducted to ascertain the susceptibility of CAC concrete to ASR; however, results described in subsequent chapters of this dissertation suggest it is highly unlikely.

Sulfate Resistance

The durability of CAC concrete in aggressive environments is often cited as one of the greatest benefits of the material. As previously mentioned, CACs were originally developed in an attempt to provide superior resistance to external sulfate attack (including sulfuric acid attack) than that seen with portland cement concretes. In the century since the advent of CACs there have been examples of both good and poor performance, yet the myth of CAC being completely sulfate resistant has prevailed. Between 1916 and 1923, over 7,000 tons of CAC were used in the construction of the P.L.M. Railway in France through areas with soils rich in gypsum and anhydrite. Since its construction, no issues related to sulfate attack have been reported in the railway or with test specimens immersed in calcium sulfate solution (Capmas & Scrivener, 1998). In the 1930's, Miller and Manson also studied the performance of CAC concretes in the sodium sulfate waters of Medicine Lake, South Dakota. After 20 years, the test specimens were still considered to be in excellent condition (Miller & Manson, 1933). Most of the early research conducted on the sulfate resistance of CAC was conducted in regions rich in calcium sulfate or with relatively low sodium sulfate concentrations (~1.0%). However, later research conducted by the UK building Research Establishment (BRE) has highlighted potential durability issues for CACs in contact with higher concentrations of sodium sulfate and magnesium sulfate (Crammond, 1990).

Corrosion Resistance and Carbonation

Typically, good quality concrete provides adequate protection against corrosion of embedded reinforcing steel. The high alkalinity (e.g., pH of 13.2 to 13.8) of portland cement concrete helps create a passive layer on the steel which prevents corrosion. Values of pH above 11.5 are generally considered to be needed to passivate reinforcing steel. Provided that chlorides do not penetrate down to the surface of the steel in sufficient quantities to depassivate this protective layer and provided that the depth of carbonation does not reach the depth of the steel, reinforced portland cement concrete can remain durable for many years. The same holds true for CAC concrete; however, the pH of CAC concretes are typically in the range of 12.2 to 12.4. According to Macias (Macias, 1996), this range is still high enough to maintain steel in the passive state, but there is less of a safety factor should the pH drop due to carbonation and there is no portlandite, which serves as an effective buffer in portland cement systems.

The carbonation of concrete occurs when carbon dioxide in the air reacts with hydration products within concrete to produce calcium carbonate. Portland cement concretes tend to be highly resistance to carbonation due to the presence of large amounts of portlandite. Likewise, the reaction of atmospheric CO_2 and CACs will eventually lead to the formation of $CaCO_3$ and AH_3. Studies have shown that the rate of carbonation for CAC concretes is similar to portland cement concretes of similar quality (Capmas & Scrivener,1998).

1.4.2 Ettringite Based Binders

Portland cement systems rely of the formation of calcium silicate hydrate (C-S-H) and calcium hydroxide (CH) for long term strength gain; however, portland cements can

be blended with calcium aluminate cement and a small amount of calcium sulfate to create a binder which achieves high early strength through the formation of ettringite. This high early strength can also be achieved by blending portland cement with calcium sulfoaluminate cements (CSA) or by the sole use of a CSA cement. These types of systems are called ettringite based binders and typically reach a compressive strength of 20 MPa (3,000 psi) within three hours making them ideal for use in rapid repair applications.

1.4.2.1 Ternary CAC Blends

Various ternary binders can be produced by combining various proportions of CAC, PC, and calcium sulfate. These ternary blends achieve high early strengths due to rapid formation of ettringite, but also experience continued strength gain due to continued hydration of the portland cement component. The composition of these ternary blends typically fall into one of two zones as depicted in Figure 1.2. The systems in zone 1 are rich in PC (typically 70^{+} percent) and are mostly used when fast set is required. Those compositions in zone 1 that are richer in CAC and incorporate supplementary C$ are characterized by better hardening properties and shrinkage compensation. Those systems in zone 2, which are predominantly CAC and C$, provide for very fast hardening kinetics, self-drying capacity and size variation control (Lamberet, 2005). The composition of the PC:CAC:C$ blend used in the studies described in this dissertation falls in zone 1.

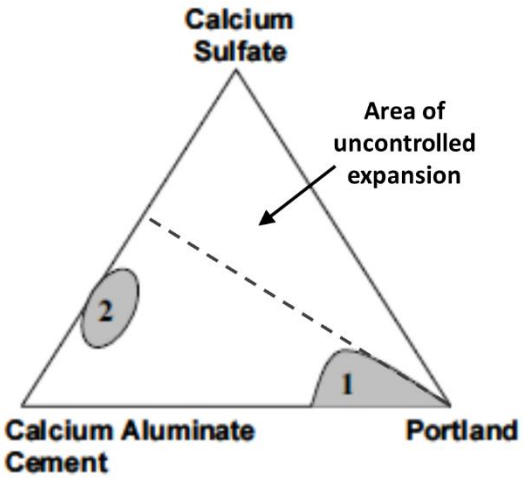

Figure 1.2: Ternary diagram depicting composition of CAC:PC:C$ blends.
Adapted from (Lamberet, 2005)

During hydration of these systems, the formation of metastable hydrates is prevented due to the addition of C$ and rapid formation of ettringite. This effectively eliminates the concern of strength loss due to conversion as seen in pure CAC systems. The hydration of this system is driven by the reaction of monocalcium aluminate and calcium sulfate which leads to the formation of ettringite and amorphous aluminum hydroxide as shown in Equation 1.6:

$$3CA + 3C\$H_x + (38 - 3x)H \rightarrow C_3A.3C\$.H_{32} + 2AH_3 \qquad (1.6)$$

Where x=0 for anhydrite, x=0.5 for hemihydrate and x=2 for gypsum. The set time of these materials decreases with the addition of C$; however, Lamberet (2005) observed uncontrolled expansion with the addition of excess hemi-hydrate. This area of uncontrolled expansion is depicted in Figure 1.2. If the amount of calcium sulfate is less than that needed

for all CA to react, calcium monosulfoaluminate will form after the depletion of calcium sulfate according (Bizzozero & et al., 2014) to equation 1.7.

$$6CA + C_3A.3C\$.H_{32} + 16H \rightarrow 3C_3A.C\$.H_{12} + 4AH_3 \quad (1.7)$$

1.4.2.2 Calcium sulfoaluminate cements and CSA blends

Calcium sulfoaluminate (CSA) cements are produced from calcium sulfate, limestone, and bauxite. These cements contain ye'elimite ($C_3A_3\$$) as a major constituent, typically 30-70%. Ye'elimite was introduced as a cementitious phase in the 1960s, when it was patented by Alexander Klein as an expansive or shrinkage compensating addition to cementitious binders ("Klein's compound") (Juenger et al., 2011). CSA cements have been used extensively throughout China since the 1960s, and have become more popular in Europe and the US in recent years.

The firing temperature for CSA cements is approximately 200 °C lower than that for portland cement clinker, and they are easier to grind compared to portland cement. These factors make CSA cements a desirable alternative to portland cement due to reduced CO_2 emissions. Usually about 15-25% of gypsum is interground with the clinker for optimum setting time, strength development and volume stability. The hydration of CSA cements depends mainly on the amount and reactivity of the added calcium sulfate (Winnefeld & Lothenbach, 2010). The main hydration product of CSA is ettringite as shown in equation 1.8.

$$C_4A_3\$ + 2C\$H_x + (38-2x)H \rightarrow C_3A.3C\$.H_{32} + 2AH_3 \quad (1.8)$$

Where *x*=0 for anhydrite, x=0.5 for hemihydrate and x=2 for gypsum Once all calcium sulfate is consumed, typically within 1-2 days monosulfate can be formed per equation 1.9.

$$C_4A_3\$ + 18H \rightarrow C_3A.C\$.H_{12} + 2AH_3 \quad (1.9)$$

Rapid strength development is related to fast hydration of monocalcium aluminate and ye'elimite. The complete reaction of ye'elimite, gypsum and water to form ettringite and aluminum hydroxide requires a high water/binder ratio (~0.6) (Bizzozero & et al., 2014).

The high cost of bauxite presents a challenge for the increased use of CSA cements. Blending CSAs with portland cement provides for a binder with rapid hardening abilities with a reduced cost and reduced carbon footprint. The hydration kinetics for the formation of ettringite in CSA:PC blended systems is similar to that for CAC:PC blends.

1.4.2.3 Durability of Ettringite Based Binders

Most standardized test methods were developed to evaluate portland cement mixtures. As a result, insufficient test methods exist for detailing the durability and long-term performance of ettringite based binders. The durability data that are available is summarized in the following sections.

Alkali-Silica Reactivity

There is little concern regarding ASR in mixtures which utilize 100% CAC as the binder; however, there is very little information on the subject of ASR in PC:CAC:C$ and PC:CSA blends. The portland cement used in such mixtures could instigate ASR if sufficient alkalis and reactive aggregate are present. No literature regarding ASR in such

systems was found; however, the aim of the research described in the next chapter was to evaluate the potential for ASR in CAC and CSA based binders.

Sulfate Resistance

As stated earlier, CACs have been touted for their sulfate resistance for over a century. Lamberet (2005) reports on the sulfate resistance of several PC:CAC:C$ binders of varying proportions. In that study, cement paste cubes were exposed to sulfate solutions and compressive strength changes were monitored over a 90 day period. Results of that study suggest that ternary blends with higher CAC contents tended to have a greater sulfate resistance.

There is dispute over the mechanisms involved in external sulfate attack, but it is generally agreed that two key reaction have the most impact on sulfate resistance: (1) C_3A, monosulfoaluminate or calcium aluminate reacts with sulfates to form ettringite, and (2) calcium hydroxide reacts with sulfates to form gypsum. The PC:CAC:C$ and PC:CSA blends rely on the formation of large amounts of ettringite for high early strength. This ettringite, however, is not stable and will eventually transform into monosulfoaluminate. The transformation provides for large amounts of monosulfoaluminate available to react with sulfate to initiate sulfate attack.

The chemistry of these blended systems also raises questions regarding the potential for internal sulfate attack otherwise known as delayed ettringite formation (DEF). In portland cement systems curing at elevated temperatures leads to the rapid formation of C-S-H. This leads to the encapsulation of sulfates and aluminates, which usually form ettringite, within the C-S-H. Later, in the presence of sufficient moisture, the sulfates and aluminates are slowly released from the C-S-H and are then available to form ettringite. This process can take weeks or years to occur. By this time the system has hardened, and the formation of ettringite can result in high levels of expansion. Most blended systems

incorporate at least 70% PC which in theory would provide adequate C-S-H formation to encapsulate the sulfates and aluminates needed for rapid ettringite formation. Little to no literature exists on DEF in CAC or CSA systems. Research described in subsequent sections of this dissertation aimed to evaluate the potential for DEF in such systems.

Corrosion Resistance and Carbonation

As with PC and CAC concrete, the potential for chloride induced corrosion in blended systems is dependent on the pore structure of the concrete. Research conducted by Moffatt (2016) revealed that CSAs were less resistant to chloride induced corrosion than blends of PC:CAC:C$ and PC:CSA as well as pure PC mixtures. This is attributed to the inability of CSAs to bind chlorides due to the presence of ettringite. The other systems are abundant in monosulfoaluminate which have the ability to convert to Friedel's salt thereby reducing the available chlorides needed to destroy the passive layer of embedded reinforcing steel.

Likewise it seems ettringite-based binders tend to be less resistant to carbonation than portland cement systems (Moffatt, 2016) (Lamberet, 2005). Portland cement systems are resistant to carbonation due to the presence of calcium hydroxide which acts as a pH buffer. Additionally, the carbonation of PC systems tends to result in a decrease in porosity, effectively reducing the rate of further carbonation. Conversely, the carbonation of ettringite-rich binders generally results in the decomposition of ettringite into denser products such as calcite and gypsum which results in an increase in porosity. This increased porosity then allows for faster diffusion of CO_2 and faster rate of carbonation at later ages.

1.4.3 Activated Fly Ash Mixtures

In the push to "go green," the production of alternative binders has increased in an effort to reduce CO_2 emissions from portland cement manufacturing. One such type of

alternative binder is a mixture of fly ashes that is chemically activated by liquid additives. Mix design and dosage of chemically activated fly ashes can be difficult in the field; therefore, some manufacturers have opted to pre-package the binder and additives with aggregate so that the user need only add water to produce a concrete mixture. Typically, chemically activated binders are made by mixing solid aluminosilicate powers such as fly ash, blast furnace slag or metakaolin with an activating solution. The composition of the activating solution can vary quite significantly depending on the manufacturer.

Specific information regarding the reaction kinetics of activated fly ashes varies greatly depending on the composition of both the powders and activators used. For aluminosilicate systems, it is generally agreed that the reaction results in the production of an extremely dense, interlocking crystalline calcium or sodium aluminum silicate hydrate (C-A-S-H) structure. The precise nature of the binder gel depends on the calcium content available for reaction (Juenger et al., 2011).

A pre-packaged chemically activated fly ash concrete mixture was used in several of the studies discussed in this dissertation. This product utilized the formation of C-A-S-H to achieve extremely high early strength, typically of 20 MPa (3,000 psi) in three hours. Little durability information exists for chemically activated fly ash mixtures. Carbonation may be problematic is such systems as there is no portlandite available to act as a pH buffer. The durability of these systems is highly dependent on the formation of an extremely dense pore structure. Also, some of the activating chemicals used in such systems can be quite caustic. The use of pre-packaged concrete mixtures minimizes the user's exposure to these chemicals.

1.5 REFERENCES

Adams, M. (2015). Factors Influencing Conversion and Volume Stability in Calcium Aluminate Cement Systems (Dissertation). Corvalis, OR: Oregon State University.

Bentivegna, A. (2012). Multi-Scale Characterization, Implementation, and Monitoring of Calcium Aluminte Cement Based Systems (Dissertation). Austin, TX: The University of Texas at Austin.

Bizzozero, J., & et al. (2014). Expansion mechanisms in calcium aluminate and sulfoaluminate systems with calcium sulfate. Cement and Concrete Research, 56, 190-202.

Capmas, A., & Scrivener, K. (1998). Lea's Chemistry of Cement and Concrete (Fourth Ed. ed.). (P. Hewlett, Ed.) New York: Arnold.

Crammond, N. (1990). Long term performance of high alumina cement in sulfate-bearing environments. In M. RJ (Ed.), Calcium Aluminate Cements, (pp. 208-221). London.

Ideker, J. (2008). Early-Age Behaviour of Calcium Aluminate Cement Systems (Dissertation). Austin, TX: The University of Texas at Austin.

Juenger, M.C.G.,Winnefeld,F., Provis, J.L, & Ideker, J.H. (2011). Advances in alternative cementitious binders. Cement and Concrete Research, 41, 12-32-1243.

Lamberet, S. (2005). Durability of Ternary Binders Based on Portland Cement, Calcium Aluminate Cement and Calcium Sulfate (Thesis). Lausanne, Switzerland: Ecole Polytechnique Federale de Lausanne.

Macias, A., Kindness, A., Glasser, FP (1996). Corrosion behaviour of steel in high alumina cement mortar cured at 5, 25, and 55C: chemical and physical factors. Journal of Materials Science, 31, 2279-89.

Miller, D., & Manson, P. (1933). Technical Bulletin 358. United States Department of Agriculture.

Moffatt, E. (2016). Durability of Rapid-set (ettringite based) Concrete (Dissertation). Frederickton, New Brunswick: University of New Brunswick.

Scrivener, K. (2001). Historical and Present Day Applications of Calcium Aluminate Cements. Proceedings of the International Conference on Calcium Aluminate Cements (CAC). Edinburgh, Scotland.

Winnefeld, F., Lothenbach, B. (2010). Hydration of calcium sulfoaluminate cements - experiemental findings and thermodynamic modelling. Cement and Concrete Research, 40, 1239-1247.

Chapter 2: Evaluation of Alkali-Silica Reaction in Calcium-Aluminate Based Binders

2.1 INTRODUCTION

Alkali-silica reaction (ASR) in ordinary portland cement based systems has been studied in-depth for over 75 years (Stanton, 1940). The components necessary to initiate ASR have been identified and a multitude of prevention techniques have been developed for use when less than ideal materials must be utilized. The behavior and long-term performance of blended mixtures comprised of fly ash and other supplementary cementitious materials with ordinary portland cement is also well known.

In recent years, the use of calcium aluminate cements (CAC) has become increasingly popular. CAC is a rapid hardening binder that is used for specialty applications where high early strength and increased durability are desired. In more recent years, blended cement systems incorporating both CAC and ordinary portland cement (OPC) have been developed to utilize the rapid hardening characteristics of CAC but at a reduced cost. While the durability of CAC has been studied over the years, the durability of these new blended systems is not yet fully understood. There is little concern regarding ASR in mixtures which utilize 100% CAC as the binder; however, there is very little information on the subject of ASR in OPC-CAC blends. The focus of this research was to evaluate the performance and long-term durability of various blended systems which utilize CAC or calcium sulfoaluminate cement (CSA) in conjunction with OPC to attain rapid hardening.

Commonly used accelerated lab tests, including ASTM C 1293 (concrete prism test) and ASTM C 1260 (accelerated mortar bar test), were used to evaluate ASR susceptibility of six binders. In addition to traditional laboratory testing, large scale exposure blocks were also cast to provide more realistic information on the behavior of

these materials in field applications. The methods used in this study were developed for use with portland cement based on the wealth of knowledge on the properties and behavior of ASR in OPC. A secondary aspect of this study was to determine whether or not current lab methods are also suitable for the evaluation of alternative binders.

2.2 Review of Alkali-Silica Reaction

Alkali-silica reaction (ASR) is a deleterious chemical reaction that leads to expansion and cracking in concrete structures. It is also one of the most recognized modes of deterioration of highway concrete structures and pavements in the United States (Tuan, 2005). ASR was first identified as a source of cracking in concrete by Stanton in 1940 (Stanton, 1940). Through evaluation of concrete pavement failures and subsequent laboratory research Stanton identified the use of certain aggregates in combination with high alkali cements as the leading catalyst for expansion.

2.2.1 Essential Components of ASR

Since Stanton's original findings, countless studies have been conducted on ASR. These studies have produced a wealth of information identifying four essential components necessary to trigger ASR: (1) high alkali concentration in pore solution, (2) reactive silica, (3) high calcium concentration in pore solution, and (4) sufficient moisture. During the hydration process, hydroxyl ions and alkalis in the pore solution combine with reactive silica present in the aggregates to form an expansive alkali-silica gel. In the presence of sufficient moisture the gel will imbibe water and continue to expand. This expansion leads to cracking and spalling.

2.2.1.1 High Alkali Concentration in Pore Solution

High alkali concentration in the pore solution of concrete mixtures is the leading catalyst for expansion due to ASR. The most common source of alkalis (sodium and

potassium) comes from the ordinary portland cement, but they can also be present in supplementary cementing materials, admixtures, or external sources (de-icing chemicals). In an alkaline environment amorphous silica present in the aggregates is attacked by hydroxyl ions (OH^-) and subsequently by Na^+ and K^+, present in the cement paste. This reaction leads to the creation of an expansive gel around the aggregate. The expansion of concrete generally increases as the total alkali content in concrete increases. The total alkali content of ordinary portland cement is expressed via the following equation (2.1):

$$Na_2O_e = Na_2O + 0.658K_2O \quad (2.1)$$

where Na_2O_e is the total sodium oxide equivalent (percent by mass of the total cement), Na_2O is the sodium oxide content (percent by mass), and K_2O is the potassium oxide content (percent by mass).

2.2.1.2 Reactive Silica

Not all siliceous aggregates are prone to ASR. The inherent reactivity of aggregates depends on several factors, including aggregate mineralogy, degree of crystallinity, and solubility (of the silica in high-pH concrete pore solution). The most reactive forms of silica tend to derive from those with amorphous, disordered, or poorly crystalline structures. The following aggregates and minerals have proven to contain reactive silica: opal, chert, greywacke, quartz, granite, shale, flint, slate, hornfels, gneiss, rhyolite, obsidian, volcanic glass, arenite, arkose, perlite, andesite, cristobalite, and tridymite (Folliard et al., 2006).

2.2.1.3 Sufficient Moisture

Sufficient moisture is necessary to drive ASR. After ASR gel is formed it will continue to imbibe water and expand. Continued expansion will eventually lead to

cracking which then allows for further ingress of moisture and additional expansion. Concrete mixtures comprised of highly reactive aggregates and high alkali cement have shown little or no expansion in certain very dry environments (Folliard et al, 2006). Likewise, research conducted by Stark (Stark, 1991) concluded that the threshold relative humidity necessary to support expansive ASR in concrete is 80% at ambient temperature.

2.2.1.4 High Calcium Concentration in Pore Solution

Recently more attention has been placed on the role of calcium in ASR related expansion. A number of studies have concluded that significant expansion only occurs when an adequate supply of calcium in available in the form of portlandite. In systems with abundant alkali hydroxides and reactive silica, but no portlandite, silica dissolves and remains in solution. Generally it is suggested that calcium increases the viscosity and yield strength of gel, resulting in larger stress magnitudes generated by gel expansion. (Rajabipour, 2015; Gaboriaud, 1999; Leemann, 2011; Bleszynski, 1998).

2.2.2 Mechanism of Expansion

Though a high concentration of alkalis (sodium and potassium) is necessary to trigger ASR, the alkalis themselves do not instigate the reaction. Instead, the initial reaction is between hydroxyl (OH^-) ions in the pore solution and reactive silica present in the aggregate. The high concentration of alkalis is important in that their presence results in an equally high concentration of OH^- ions to maintain charge equilibrium. Therefore, it is the OH^- concentration, and thus high pH, that leads to the initial breakdown of reactive silica within the aggregate (Folliard et al., 2006). Later, Na^+ and K^+ diffuse into the system to again maintain charge balance resulting in the dissolution of the silica present in the aggregate and the formation of an expansive gel comprised of Na, K, and Si with small

amounts of Ca. In the presence of sufficient moisture this gel will swell resulting in bulk expansion of the system.

2.3 MATERIALS

2.3.1 Binders

Six different binders were evaluated in this study. An ASTM C 150 (ASTM, 2015) Type I cement was selected as the control binder. Other binders evaluated include a calcium-aluminate cement, a calcium-sulfoaluminate cement, commonly used in commercial applications, blended systems which incorporate CAC or CSA with Type I cement, and a pre-bagged chemically activated concrete mixture. Table 2.1 shows the oxide analysis for the binders described below.

Table 2.1: Oxide Composition of Binders

Oxide (%wt)	Binder				
	OPC	**CAC-1**	**PC:CAC-2**	**CSA-1**	**PC:CSA-2**
SiO_2	20.14	4.57	15.15	14.46	9.02
Al_2O_3	5.42	41.21	14.98	16.21	23.88
Fe_2O_3	2.47	14.29	2.12	0.94	2.56
CaO	63.63	37.49	56.32	50.30	44.03
MgO	1.32	0.61	0.97	1.34	0.86
SO_3	3.09	0.00	8.44	17.09	21.37
Na_2O	0.17	0.06	0.14	0.21	0.12
K_2O	0.95	0.21	0.73	0.73	0.35
ZnO	0.01	0.01	0.01	0.02	0.01
SrO	0.08	0.02	0.07	0.14	0.07
Mn_2O_3	0.06	0.18	0.04	0.03	0.08
P_2O_5	0.26	0.13	0.21	0.09	0.11
TiO_2	0.28	1.79	0.61	0.58	0.91
Cl	0.00	0.00	0.00	0.02	0.00
Cr_2O_3	0.01	0.08	0.02	0.02	0.01
Na_2O_e	0.79	0.20	0.61	0.69	0.35

2.3.1.1. Portland Cement

A locally sourced Type I portland cement was chosen as the control binder for this study. This cement has been used extensively within this lab as a control binder for various studies; therefore, the long-term performance of this material is well documented and understood making it the clear choice for the control for this study. The total alkali equivalent (Na_2O_{eq}) for this cement is 0.79%.

2.3.1.2 Calcium Aluminate Cement and Blended System

A single source of calcium aluminate cement was used in this study and is referred to herein as CAC-1 and represents a binder containing 100 percent CAC. A blended CAC binder, designated as PC:CAC-2, was also evaluated and the blend contained a mixture of calcium-aluminate cement and calcium sulfate at a ratio of 2.2:1. This blend was then combined with Type I cement at a 30% replacement level (by total mass).

2.3.1.3 Calcium Sulfoaluminate Cement and Blended System

A single source of calcium sulfoaluminate cement, refered to as CSA-1, was used in this study and is widely available within the US and abroad. The main phases of this CSA are ye'elimite ($C_4A_3\$$), belite (ß-C_2S), and calcium sulfate (C$).

The blended CSA system, designated as PC-CSA-2, utilized a combination of CSA in which the main phase was ye'elimite and calcium sulfate. The ratio of these components is not reported by the manufacturer. Similar to PC:CAC-2, PC:CSA-2 was also combined with Type I cement at a 30% replacement level. CSA-1 and CSA-2 are manufactured by different sources and have different chemical compositions.

2.3.1.4 Chemically Activated Fly Ash Mixture

A commercially available pre-packaged concrete mixture, designated as AFA, was also evaluated in this study. The binder in this mixture is a chemically activated fly ash blend which contains both Class C and Class F fly ashes. The hydration of this product is controlled by a specific dose of an unreported chemical activator. Coarse aggregate with a maximum size of 9.5 mm (3/8 in) and fine graded sand are also included in each unit of the product. The manufacturer's recommendations prescribe the amount of water necessary to utilize this product.

2.3.2 Admixtures

A superplasticizer and a lithium-based accelerator were used for all CAC-1 mixtures. The superplasticizer and accelerator were dosed at 0.50% and 1.00% by mass of cement, respectively.

For all PC:CAC-2 mixtures, powdered citric acid was used as a retarder at a dose of 0.35% by mass of cement in conjunction with a superplasticizer in the form of sulfonated melamine formaldehyde (SMF) at a dose of 0.85% by mass of cement.

All CSA-1 and PC:CSA-2 mixtures utilized a combination of citric acid and SMF to attain the desired workability and three-hour compressive strength of 20 MPa (3,000 psi). The dosage for SMF was 0.1% by mass of the dry materials in the mix for both mixtures, and the citric acid was dosed at 0.2% and 0.35% by mass of cement for CSA-1 and PC:CSA-2, respectively.

2.3.3 Aggregates

The combination of fine and coarse aggregate remained constant for the concrete exposure block and ASTM C 1293 mixtures, excluding the AFA mixtures. The fine

aggregate was a natural, highly-reactive (with regard to ASR) siliceous sand containing quartz (64.0 %) chert (17.1 %), and feldspar (11.5 %) from El Paso, Texas. The sieve analysis results showed that this aggregate conforms to the requirements of fine aggregate for concrete based on ASTM C 33 (ASTM, 2016). In previous research (Folliard et al., 2006), this aggregate has shown to be highly alkali-silica reactive in ASTM C 1260 (ASTM, 2014) and ASTM C 1293 (ASTM, 2008).

The coarse aggregate used for all concrete mixtures was a non-reactive dolomitic limestone. The coarse aggregate was sieved using a SIMCO Fractionator sieve machine into three equal parts of the three gradation sizes: 12.5mm (1/2 in), 9.5mm (3/8 in), 4.75mm (1/5 in or No.4) for all mixtures. The absorption capacity of the coarse aggregate was determined to be 3.12%. Aggregate mixture proportions were determined according to ASTM C 1293.

The fine aggregate used for the ASTM C 1260 mortar mixtures was a mixed quartz/chert sand from Robstown, Texas. The aggregate was pulverized, sieved, and proportioned according to ASTM C 1260 (Table 2.2).

Table 2.2: Aggregate Grading Requirements for ASTM C 1260

Sieve Size		Mass, %
Passing	Retained on	
4.75 mm (No. 4)	2.36 mm (No. 8)	10
2.36 mm (No. 8)	1.18 mm(No. 16)	25
1.18 mm (No.16)	600 μm (No.30)	25
600 μm (No. 30)	300 μm (No. 50)	25
300 μm (No.50)	150 μm (No. 100)	15

2.4 MIXTURE PROPORTIONS

Generally, to achieve good long-term strength and durability with CAC a water/cement ratio below 0.4 and a cement content above 400 kg/m^3 (674 lb/yd^3) are

recommended (Campas & Scrivener, 1998). Therefore, the cement content of the mixtures was 440 kg/m^3 (742 lb/yd^3) for the CAC-1 mixture. The cement content for all other mixtures was 446 kg/m^3 (752 lb/yd^3). This value was chosen over the 440 kg/m^3 used for the CAC-1 mixture to correspond to the colloquial "8 sack" mix design often used by construction contractors. The water to cement ratio (w/c) was 0.35 by mass for all mixtures except, of course, the pre-packaged AFA product. The mixtures labels and binder mixture proportions are listed in Table 2.2.

Table 2.3: Mixture Proportions

Mixture Label	w/c	Total Binder Content (kg/m^3)	PC Content (kg/m^3)	CAC-2 Content (kg/m^3)	CSA-2 Content (kg/m^3)
OPC	0.35	446.0	446.0		
CAC-1	0.35	440.0			
PC:CAC-2	0.35	446.0	312.2	133.8	
CSA-1	0.35	446.0			
PC:CSA-2	0.35	446.0	312.2		133.8
AFA	~0.26	n/a			

ASTM C 1293 specifies "boosting" of the alkali content of the cement to 1.25% Na_2O_{eq} by the addition of NaOH to the mixing water; however, in order to obtain a realistic evaluation of these binders all mixtures remained unboosted. The results of the oxide analyses listed in Table 2.1 allowed for the calculation of the total alkali equivalent for each binder. These values are typically used to determine potential for alkali-silica reactivity.

2.5 EXPERIMENTAL PROCEDURES

2.5.1 ASTM C 1293

Four concrete prisms were cast according to ASTM C 1293 (ASTM, 2008) for each binder. The dimensions of the prisms are 75 x 75 x 290 mm (3 x 3 x 11.25 in). Gauge studs were cast into each end of the prisms to provide an effective length of 250 mm (10 in). The prisms were wet cured in a temperature-controlled fog room for 24-hours and then demolded. Once demolded initial length measurements were obtained. The prisms were then placed in a 3.78 L (5 gal) bucket conforming to ASTM C 1293. A perforated rack was placed in the bucket so the prisms were approximately 40 mm (1.5 in) above the bottom, and water was added to a depth of 25 mm (1 in) above the bottom. The bucket was also lined with felt fabric to facilitate wicking of the water from the bottom to simulate a high humidity environment. The buckets were stored at 38 °C (100 °F) between measurements. Expansion measurements were obtained at intervals as specified within the standard.

2.5.2 Water Soluble Alkali Testing

As stated earlier, the most essential component necessary to trigger ASR is a high alkali concentration in the pore solution. Water soluble alkali analysis in an indirect method for determining the alkali concentration in the pore-solution of the concrete in question. Samples were taken from each of the ASTM C 1293 tests at the end of the 2-year test period for water soluble alkali analysis. A 50 x 50 mm (2 x 2 inch) slice was taken from one prism within each test set for analysis. The slice was pulverized and three 10 g samples were taken from each sample. Each 10 g sample was combined with 100 mL of deionized water and boiled for 10 minutes to promote alkali leaching. The samples were allowed to sit for 24 hours before being analyzed. Flame photometry was used to measure the sodium

and potassium concentrations in each sample. The procedure and calculations for water soluble alkali analysis summarized here is described in more detail by Williams (Williams, 2005) and Bérubé (Berube, 2002).

2.5.3 Damage Rating Index

The Damage Rating Index (DRI) is a semi-quantitative petrographic method designed to evaluate concrete damaged by ASR. The method was developed in the early 1990's by Gratan-Bellew (Grattan-Bellew & Danay, 1992) and subsequently updated and modified by Villenueve et al. (Villenueve, 2012) and Fournier (Fournier et al., 2015). With this method polished concrete samples are visually assessed under a stereomicroscope and certain features associated with ASR damage are identified and counted. The total count for each feature is then multiplied by a weighting factor. The weighting factors were chosen to accurately assess each feature according to its importance in relation to ASR damage. Initial weighing factors were proposed by Grattan-Bellew and Mitchell (2006); however, modified weighting factors recently proposed by Villenueve et al. (2012) and the most recent guidance by Fournier et al. (2015) was followed in this study.

After the completion of the two-year monitoring period required for ASTM C 1293, samples were obtained from the concrete prisms to determine the DRI for each binder. A 50 mm (2 in) slice was taken from one concrete prism for each binder. The samples were then polished with SiC papers of increasing fineness (#120, #400, #600, #800, and #1200) until a mirror-like surface was achieved. Next a 1 cm^2 (0.4 in^2) grid was drawn on each sample with permanent marker as illustrated in Figure 2.1.

Figure 2.1: Example of 1cm^2 grid used for Damage Rating Index

Using a stereomicroscope with a Nikon camera each 1 cm (0.4 in) square was carefully visually examined at a magnification of 15x. The following petrographic features were identified and counted in each square:

- Cracks in aggregate particles (with and without reaction product)
- Cracks in cement paste (with and without reaction product)
- Debonded aggregate
- Reacted aggregate particle

- Reaction rim on aggregate particle
- Voids filled with reaction product

Once all features were counted for the entire sample they were summed and multiplied by the corresponding weighting factor. The modified weighting factors proposed by Villenueve (2012) and used in this study are listed in Table 2.4. Finally, the summation of the factored counts provided the Damage Rating Index for each sample.

Table 2.4: Weighting Factors used to Determine Damage Rating Index

Petrographic Features		**Weighting Factors**
Cracks in the Aggregate particle	Closed or (line), **without** reaction products	0.25
	Opened or in a fine network, **without** reaction products	2
	Opened or in a fine network, **with** reaction products	2
Cracks in the Cement Paste	**without** reaction products	3
	with reaction products	3
Debonded Aggregate		3
Reacted Aggregate Particle		2
Reaction Rim on Aggregate		0
Voids Filled with Reaction product		0

When using the modified method, weighting factors are not applied to the last two petrographic features listed in Table 2.4: (1) reaction rim on aggregate, and (2) voids filled with reaction product. Experience has shown that including these features in the DRI count can inadvertently increase the DRI value by misidentifying natural weathering as a reaction rim or can lead to significant variations in DRI values between petrographers due to difficulty of accurately counting air voids at 15x magnification (Fournier et al., 2015). These features were still counted as they are considered characteristic of ASR related damage in concrete.

The DRI values are divided into four damage groups (Villenueve, 2012) (Fournier, et al., 2015) which are summarized in Table 2.5 and 2.6.

Table 2.5: Description of DRI Damage Groups
((Villenueve, 2012) (Fournier, et al., 2015))

Damage Group	DRI values	Key Characteristics
1	**<200/250**	Concrete is in **good** condition with no signs of deterioration visible at macro level and limited signs of deterioration at micro level (~15x magnification) Signs of ASR of samples in this group are generally considered to be at **trace level**
2	**200/250 - 400**	Concrete is in generally good condition with **fair** signs of deterioration visible at the macro level, but fair to moderate signs of deterioration at the microlevel Signs of ASR of samples in this group are generally considered to be at **fair to moderate levels**
3	**~400 - 700/750**	Concrete with **moderate** signs of deterioration visible at the macro level and important signs of damge visible at the micro level Signs of ASR of samples in this group are generally considered **moderate to severe**
4	**>700/750**	Concrete with **severe** signs of deterioration visible both at macro and micro levels and important signs of damage visible at micro level Signs of ASR of samples in this group are generally considered **severe to very severe**

Table 2.6: Summary of DRI Values Relative to Degree of ASR
((Villenueve, 2012) (Fournier et al., 2015))

DRI	Degree of ASR
<200/250	Trace
200/250 - 400	Fair to Moderate
400 - 700/750	Moderate to Severe
> 700/750	Severe to Very Severe

2.5.4 Scanning Electron Microscopy

Samples for evaluation via scanning electron microscopy were selected from the ASTM C 1293 concrete prisms after the completion of the two year measurement period. One sample was taken from the center of one concrete prism from each binder set and sawn to a size of approximately 25 mm x 25 mm x 4 mm (1 in x 1 in x 0.15 in). After the sample was sawn, visible saw marks were removed using #120 SiC paper. Debris were removed from the surface of the sample with compressed air and the sample was placed in a desiccator and remained under vacuum for at least 24 hours prior to epoxy impregnation. Details for the epoxy impregnation procedure used in this study can be found in (Williams, 2005). After epoxy impregnation the surface of each sample was prepared through a series of fixed grinding and polishing steps. The grinding process entailed hand grinding the sample with #120 SiC paper until approximately 70% of the concrete surface was exposed. At this point, the sample was ground by hand with SiC paper of increasing fineness (#400, #600, #800, and #1200) until the center of the sample was flat and free of scratches. Next, the sample was polished with diamond spray of increasing fineness using an automated polishing head on a Buehler variable speed grinder-polisher. The duration of polishing for each polishing step is listed in Table 2.7. Polishing was considered complete once a mirror-like surface was achieved.

Table 2.7: Polishing Steps and Duration

Polishing Stage	Duration
9 μm	3 hrs
3 μm	2 hrs
1 μm	2hrs
1/4 μm	1 hr

A JEOL JSM-6490 SEM was used under low vacuum to acquire images and conduct EDS point analysis.

2.5.5 Outdoor Exposure Block Testing

For each concrete mixture, one large-scale exposure block was cast. The exposure block mold is wooden and its interior measurements are 710 x 380 x 380 mm (28 x 15 x 15 in). The concrete was cast in the mold in two lifts and consolidation was achieved with a portable vibrating rod after each lift. Each block was instrumented with 12 cast-in-place stainless steel bolts that were later used to measure expansion. Each 9.5 mm (3/8 in) diameter bolt was screwed into wood inserts located within each side of the exposure block mold. After concrete was cast within the mold only the tip of the bolt remained visible on the exterior of the block. Prior to casting, a 1 mm (0.04 in) "demec" hole was machined into the end of each bolt using a drill press with a 1 mm (0.04 in) diameter drill bit. Twelve expansion measurements were collected using these "demec" points. Each exposure block was covered in burlap and wet cured for seven days at ambient temperature prior to taking initial expansion measurements. Once initial measurements were obtained the block was

placed outside on the exposure site. Subsequent measurements were taken when outside temperatures are approximately 23 °C (73 °F).

2.5.6 ASTM C 1260

Three mortar bars were cast according to ASTM C 1260 for each binder. Stainless steel molds were used to cast mortar bars with dimensions of 25 x 25 x 285 mm (1.0 x 1.0 x 11.25 in). After casting, the mortar bars were cured at ambient temperature for 24 hours and then demolded. Upon demolding the bars were placed in water at 80 °C for 1 day. At this point initial length measurements were taken and the bars were placed in 1 M NaOH solution and stored at 80 °C. Length measurements were recorded three times between 1 and 14 days. In addition, 21- and 28-day measurement were taken; however, an expansion limit of 0.10% at 14 days was generally followed, as it is the typical convention for portland cement concrete.

2.6 Results and Discussion

2.6.1 ASTM C 1293 – Concrete Prism Test

ASTM C 1293 is a standard test method used to assess the ASR reactivity of an aggregate source. However, for this study an aggregate of known reactivity was used to assess the susceptibility of alternative binders to ASR. The ASTM C 1293 concrete prisms were monitored for 2 years. As expected the OPC mixture experienced the highest amount of expansion of the six binders evaluated. Conversely, it was quite unexpected to see such high levels of expansion in the PC:CAC-2 and PC:CSA-2 mixtures, especially as such early ages. As illustrated in Figure 2.2, both PC:CAC-2 and PC:CSA-2 surpass the expansion limit of 0.04% within 90 days with the OPC mixture following close behind. The CSA-1

mixture surpassed the expansion limit at 1.5 years and the CAC-1 and AFA mixtures remained below the 0.04% expansion limit for the entirety of the test period, as expected.

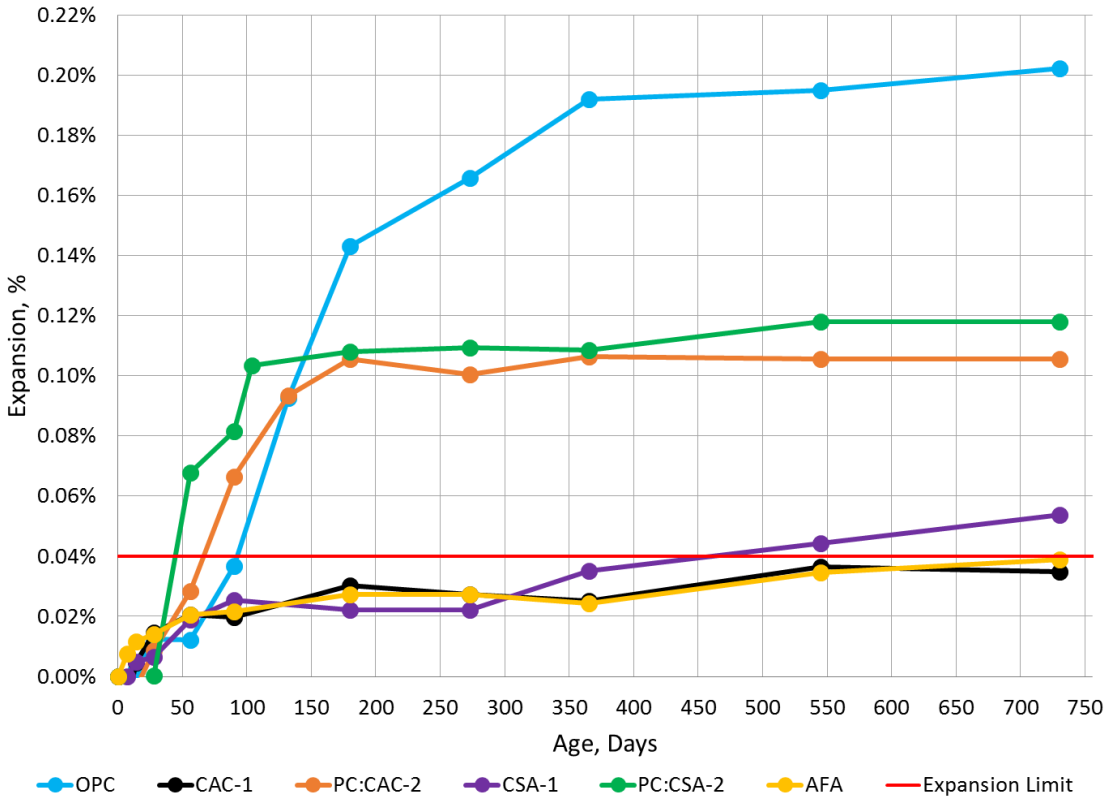

Figure 2.2: Expansion Results for ASTM C 1293 Concrete Prisms

ASTM C 1293 was designed for use with portland cement and ternary blends which utilize portland cement and supplementary cementing materials; therefore, it is yet to be seen if it is appropriate to use this method to also characterize alternative binders. Additional analytical techniques including water soluble alkali analysis, petrographic analysis, and scanning election microscopy were used to evaluate the ASTM C 1293 prisms at the end of the testing period in an attempt to verify the presence of ASR in the PC:CAC-2, CSA-1, and PC:CAC-2 mixtures. Results from these methods are discussed in detail in the following sections.

2.6.1.1 Water-Soluble Alkali Analysis

The hot-water extraction method described by Berube et al. (Berube, 2002) was used to quantify the water-soluble alkali content of the ASTM C 1293 test specimens at the end of the two year test period. The results of this analysis are listed in Table 2.8. It should be noted that these values are considered estimates and not precise measured values. The nature of the hot-water extraction method can lead to an underestimation of alkali loading due to the possibility that some alkalis originally dissolved in the pore solution do not return to solution when boiled. Conversely, the method can also lead to an overestimation of alkali loading due to the release of alkalis present in the aggregate during grinding.

Table 2.8 Water Soluble Alkali Test Results

Sample	Estimated Alkali Loading	
	kg/m^3	lb/yd^3
OPC	3.06	5.16
CAC-1	0.67	1.14
PC:CAC-2	3.15	5.32
CSA-1	2.04	3.45
PC:CSA-2	2.17	3.66
AFA	3.99	6.75

Aside from the AFA mixture, the estimated alkali loading values correlated reasonably well with the expansion data from ASTM C 1293. The AFA mixture showed the least amount of expansion in ASTM C 1293, but has the highest estimated alkali loading. This is likely due to the composition of the fly ashes and chemical (alkali based) activators used in this mixture. Many of these alkalis are quickly consumed and bound in the beginning stages of the hydration process and are not available at later time periods to contribute to alkali-silica reaction. The aggregates provided within the package are also

likely to be non-reactive. The OPC, PC:CSA-2, and PC:CAC-2 mixtures reached 0.20%, 0.12%, and 0.11% expansion at two years, respectively; however, the estimated alkali loading is highest in the PC:CAC-2 mixture. This could be an effect of alkali leaching caused by the storage condition of the concrete prisms within the ASTM C 1293 test set-up prior to analysis.

2.6.1.2 Petrographic Analysis – Damage Rating Index

One concrete sample was taken from each ASTM C 1293 test set for petrographic analysis. Visual observations were made of each sample using a stereomicroscope at 15x magnification. Certain features associated with damage caused by ASR were identified and counted to provide a Damage Rating Index value. These values were used to categorize the samples into Damage Groups which rate the degree of ASR present from Trace to Severe. The final DRI values for each sample are listed in Table 2.9 and detailed observations are tabulated in Appendix A.

Table 2.9: DRI values for ASTM C 1293 Specimens

Sample ID	DRI	Damage Group	Degree of ASR
OPC	708	3	Moderate to Severe
CAC-1	88	1	Trace
PC:CAC-2	323	2	Fair to Moderate
CSA-1	586	2	Fair to Moderate
PC:CSA-2	775	4	Severe
AFA	82	1	Trace

The DRI values correlate well with the level of expansion seen in ASTM C 1293. The OPC mixture showed the highest level of expansion and the DRI examination revealed extensive cracking in the cement paste with many cracks filled with reaction product (Figure 2.3). Cracking was also observed in a large number of the non-reactive coarse

aggregates (Figure 2.4). It was unexpected to see such so many cracks that propagate through the non-reactive coarse aggregate. Likely, the tensile forces created within the bulk paste due to ASR induced by the fine aggregate exceeded the low strength of the limestone coarse aggregate. What appears to be a reaction rim was also noted around many of the coarse aggregate particles. This reaction rim could be an indication of alkali-carbonate reaction (ACR). ACR is somewhat similar to ASR but occurs only in some dolomitic limestones rather than siliceous aggregates. ACR is quite rare as most susceptible aggregates are typically unsuitable for concrete mixtures. Further analysis is necessary to identify the reaction present within the OPC mixture as ACR.

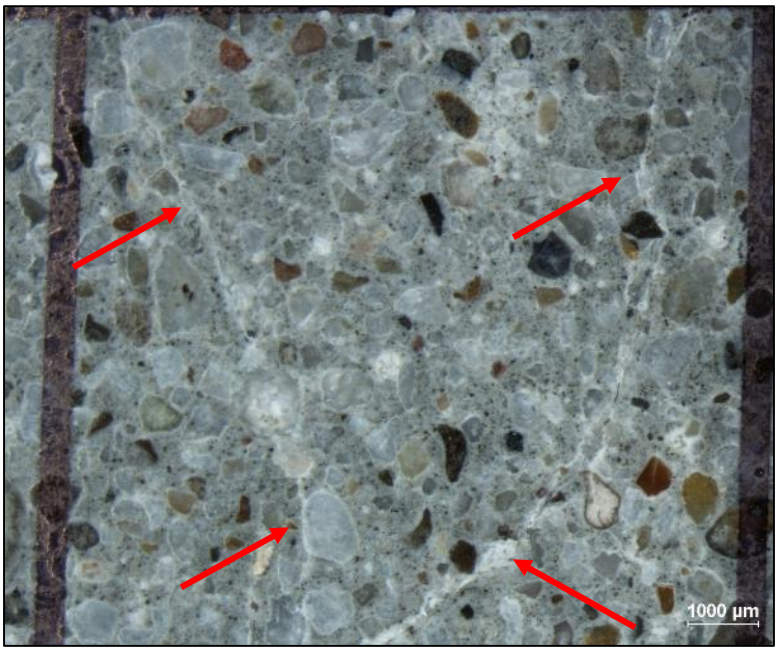

Figure 2.3: Photo of OPC mixture showing several cracks with reaction products which pass through cement paste

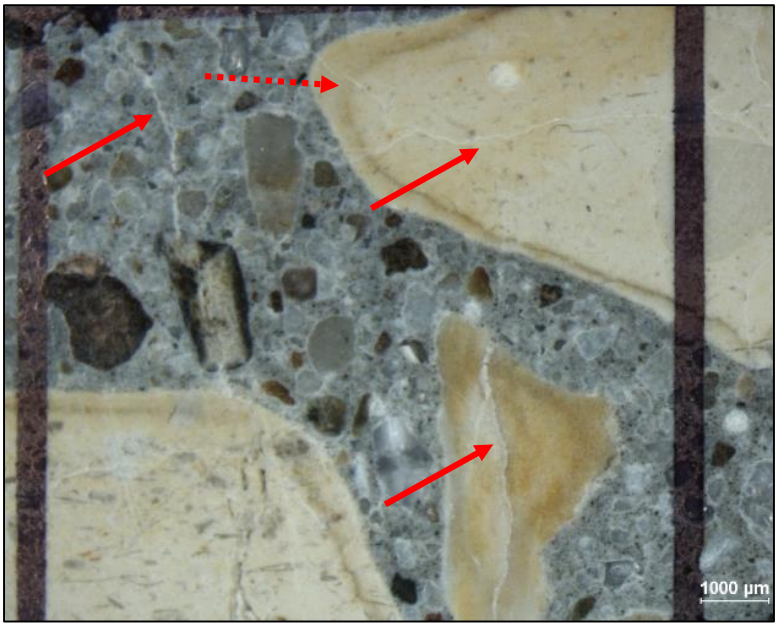

Figure 2.4: Photo of OPC mixture showing several cracks with reaction products which pass through cement paste and non-reactive coarse aggregate (solid arrow). Reaction rim noted around coarse aggregate (dashed arrow)

Very little cracking was noted in the CAC-1 sample as evidenced in Figure 2.5 and in turn the sample had a very low DRI value. However, the PC:CAC-2 sample was riddled with cracks throughout the cement paste and reaction product which accumulated around the coarse aggregate. Again, it is unusual to see such amounts of reaction product around non-reactive aggregates. PC:CAC-2 had a DRI value of 323, placing it in Damage Group 2 with fair to moderate ASR damage.

Figure 2.5: Photo of CAC-1 mixture showing no cracks in the cement paste or aggregates.

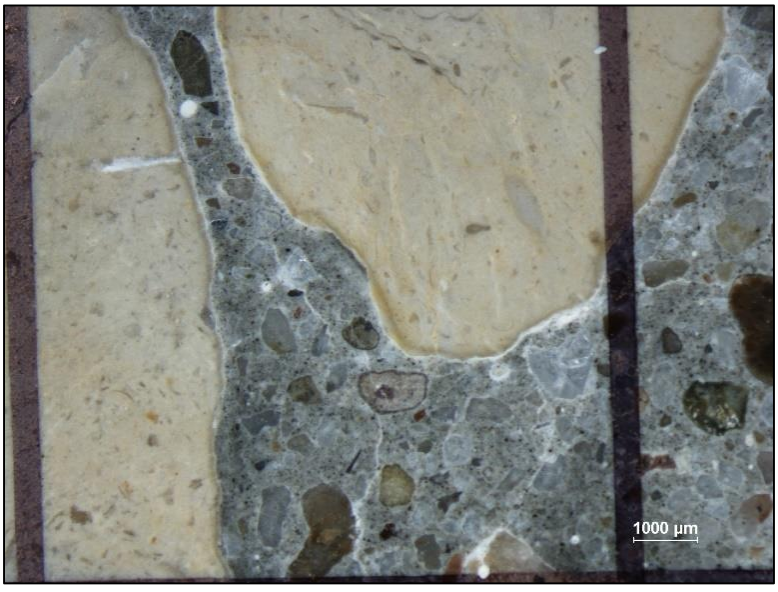

Figure 2.6: Photo of PC:CAC-2 mixture showing several cracks in the cement paste and reaction product around non-reactive coarse aggregates.

The CSA-1 sample reached a relatively low level of expansion in ASTM C 1293; however, the DRI examination revealed moderate cracking in the paste and coarse

aggregates resulting in a DRI value of 586. This value corresponds to a fair to moderate degree of ASR damage. Again, reaction rims were noted around the non-reactive coarse aggregates (Figure 2.7) and in some cases cracks propagated from the aggregate to the surrounding paste (Figure 2.8). The propagation of cracks from aggregate to the cement paste is a tell-tale sign of ASR.

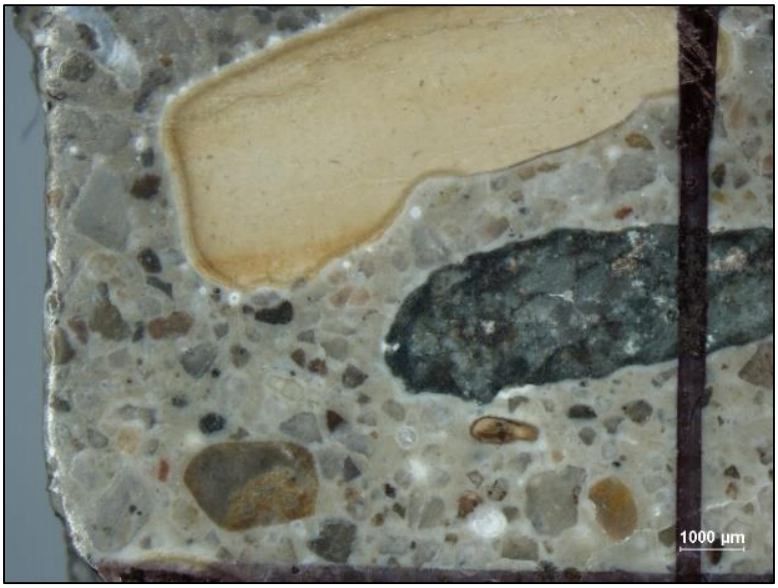

Figure 2.7: Photo of CSA-1 mixture showing reaction rim around limestone aggregate and reaction product deposits within the cement paste.

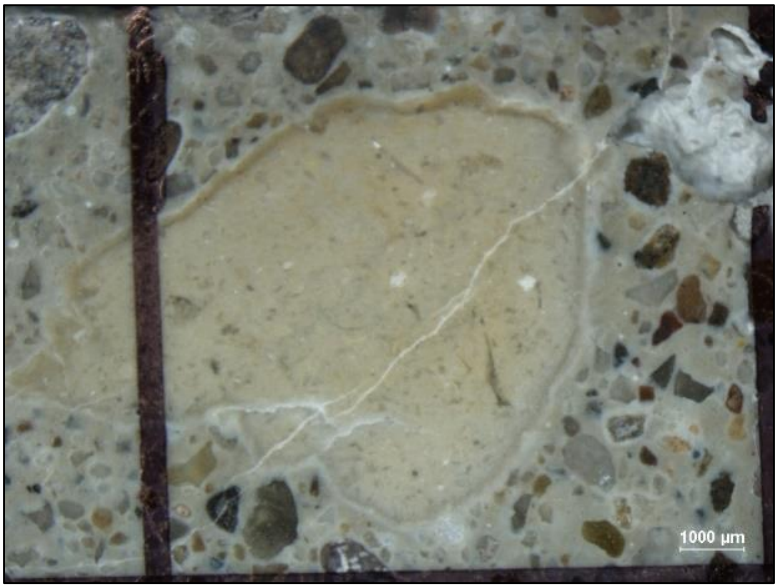

Figure 2.8: Photo of CSA-1 mixture showing reaction rim around limestone aggregate and crack propagating through aggregate and surrounding paste.

The PC:CSA-2 sample received the highest DRI value of 775 placing it the group for severe degree of ASR related damage. A large amount of cracks filled with reaction product were noted throughout the cement paste, and many cracked and reacted aggregate particles were also noted. Figures 2.9 and 2.10 show multiple reacted fine aggregate particles and cracks in the cement paste.

Figure 2.9: Photo of PC:CSA-2 mixture showing reacted fine aggregate particles

Figure 2.10: Photo of PC:CSA-2 mixture showing cracked aggregate particles and cracks in cement paste filled with reaction product.

The AFA sample showed little to no signs of ASR damage during the DRI examination. Figure 2.11 shows a typical view of the AFA sample showing little or no cracking in the paste or aggregate.

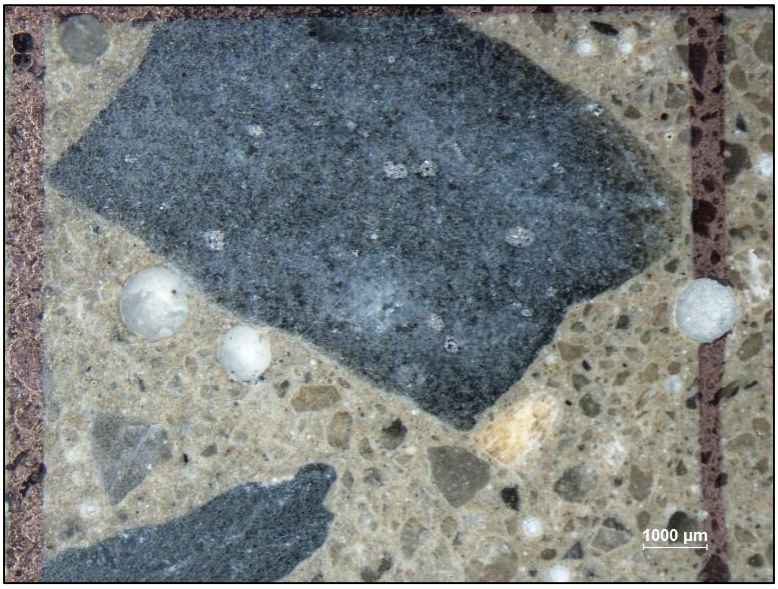

Figure 2.11: Photo of AFA mixture showing sound concrete with no cracking.

The results of the petrographic analysis of ASTM C 1293 samples using the Damage Rating Index correlate quite well with the levels of expansion reached in ASTM C 1293. In general, those samples with higher levels of expansion also had higher DRI values. The added benefit of using the Damage Rating Index in conjunction with ASTM C 1293 is the ability to visually verify the presence of alkali-silica gel, reacted aggregates, and cracks within the cement paste. This is especially useful and necessary when attempting to confirm the presence of ASR in alternative binders. As previously stated, most accelerated laboratory test methods were developed for use with ordinary portland cement; therefore, the employment of additional analytical methods is essential until it is determined that these methods are also suitable for the evaluation of alternative binders.

2.6.1.3 Scanning Electron Microscopy and Image Analysis

The results from the petrographic analysis prompted the use of scanning electron microscopy to verify the presence of ASR gel and identify other observed features present in the ASTM C 1293 samples. Of particular interest was the presence of what appeared to be reaction rims around the non-reactive limestone coarse aggregate particles in the OPC, PC:CAC-2, and CSA-1 mixtures. Also, the DRI value for the CSA-1 mixture was surprisingly high considering the relatively low level of expansion in ASTM C 1293; therefore, SEM was used to verify the nature of the features observed in the petrographic analysis.

Figures 2.12 and 2.13 from a sample of the OPC mixture taken after two years in ASTM C 1293 shows evidence of some cracking and reacted fine aggregate particles. EDS point analysis was conducted on the rim of the reacted aggregate particle shown in Figure 2.13; however, no ASR gel was detected. It is assumed that the gel was disturbed or removed during the extensive grinding and polishing performed during sample preparation. Fortunately, the presence of reacted fine aggregates is evidence enough to verify ASR within the sample.

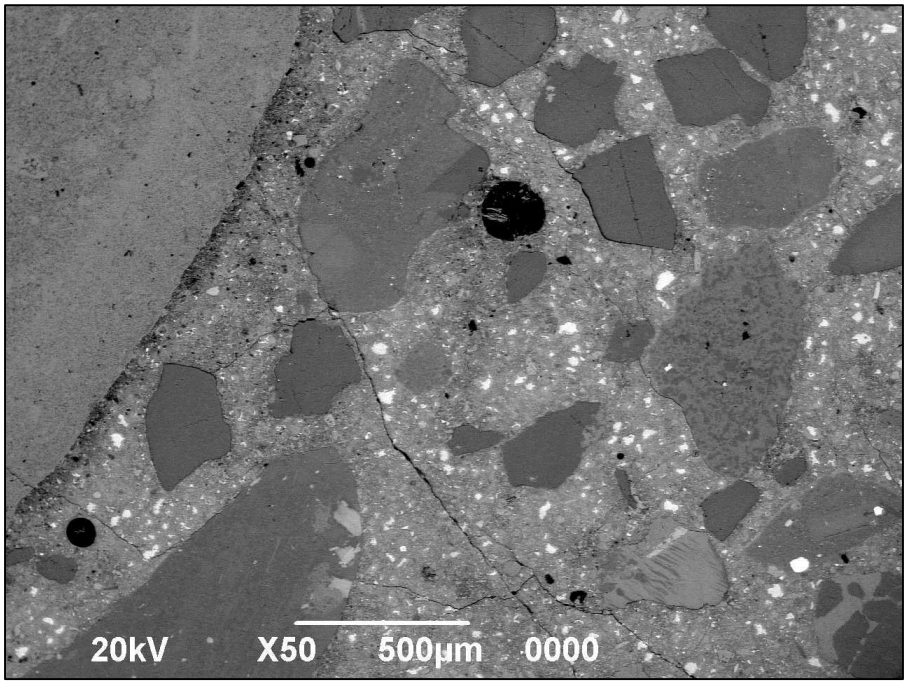

Figure 2.12: SEM image of OPC mixture showing cracks within cement paste

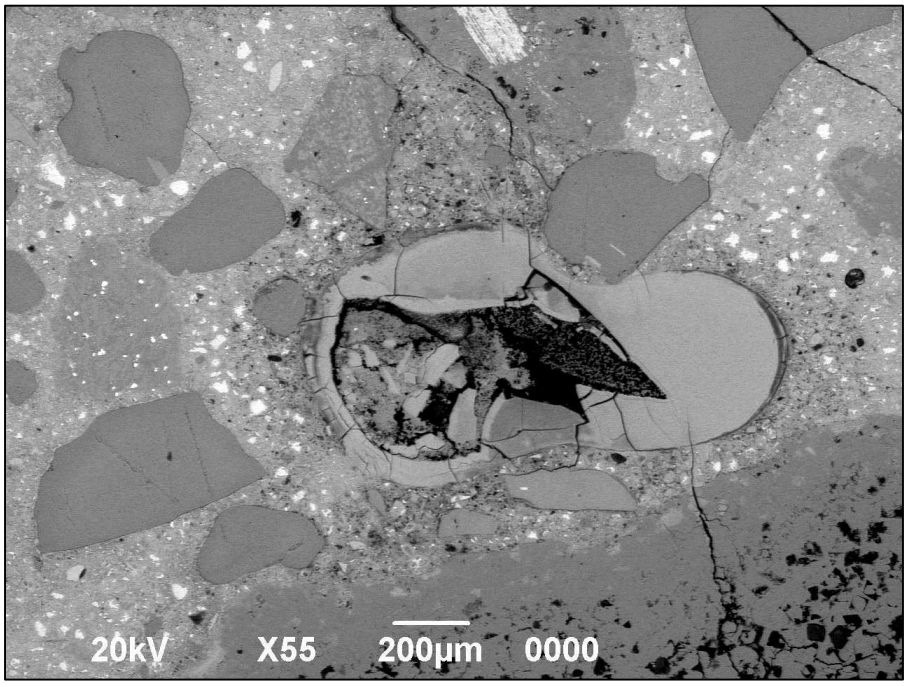

Figure 2.13: SEM image of OPC mixture showing a reacted aggregate particle and cracking within cement paste

Figure 2.14 shows an SEM image of a sample of the PC:CAC-2 mixture also taken after 2 years in ASTM C 1293. This image shows extensive cracking within the cement paste but no cracking within the aggregate particles. There was also no evidence of reacted aggregate particles within the SEM sample. The main reactive material in the sand used in these mixtures is chert which is typically present in the coarser fractions of the aggregate material (~1.25 – 5 mm fractions). The aggregate particles viewed via SEM are typically smaller than those which are most reactive. Figures 2.15 and 2.16 show SEM images of CSA-1 and PC:CSA-2, respectively. These images show cracking throughout the paste similar to that seen in PC:CAC-2. Most of the fine aggregate particles are too small for complete aggregate deterioration; however, due to the large surface area of the fine aggregate the extensive cracking within all four samples can be attributed to bulk expansion from alkali-silica reaction around the fine aggregate.

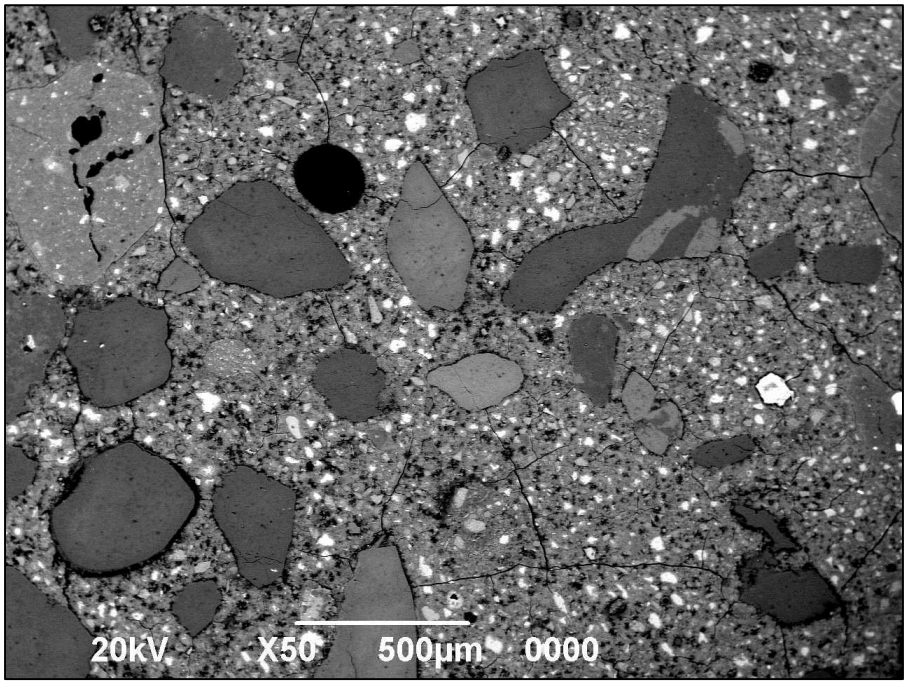

Figure 2.14: SEM image of PC:CAC-2 showing extensive cracking in paste.

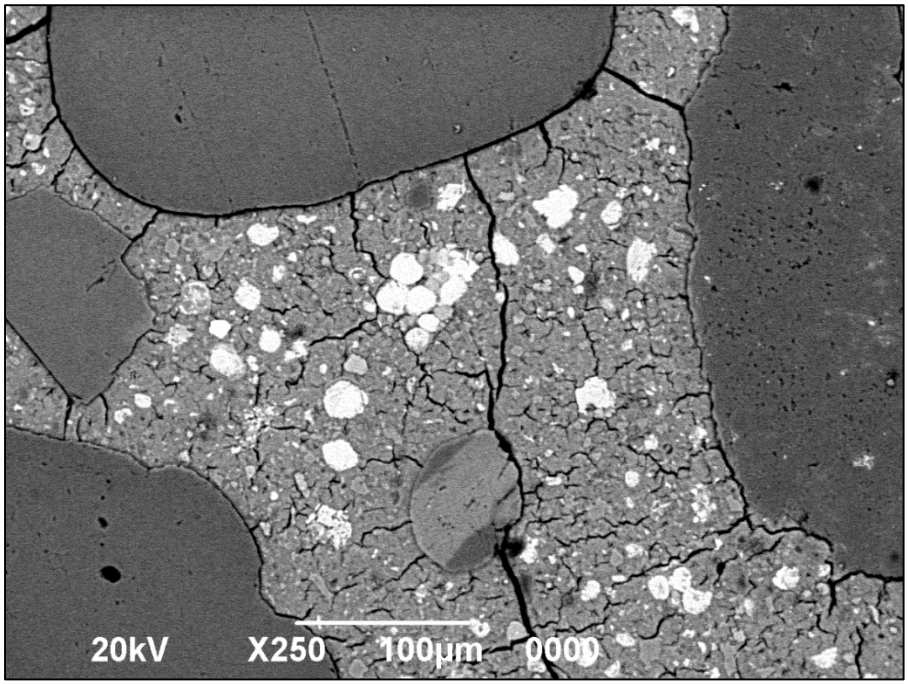

Figure 2.15: SEM image of CSA-1 showing cracks in paste and around aggregate particles

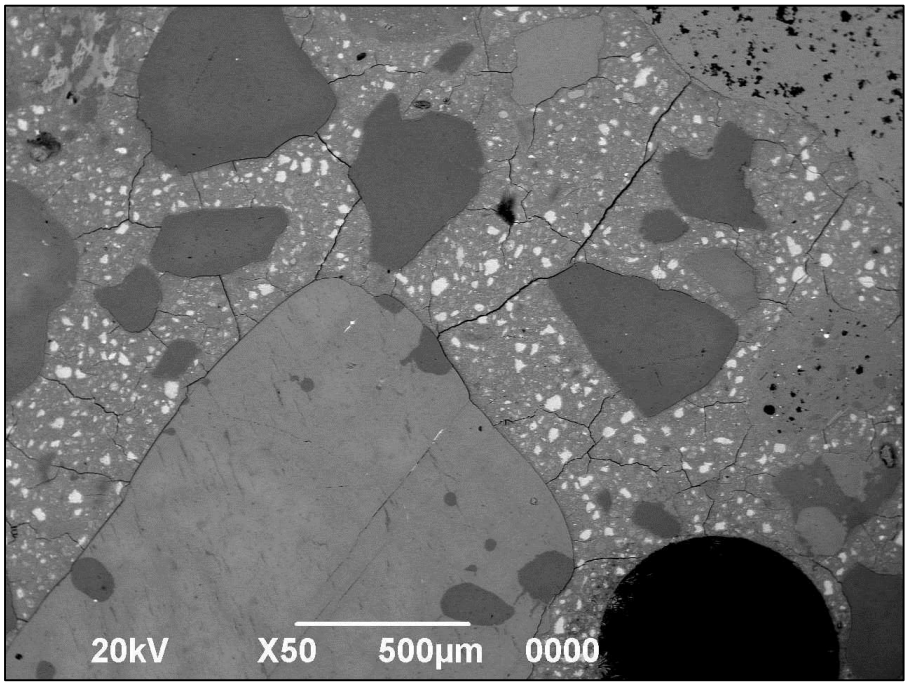

Figure 2.16: SEM image of PC:CSA-2 cracks in paste and showing cracks in cement paste and around aggregate particles

The SEM images presented in this section verified the presence of ASR in those samples which surpassed the expansion limit in ASTM C 1293 and provided a more detailed look at the micro-cracking associated with ASR. Unfortunately, the "reaction rims" noted on the coarse aggregate during the DRI examination were not visible under SEM. The nature and impact of these features is still undetermined.

2.6.2 Exposure Block Testing

All six exposure blocks were monitored periodically for over two years. The expansion values for each block at the last measurement are listed in Table 2.10 and illustrated in Figure 2.17. As expected, the OPC block showed the highest level of expansion reaching 1.27% at just under 2.5 years. Heavy map cracking is visible on the OPC block. Very little expansion has been recorded on the other five blocks in the same amount of time; however, an upswing in expansion was noted in the last few months in the PC:CAC-2, CSA-1, and PC:CSA-2 blocks as illustrated in Figure 2.18.

Table 2.10: Expansion Data for ASR Exposure Blocks

Binder	Age at Last Measurement, days	Expansion at Last Measurement, %
OPC	883	1.27%
CAC-1	720	0.02%
PC:CAC-2	883	0.03%
CSA-1	825	0.01%
PC:CSA-2	868	0.02%
AFA	846	0.01%

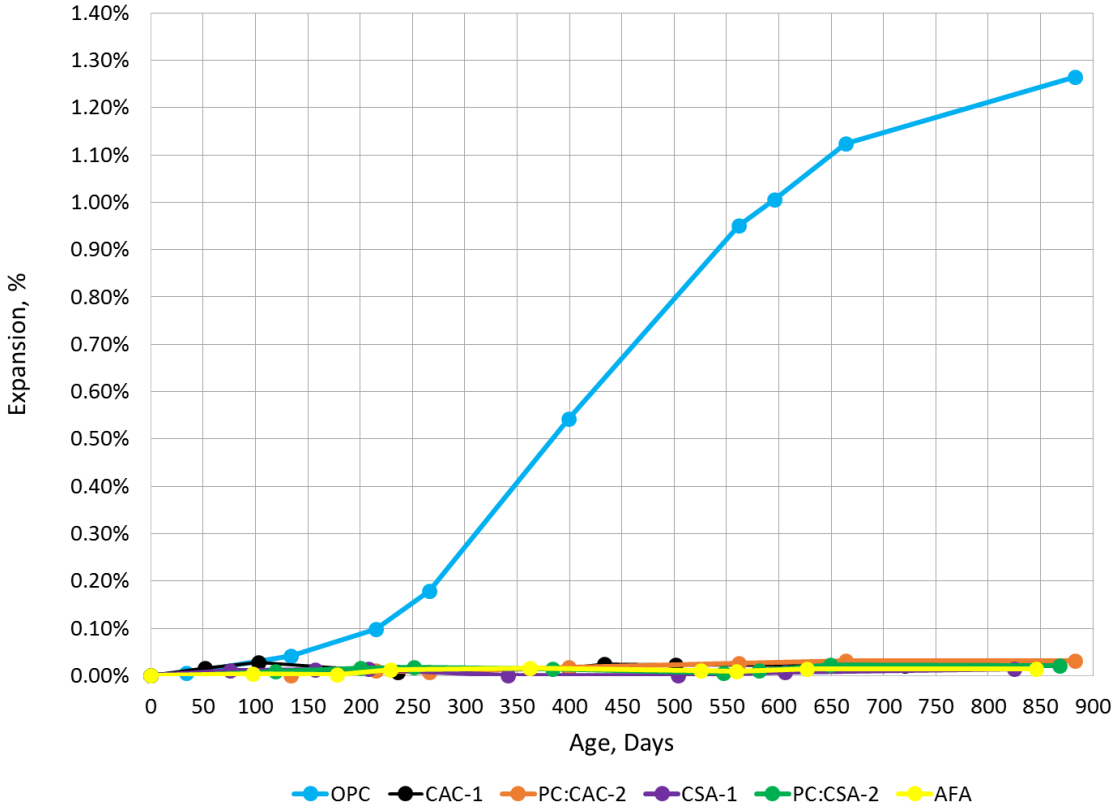

Figure 2.17: Expansion of Outdoor Exposure Blocks

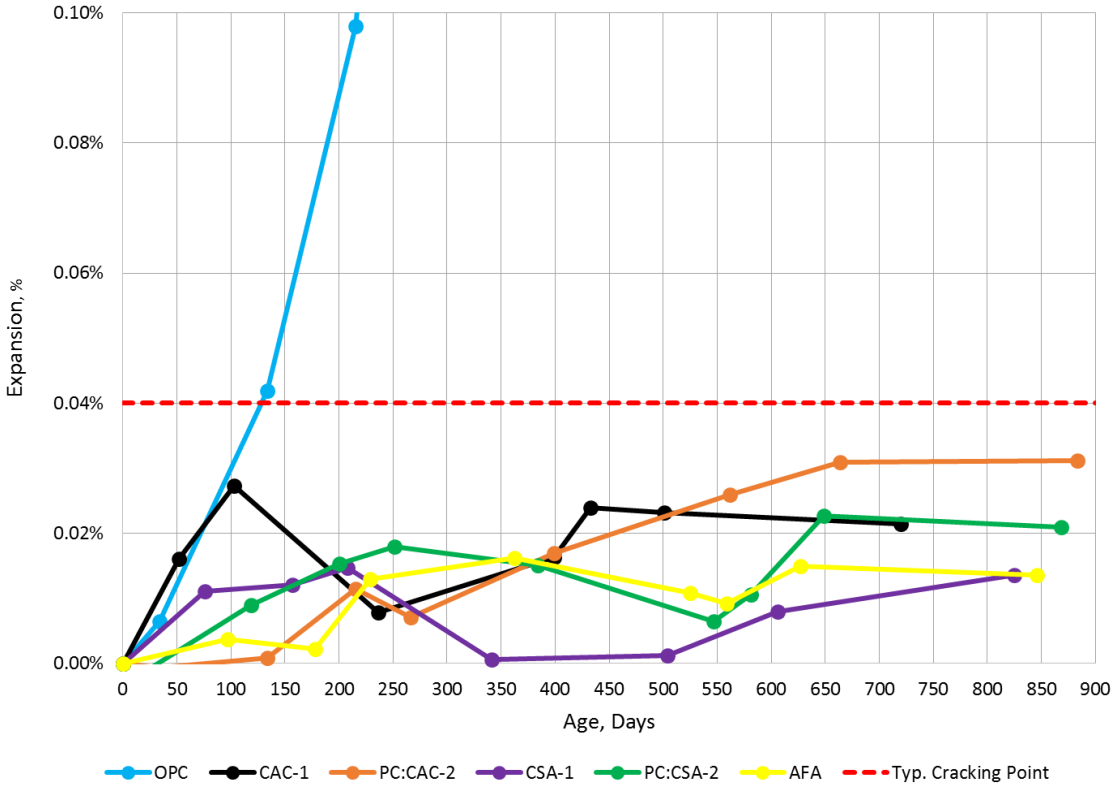

Figure 2.18: Expansion of Outdoor Exposure Blocks, zoomed

The results of the exposure block testing highlight the significant differences that can be seen between accelerated laboratory methods and field exposure. The same mixture designs were utilized in both the ASTM C 1293 and exposure block testing; however, we see much greater amounts of expansion in the PC:CAC-2 and PC:CSA-2 mixtures in ASTM C 1293 than in the exposure blocks. The recent upswing in expansion in the blocks may indicate that the blended systems just require more time to trigger ASR in field applications. Future monitoring of these blocks is essential and should provide a more accurate basis for comparison with the accelerated laboratory test results.

2.6.3 ASTM C 1260 – Mortar Bar Test

Similar to ASTM C 1293, ASTM C 1260 is typically used to determine reactivity of an aggregate source. However, in this study an aggregate of known reactivity was used in an attempt to characterize the reactivity of a binder alone. ASTM C 1260 is an accelerated and extremely aggressive test method that has been known to identify aggregates as being reactive that were otherwise considered non-reactive according to ASTM C 1293 (Folliard et al., 2006). ASTM C 1260 was used to characterize all binders except for the pre-bagged AFA mixture.

The ASTM C 1260 expansion results are shown in Figure 2.19. The OPC, PC:CSA-2, PC:CAC-2, and CSA-1 mixtures failed the test within the prescribed testing period of 14 days. All mixtures were monitored for an additional 14 days to acquire more information about the mixtures. An expansion limit of 0.10% at 14 days was used. The trends in these results track very closely with those seen in the ASTM C 1293 tests. The data acquired in the two weeks after the 14 day test period is quite telling. Very little expansion was observed with the CAC-1 mixture; however, the CSA-1 mixture continued to expand to 0.25%, which is well over two times the expansion limit at 14 days.

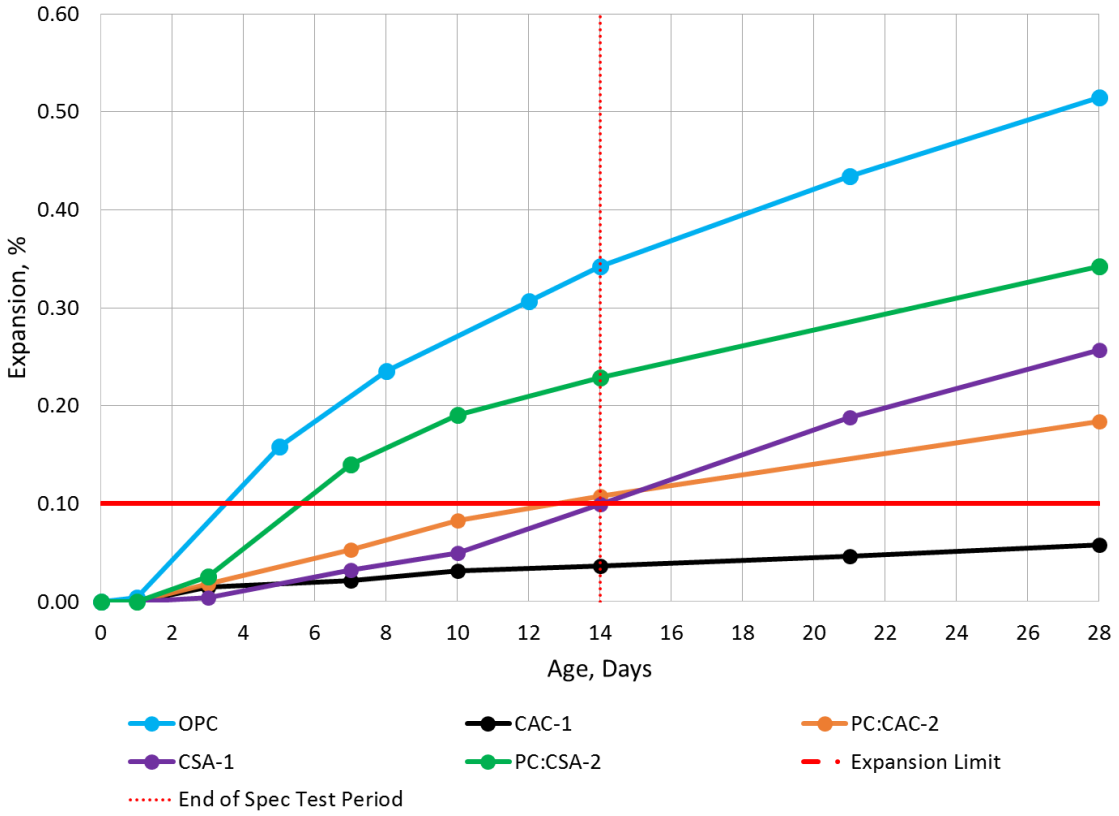

Figure 2.19: Expansion Results of Mortar Bars in ASTM C 1260

2.7 CONCLUSIONS

The purpose of this study was to produce information regarding the potential for ASR in blended systems incorporating portland cement and calcium aluminate cement or calcium sulfoaluminate cement. The secondary purpose of this study was to determine whether or not current standard test methods could be used to effectively characterize alternative binders. Five alternative binders were evaluated through standard laboratory tests including, ASTM C 1293 and ASTM C 1260, as well as outdoor exposure block testing. The ASTM C 1293 specimens were further evaluated through water-soluble alkali testing, petrographic analysis, and SEM-EDS analysis.

Based on the test results described in this chapter, the following conclusions can be drawn:

- Blends that incorporated portland cement, calcium aluminate cement and calcium sulfate were prone to ASR when used with reactive aggregate and high-alkali portland cement.
- Blends that incorporated portland cement and calcium sulfoaluminate cement were also prone to ASR when used with reactive aggregate and high alkali portland cement.
- Calcium sulfoaluminate cement was also prone to low levels of ASR when used with reactive aggregate.
- When used as 100% of the binder, calcium aluminate cement did not trigger ASR, presumably due to the lower inherent pore solution pH.
- Current standard lab tests (ASTM C 1293 and ASTM C 1260) were found to be effective in evaluating alternative binders. However, it should be noted that the 1 N NaOH solution used in ASTM C 1260 provides essentially an unlimited reservoir of alkalies and may overwhelm any effects of the binders being tested. Ultimately, the results of these laboratory tests need to be correlated with long-term exposure block performance.
- The Damage Rating Index was found to be a useful and necessary tool for verifying the presence of ASR in new or alternative binders.

The use of calcium aluminate cements and calcium sulfoaluminate cements in blended systems can provide many desirable results including but not limited to, high early strength and cost reduction; however, these mixtures can lead to some durability concerns

as well, such as alkali-silica reaction. More research is needed to evaluate the effect of mitigation measures on ASR-induced expansion, such as low-alkali portland cements and supplementary cementing materials.

2.8 REFERENCES

ASTM. (2005). *ASTM C 114 Standard Test Methods for Chemical Analysis of Hydraulic Cement.* West Conshokocken, PA: ASTM International.

ASTM. (2008). *ASTM C 1293, Standard Test Method for Determination of Length Change of Concrete Due to Alkali-Silica Reaction.* West Conshokocken, PA: ASTM International.

ASTM. (2013). *ASTM C 305 Standard Practice for Mechanical Mixing of Hydraulic Cement Pastes and Mortars of Plastic Consistency.* West Conshohocken, PA: ASTM International.

ASTM. (2014). *ASTM C 1260 Standard Test Method for Potential Alkali Reactivity of Aggregates (Mortar-Bar Method).* West Conshokocken, PA: ASTM International.

ASTM. (2015). *ASTM C 150, Standard Specification for Portland Cement.* West Conshokocken, PA: ASTM International.

ASTM. (2016). *ASTM C 33, Standard Specification for Concrete Aggregates.* West Conshokocken, PA: ASTM International.

Berube, M., et al. (2002). Measurement of the Alkali Content of Concrete Using Hot-Water Extraction . *Cement, Concrete, and Aggregates, 24*(1), pp. 28-36.

Bleszynski, R. T. (1998). Microstructural Studies of Alkali-Silica Reaction in Fly Ash Concrete Immersed in Alkaline Solutions. *Advanced Cement Based Materials, 7*, 66-78.

Campas, A., & Scrivener, K. (1998). *Lea's Chemistry of Cement and Concrete* (Fourth Ed. ed.). (P. Hewlett, Ed.) New York: Arnold.

Folliard, K. et al. (2006). *Interim Recommendations for the Use of Lithium to Mitigate or Prevent Alkali-Silica Reaction.* McLean, VA: FHWA.

Folliard, K., et al. (2006). *Preventing ASR/DEF in New Concrete: Final Report.* Report No. FHWA/TX-06/0-4085-5.

Fournier, B., et al. (2015). *Description of petrogrpahic features of damage in concrete used in the determination of the Damage Rating Index (DRI).* Quebec City, Quebec: Universite Laval, Geology and Geological Department.

Gaboriaud, F. et al. (1999). Aggregation and gel formation in basic silico-calco-alkaline solutions studied: A SAXS, SANS, and ELS study. *J. Phys.Chem. B, 103*, 5775-5781.

Grattan-Bellew, P., & Danay, A. (1992). Comparison of laboratory and field evaluation of alkali-silica reaction in large dams. *Proceedings of the International Conference on Concrete Alkali-Aggregate Reactions in Hydraulic Plants and Dams.* Fredericton: Canadian Electrical Association.

Grattan-Bellew, P., & Mitchell, L. (2006). Quantitative petrographic analysis of concrete - The Damage Rating Index (DRI) method, a review. *8th International CANMET-ACI Conference on Recent Advances in Concrete Technology - Marc-Andre Berube Symposium on AAR in Concrete*, (pp. 321-334). Montreal (Canada).

Leemann, A. et al. (2011). Alkali-silica Reaction: the Influence of Calsium on Silica Dissolution and the Formation of Reaction Products. *Journal of the American Ceramic Society, 94*(4), 1243-1249.

Rajabipour, F. et al. (2015). Alkali-silica reaction: Current Understanding of the reaction mechanisms and the knowledge gaps. *Cement and Concrete Research, 76*, 130-146.

Stanton, T. (1940). Expansion of Concrete Through Reaction Between Cement and Aggregate. *66* (10), p. 1781 - 1811.

Stark, D. (1991). The Moisture Condition of Field Concrete Exhibiting Alkali-Silica Reactivity. *ACI Special Publication, 126*, 973-988.

Tuan, C. (2005). Evaluation of Use of Lithium Nitrate in Controlling Alkali-Silica Reactivity in Existing Concrete Pavement. *Journal of the Transportaion Reserach Board, No. 1914*, 34-44.

Villenueve, V. F. (2012). Determination of the damage in concrete affected by AST - the Damage Rating Index (DRI). *14th International Conference of alkali aggregate reaction (AAR) in concrete.* Austin, TX.

Williams, S. (2005). *Structures Affected by Premature Concrete Deterioration: Diagnosis and Assessment of Deterioration Mechanisms (Thesis).* Austin: Civil Engineering Department, The University of Texas.

Chapter 3: Evaluation of Calcium-Aluminate Based Binders Exposed to Sulfate Environments

3.1 INTRODUCTION

Although the deterioration of concrete structures by external sulfate attack has been investigated quite extensively, it still remains a complicated and somewhat unclear durability issue. It is generally agreed that minimizing permeability and using sulfate resistant cements (with or without SCMs) are effective in ensuring good long-term performance for concrete exposed to sulfate-rich environments.

Calcium aluminate cements (CAC) were originally developed in an attempt to provide superior resistance to external sulfate attack (including sulfuric acid attack), as compared to portland cement concretes. In the century since the advent of CACs, there have been examples of both good and poor performance, yet the inherent assumption of CAC being sulfate resistant has generally prevailed. Between 1916 and 1923, over 7,000 tons of CAC were used in the construction of the P.L.M. Railway in France through areas with soils rich in gypsum and anhydrite. Since its construction, no issues related to sulfate attack have been reported in the railway or with test specimens immersed in calcium sulfate solution (Capmas & Scrivener, 1998). In the 1930s, Miller and Manson also studied the performance of CAC concretes in the sodium sulfate waters of Medicine Lake, South Dakota. After 20 years, the test specimens were still considered to be in excellent condition (Miller & Manson, 1933). Most of the early research conducted on the sulfate resistance of CAC was conducted in regions rich in calcium sulfate or with relatively low sodium sulfate concentrations (~1.0%). However, later research conducted by the UK building Research Establishment (BRE) has highlighted potential durability issues for CACs in contact with higher concentrations of sodium sulfate and magnesium sulfate (Crammond, 1990).

The lack of research focusing on the sulfate resistance of CAC may be attributed to the decline of its use following several structural collapses in the UK in the early 1970s. These collapses were initially attributed to a characteristic of the hydration process of CAC called "conversion". Unlike portland cement systems which experience continual strength gain over time, CAC systems inevitably experience strength loss over time due to "conversion". During the hydration of CAC at ambient temperatures, metastable hydrates (CAH_{10} and C_2AH_8) are formed; however, with time or an increase in temperature these metastable hydrates will convert to C_3AH_6 and AH_3 which are more thermodynamically stable hydrates. Conversion also causes an increase in porosity which can lead to significant strength loss. The increase in porosity associated with conversion is of significant interest in terms of sulfate resistance as most previously reported research has focused on unconverted CAC. In recent years, blended systems which incorporate calcium aluminate cement, calcium sulfate, and portland cement have been embraced because they offer the benefits of rapid strength gain without later strength issues associated with conversion. The increased use of these blended systems has further increased the confusion regarding the sulfate resistance of CAC as well as the need for additional research and long-term performance data.

ASTM C 1012 (ASTM, 2012) is the most commonly used test method for assessing the potential for sulfate attack in portland cement systems. This method entails the casting of mortar bars which are subsequently stored in a 5% sodium sulfate solution. Length change of the bars is measured periodically for up to 18 months, and the level of expansion observed in the mortar bars is used to determine the sulfate resistance of the mixture. This test method is the only method cited for equivalent testing in ACI 201.2R – Guide to Durable Concrete. ACI 201.2R provides requirements for concrete mixtures based on the severity of potential exposure. ASTM C 1012 is then used to determine whether or not

certain proposed materials will provide adequate sulfate resistance. While ASTM C 1012 is the most commonly used test method it is not without limitations. This method only allows for evaluation of mortar in contact with sodium sulfate. There is a lack of good correlation between the performance of mortar in a laboratory setting and concrete used in field applications. Likewise, there are significant differences in the sulfate resistance of most concrete mixtures depending on the type of sulfate present (calcium, sodium, or magnesium).

The aim of the research described herein was to use ASTM C 1012 and appropriate modifications to the test method to characterize the sulfate resistance of several blended systems which incorporate portland cement and calcium aluminate cement or calcium sulfoaluminate cement. A secondary goal was to obtain long-term performance data for concrete exposed to both high and low concentrations of sodium sulfate in an attempt to correlate field performance of concrete with laboratory results from mortar testing.

3.2 Review of External Sulfate Attack

Sulfate attack is a form of concrete deterioration that can be caused by the external ingress of sulfates or by an internal process known as delayed ettringite formation. External sulfate attack is considered the "classical" form of sulfate attack and is the focus of this study. Sulfate attack occurs when water containing sulfate ions penetrates into concrete. The sulfates are then available to the react with hydration products present in the concrete resulting in microstructural changes that can cause expansion and cracking.

The most common types of sulfates involved in sulfate attack are calcium, sodium, and magnesium sulfate. The reaction processes involved in sulfate attack vary depending on the type of sulfates present. The research discussed here involved the use of sodium sulfate; therefore, only the reaction processes for sulfate attack by sodium sulfate will be

reviewed. In general, sodium sulfate reacts with available hydration products to produce ettringite. In portland cement systems this typically happens two ways: (1) sodium sulfate reacts with calcium hydroxide to form gypsum which can then react with monosulfoaluminate to form ettringite (Equations 3.1 and 3.2), and (2) sodium sulfate reacts with C_3A to form ettringite (Equation 3.3) (Drimalas, 2011).

$$CH + N_2\$H10 \rightarrow C\$H_2 + 2NH + 8H \quad \text{(Equation 3.1)}$$

$$C_3A(C\$)H_{12} + 2C\$H_2 + 16H \rightarrow C_3A(C\$)3H_{32} \quad \text{(Equation 3.2)}$$

$$2C_3AH_6 + 3N_2\$H_{10} \rightarrow C_3A(C\$)3H_{32} + 2AH_3 + 6NH + 5H \quad \text{(Equation 3.3)}$$

For blended systems containing OPC and CAC or CSA the reaction of monosulfate hydrates and calcium aluminate hydrates with external sulfates is of greatest concern. The blending of OPC with CAC and a small amount of calcium sulfate (C$) results in a binder which, when mixed with water, generates large amounts of ettringite, resulting in high early compressive strengths. This is also the case for systems which blend OPC with calcium sulfoaluminate cements (CSA). However, the ettringite that is formed early on is not stable and will slowly convert to monosulfoaluminate within a few weeks. This conversion provides a large cache of monosulfoaluminate ready to interact with external sulfates to cause sulfate attack.

3.3 MATERIALS

3.3.1 Binders

Five different binders were selected for evaluation under this study. An ASTM C 150 (ASTM, 2015) Type I cement was selected as the control binder. Other binders

selected include, a calcium-aluminate cement, a calcium-sulfoaluminate cement, commonly used in commercial applications, and blended systems which incorporate CAC or CSA with Type I cement. Samples of all binders were sent to a testing laboratory where the chemical compositions of each were determined via ASTM C 114 (ASTM, 2015). Table 3.1 provides the oxide analysis for the binders described below.

Table 3.1: Oxide Analysis of Binders

Oxide (%wt)	Binder				
	OPC	**CAC-1**	**PC:CAC-2**	**CSA-1**	**PC:CSA-2**
SiO_2	20.14	4.57	15.15	14.46	9.02
Al_2O_3	5.42	41.21	14.98	16.21	23.88
Fe_2O_3	2.47	14.29	2.12	0.94	2.56
CaO	63.63	37.49	56.32	50.30	44.03
MgO	1.32	0.61	0.97	1.34	0.86
SO_3	3.09	0.00	8.44	17.09	21.37
Na_2O	0.17	0.06	0.14	0.21	0.12
K_2O	0.95	0.21	0.73	0.73	0.35
ZnO	0.01	0.01	0.01	0.02	0.01
SrO	0.08	0.02	0.07	0.14	0.07
Mn_2O_3	0.06	0.18	0.04	0.03	0.08
P_2O_5	0.26	0.13	0.21	0.09	0.11
TiO_2	0.28	1.79	0.61	0.58	0.91
Cl	0.00	0.00	0.00	0.02	0.00
Cr_2O_3	0.01	0.08	0.02	0.02	0.01
Na_2O_e	0.79	0.20	0.61	0.69	0.35

Bogue calculations were conducted for OPC using the values from the oxide analysis. The C_3A content of a cement has a great influence on sulfate resistance. For this reason ASTM C150 limits the C_3A content of sulfate resistant cements, Type V and Type II, to 5% and 8%, respectively. The C_3A content of the OPC binder used in this study was 10.2%; therefore, it was expected to be susceptible to sulfate attack.

3.3.1.1 Portland Cement

A locally sourced ASTM C 150 Type I portland cement was chosen as the control binder for this study. This cement has been used extensively within this lab as a control binder for various studies; therefore, the long term performance of this material is well documented and understood making it the clear choice for the control for this study.

3.3.1.2 Calcium Aluminate Cement and Blended System

A single source of calcium aluminate cement was used in this study and is referred to herein as CAC-1 and represents a binder containing 100 percent CAC. A blended CAC binder, designated as PC:CAC-2, was also evaluated and blend contained a mixture of calcium-aluminate cement and calcium sulfate at a ratio of 2.2:1. This blend was then combined with Type I cement at a 30% replacement level (by total mass).

3.3.1.3 Calcium Sulfoaluminate Cement and Blended System

A single source of calcium sulfoaluminate cement, referred to as CSA-1, was used in this study and is widely available within the US and abroad. The main phases of this CSA are ye'elimite ($C_4A_3\$$), belite (ß-C_2S), and calcium sulfate (C$).

The blended CSA system, designated as PC-CSA-2, utilized a combination of CSA in which the main phase was ye'elimite and calcium sulfate. The ratio of these components is unknown for this binder. Similar to PC:CAC-2, PC:CSA-2 was also combined with Type I cement at a 30% replacement level. CSA-1 and CSA-2 are manufactured by different sources and vary in chemical composition.

3.3.2 Admixtures

A superplasticizer and a lithium-based accelerator were used for all CAC-1 mixtures. The superplasticizer and accelerator were dosed at 0.50% and 1.00% by mass of cement, respectively.

For all PC:CAC-2 mixtures powdered citric acid was used as a retarder at a dose of 0.35% by mass of cement in conjunction with a superplasticizer in the form of sulfonated melamine formaldehyde (SMF) at a dose of 0.85% by mass of cement.

All CSA-1 and PC:CSA-2 mixtures utilized a combination of citric acid and SMF to attain the desired workability and three-hour compressive strength of 20 MPa (3,000 psi). The dosage for SMF was 0.1% by mass of the dry materials in the mix for both mixtures, and the citric acid was dosed at 0.2% and 0.35% by mass of cement for CSA-1 and PC:CSA-2, respectively.

3.3.2 Aggregates

For all mortar mixtures, per ASTM C 1012, ASTM C778 Ottawa graded sand was used at a sand to cement ratio of 2.75. The water to cement ratio stated in the standard is 0.485; however, a water to cement ratio of 0.35 was used for all mixtures. This was done to better simulate and evaluate materials used in rapid repair applications using typical field mixture design proportions. This also allows for greater possibility of correlation between results for mortar and concrete.

For all concrete mixtures, a crushed limestone coarse aggregate and manufactured limestone sand were used for all concrete mixtures. These materials are known to be non-reactive in regards to alkali-silica reaction. This distinction is important, especially for field trials, for isolation of the mechanism of deterioration to external sulfate attack only. A water to cement ratio of 0.35 was used for all concrete mixtures.

3.4 MIXTURE PROPORTIONS

Generally, to achieve good long-term strength and durability with CAC a water/cement ratio below 0.4 and a cement content above 400 kg/m^3 (674 lb/yd^3) are recommended (Capmas & Scrivener, 1998). Therefore, the cement content of the mixtures

was 440 kg/m^3 (742 lb/yd^3) for the CAC-1 mixture. The cement content for all other mixtures was 446 kg/m^3 or 752 lb/yd^3. This value was chosen over the 440 kg/m^3 (742 lb/yd^3) used for the CAC-1 mixture to correspond to the colloquial "8 sack" mix design often used by construction contractors. The water to cement ratio (w/c) was 0.35 by mass for all mixtures. The mixtures labels and binder mixture proportions are listed in Table 3.2.

Table 3.2: Mixture Labels and Proportions

Mixture Label	w/c	Total Binder Content (kg/m^3)	PC Content (kg/m^3)	CAC-2 Content (kg/m^3)	CSA-2 Content (kg/m^3)
OPC	0.35	446.0	446.0		
CAC-1	0.35	440.0			
PC:CAC-2	0.35	446.0	312.2	133.8	
CSA-1	0.35	446.0			
PC:CSA-2	0.35	446.0	312.2		133.8

3.5 EXPERIMENTAL METHODS

3.5.1 Paste and Mortar Mixtures

3.5.1.1 Casting and Curing

ASTM C 1012 was used as a guide during casting of paste and mortar bars. Stainless steel molds were used to cast paste and mortar bars with dimensions of 25 x 25 x 285 mm (1.0 x 1.0 x 11.25 in). Gauge studs were cast into each end of the bars to provide an effective length of 254 mm (10 in).

According to ASTM C 1012, specimens should be cast into molds, placed in a covered curing container and then cured at 35 ± 3 °C for 23½ h ± 30 min. This elevated temperature allows an acceleration in hydration of ordinary cementitious materials to achieve strength gain. However, the materials evaluated under this study rely on ettringite

formation for high early strength. Ettringite is more stable at ambient temperatures and the decomposition of ettringite increases with increasing temperature; therefore, heat curing was omitted from the procedure to more accurately characterize ettringite based binders. All specimens were wet cured at 23 °C (73 °F) in a temperature-controlled fog room for 24-hours and then demolded. Once demolded initial length measurements were obtained. The standard also requires the casting of mortar cubes for compressive strength testing. The companion cubes must reach 20 MPa (2,850 psi) prior to placement of mortar bars in sulfate solution. All mortar mixtures reached this required compressive strength at one day without heat curing.

A side study was conducted to investigate the effect of the conversion of CAC on sulfate resistance. For this study, two sets of mortar bars were cast using CAC-1. Both sets were cast and cured at ambient temperatures for 24 hours. After demolding, one set was placed in a 50 °C (122 °F) water bath. Companion mortar cubes were also kept in the water bath and tested daily until a drop in compressive strength was achieved signifying conversion had taken place. The other set of mortar bars was kept in the fog room at ambient temperature until conversion was achieved in the other set. At that time, both sets were placed in 5% Na_2SO_4 solution. Conversion was achieved within 5 days; therefore, all mortar bars were placed in solution 7 days after casting.

3.5.1.2 Sulfate Exposure Environments

Two sodium sulfate solution concentrations, 0.89% and 5.0% Na_2SO_4, were used in this study. ASTM C 1012 stipulates the use of a 5.0% Na_2SO_4 solution; however, it is believed that 0.89% Na_2SO_4 to be a more accurate depiction of sulfate concentration in soils (Chabrelie, 2010). One set of paste and mortar bars for each binder was exposed to each solution concentration.

For the first phase of sulfate attack testing, four paste bars were cast for each binder and exposure environment. Expansion measurements were taken from three of the bars at measurement intervals described in ASTM C 1012. The fourth bar was used for x-ray diffraction (XRD) sampling at 1, 14, and 28 days after casting. Additional XRD samples were taken at later ages when significant levels of expansion were achieved.

During the second phase of testing, a set of six mortar bars was cast for each binder and was placed in 5% Na_2SO_4 solution. Very high levels of expansion during the first round of the mortar bar testing prompted the casting of additional sets of bars that were then exposed to 0.89% and 5% Na_2SO_4 solution. Two curing regimens were also investigated: one set of bars was subjected to the same one-day ambient curing method described above, while the second set was kept in a temperature controlled fog room at 23 °C (73 °F) for 28 days before exposure to sulfate solution. Expansion measurements were taken at the intervals described in ASTM C 1012 after exposure to solution for each set.

3.5.2 Concrete Mixtures

3.5.2.1 Casting and Curing

Several concrete prisms were cast for each binder. The dimensions of the prisms are 75 x 75 x 300 mm (3 x 3 x 11.25 in). Gauge studs were cast into each end of the prisms to provide an effective length of 254 mm (10 in). The prisms were moist-cured in a temperature-controlled fog room for 24-hours and then demolded. Once demolded initial length measurements were obtained.

3.5.2.2 Sulfate Exposure Environments

After initial measurements were recorded the concrete prisms were placed in three different exposure environments: (1) indoor; static solution, (2) outdoor; partially

submerged in soil, and (3) outdoor; fully submerged in soil. Both 0.89% and 5.0% solution concentrations were investigated in all three environments.

3.5.2.3 Outdoor Sulfate Exposure Site

The outdoor sulfate exposure environments described above are located within the outdoor sulfate exposure site at the Concrete Durability Center in Austin, TX. This site was developed in 2005 to evaluate the sulfate resistance of concrete in a realistic "field" environment. Several 0.91 x 0.61 x 3.05 m (3 x 2 x 10 ft) galvanized feed troughs were used to house the concrete specimens. The troughs were filled half-way with sandy loam fill material typically used in residential construction. Sulfate solutions of specific type and concentration were added to each trough. For this study, 0.89% and 5% sodium sulfate solutions were placed into two troughs. For each binder, two concrete prisms were submerged 50 mm (2 in) below the soil level and three prims were oriented vertically. The vertical prisms were partially submerged into the sulfate bearing soil with the remaining half of the prism exposed to solution and open air as seen in Figures 3.1 and 3.2.

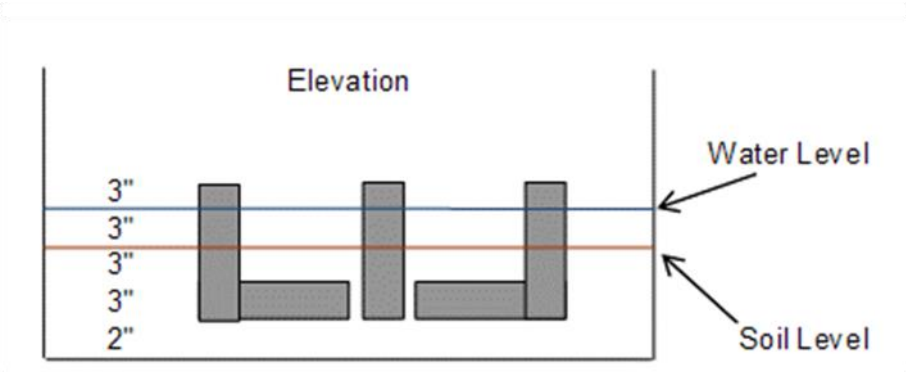

Figure 3.1: Orientation of Concrete Prisms in Outdoor Sulfate Exposure Site

Figure 3.2: Concrete Prisms in 5% Na_2SO_4 Outdoor Exposure Site

The completely submerged specimens are used to evaluate resistance to chemical sulfate attack, whereas the vertical prisms allow for evaluation of resistance to both chemical and physical sulfate attack. The soil-solution interface located at the center of the vertical prisms provides a wetting/drying zone which helps facilitate physical sulfate attack.

3.5.3 Qualitative X-Ray Diffraction Analysis

Qualitative x-ray diffraction analysis was performed on hydrated cement paste and mortar samples to characterize the microstructural development of CAC based binders exposed to sodium sulfate solutions. XRD sampling and analysis was done on all paste and ASTM C 1012 mortar bar mixtures described earlier in this section. Typically, samples were taken for analysis at 1 day after casting (prior to exposure), 14 and 28 days after exposure. Later, samples were also taken when significant levels of expansion were

reached. In addition, samples were also taken at 14 and 28 days prior to exposure for mortar bars cured in the fog room for 28 days.

The solvent exchange method was used to stop hydration of each sample after removal from sulfate solution. The following steps outline the solvent exchange method used:

1. Remove chunk of paste or mortar from bar, approximately 50 mm (2 in)
2. Cut multiple 3 - 4 mm (0.12 – 0.16 in) slices from chunk
3. Place slices in isopropanol (200-250 mL) for 5 - 7 days
4. Remove from isopropanol, dry in vacuum desiccator 2 days

After completion of the drying cycle, the samples were crushed and passed through a No. 325 sieve and returned to the desiccator until testing.

Analysis was conducted with a Siemens D500 diffractometer with a DacoMP controller. The parameters for each scan were: 5-70° 2θ, with a 0.02° 2θ step size and 4 second dwell.

3.6 Results and Discussion

3.6.1 Expansion Results

3.6.1.1 Expansion of Paste Samples in Sodium Sulfate Solution

Paste bars for all five binders were cast and placed in water, 0.89% Na_2SO_4, and 5% Na_2SO_4 solution. The expansion of the bars was monitored periodically over the course of a year. The PC:CSA-2, PC:CAC-2 and CAC-1 mixtures expanded the most in all three environments. Figure 3.3 shows the expansion of all mixtures placed in 0.89% Na_2SO_4 after a 1 day cure. The PC:CSA-2 paste bars began to deteriorate and were no longer measurable after six months. The yellow splatter mark in Figure 3.3 illustrates this

deterioration and indicates that no further measurements were possible, All other paste bar mixtures remained solid and intact despite relatively high levels of expansion in all three concentrations. Little to no expansion was noted in the CSA-1 mixture in any solution concentration. Figure 3.4 shows the expansion results for all five paste mixtures in 5.0% sodium sulfate. Similar trends were noticed in that the blended systems and CAC-1 tend to show more signs of expansion at early ages. However, as illustrated in Figure 3.5, the expansion seen in 5.0% Na_2SO_4 is almost equal to that seen in water for all five mixtures.

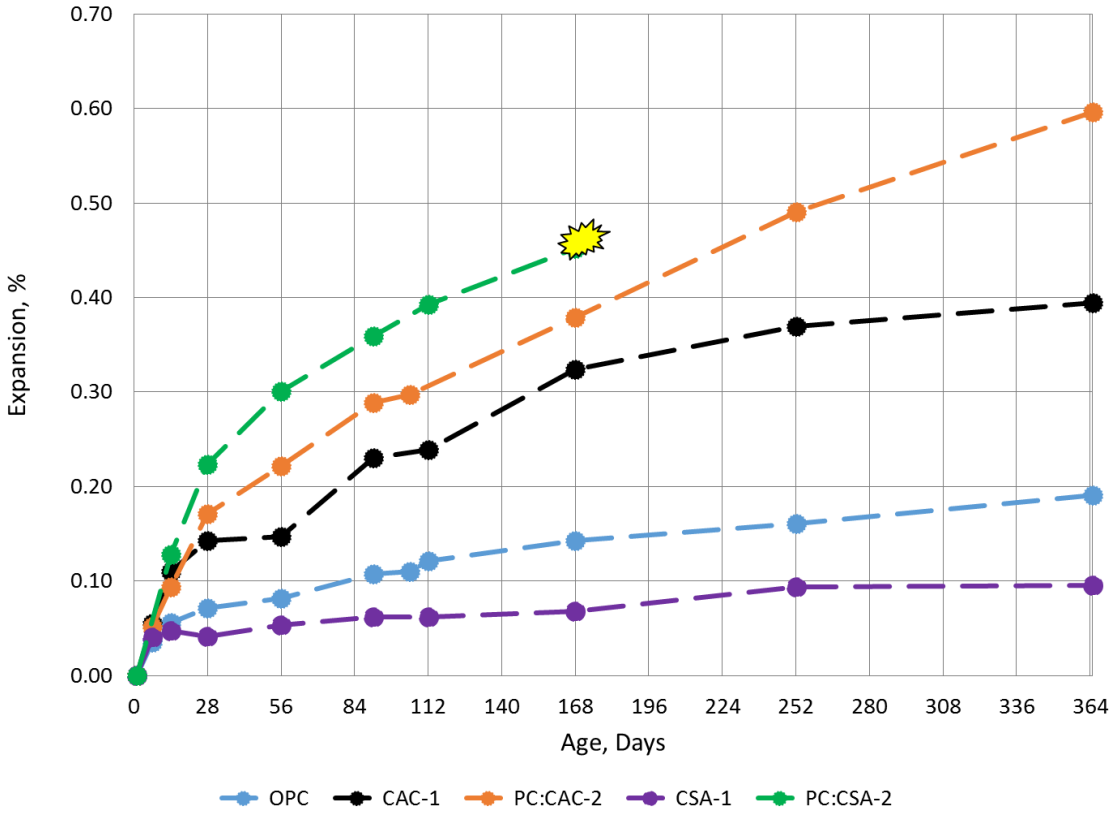

Figure 3.3: Expansion of Paste Samples Exposed to 0.89% Na_2SO_4 Solution at 1 Day

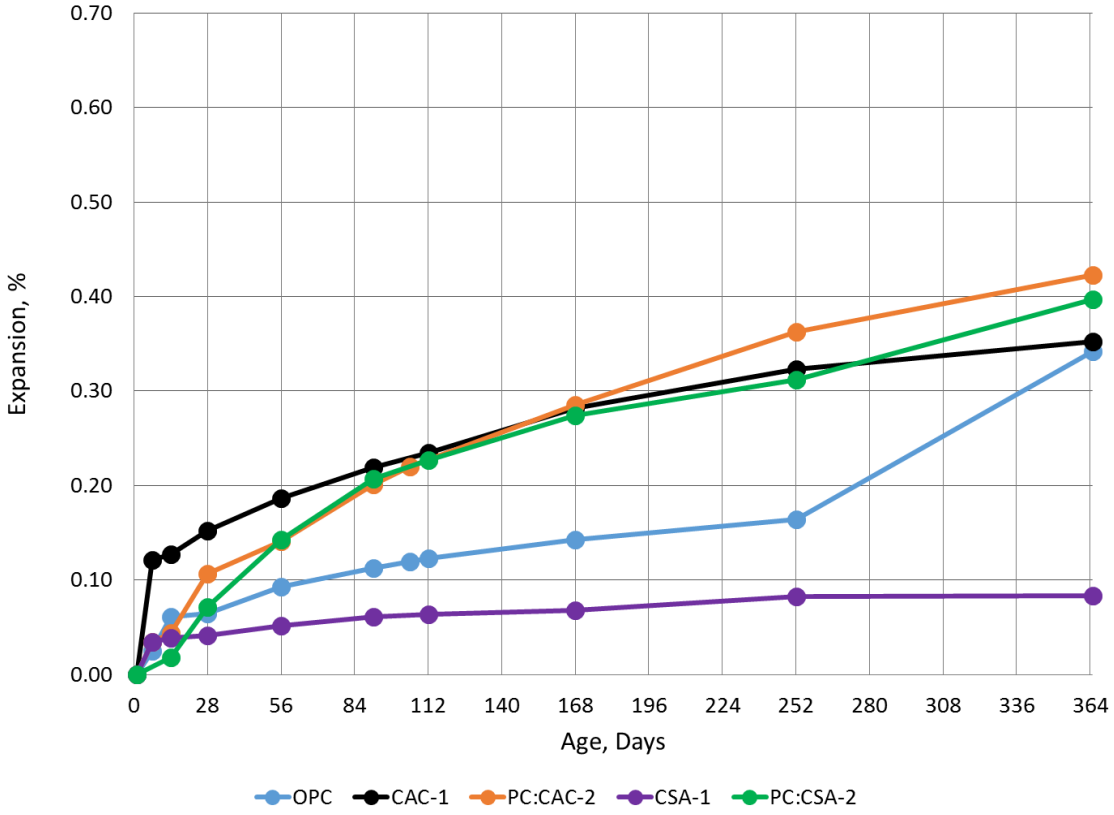

Figure 3.4: Expansion of Paste Samples Exposed to 5.0% Na_2SO_4 Solution at 1 Day

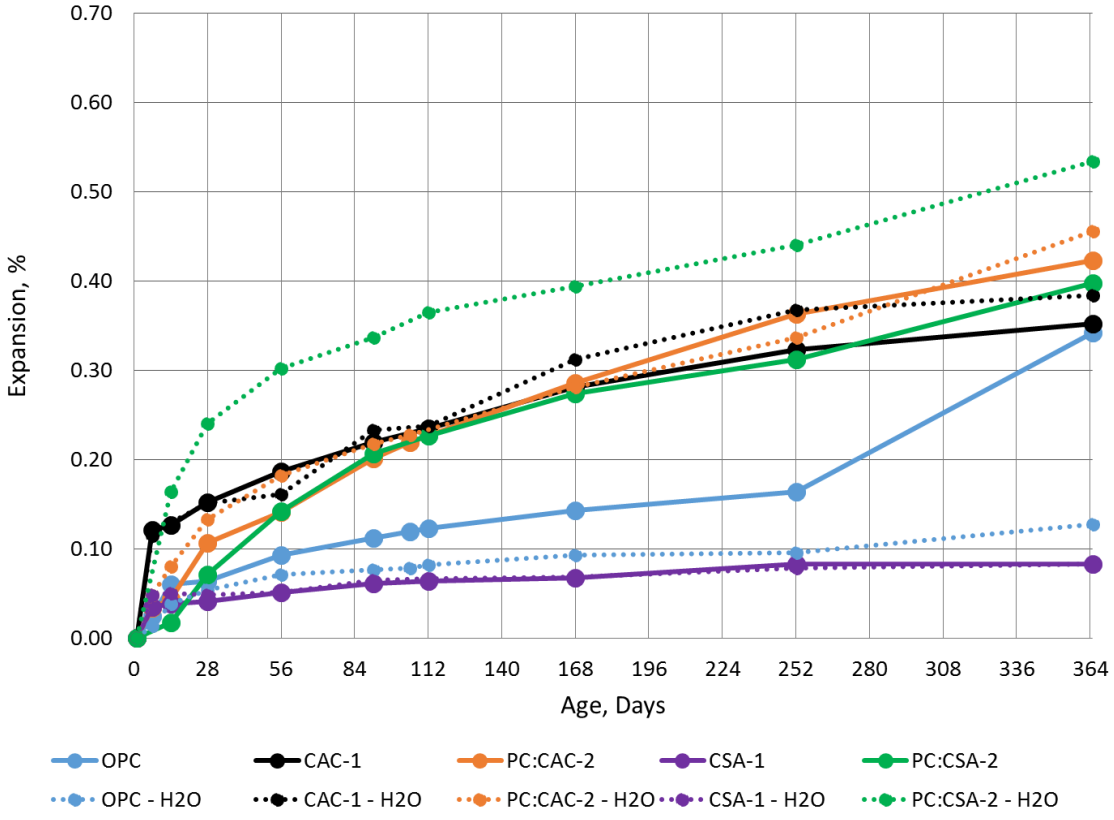

Figure 3.5: Comparison of Paste Exposed to 5% Na_2SO_4 versus Water at 1 Day

Similar trends are seen in samples that were cured in the fog room for 28 days prior to placement in solution as shown in Figures 3.6 to 3.8. The PC:CSA-2, PC:CAC-2, and CAC-1 mixtures show more expansion than OPC and CSA-1 in all three concentrations. A lower expansion was measured in all mixtures compared to the 1 day cure specimens, and expansion levels are almost equal for each mixture regardless of solution concentration.

Hydrated cement paste, especially with a low water/cement-ratio, has very low porosity. It is likely that the perceived expansion noted above is not actually from ettringite formation due to sulfate attack, but from swelling associated with water uptake or standard volumetric changes due to continued hydration of the cement paste. Also, the use of

aggregate provides dimensional stability in mortar and concrete mixtures; therefore, expansion noted could be due to volume change related to a lack of aggregate. X-ray diffraction analysis was conducted to identify the mechanism of expansion for these specimens and is discussed further in subsequent sections.

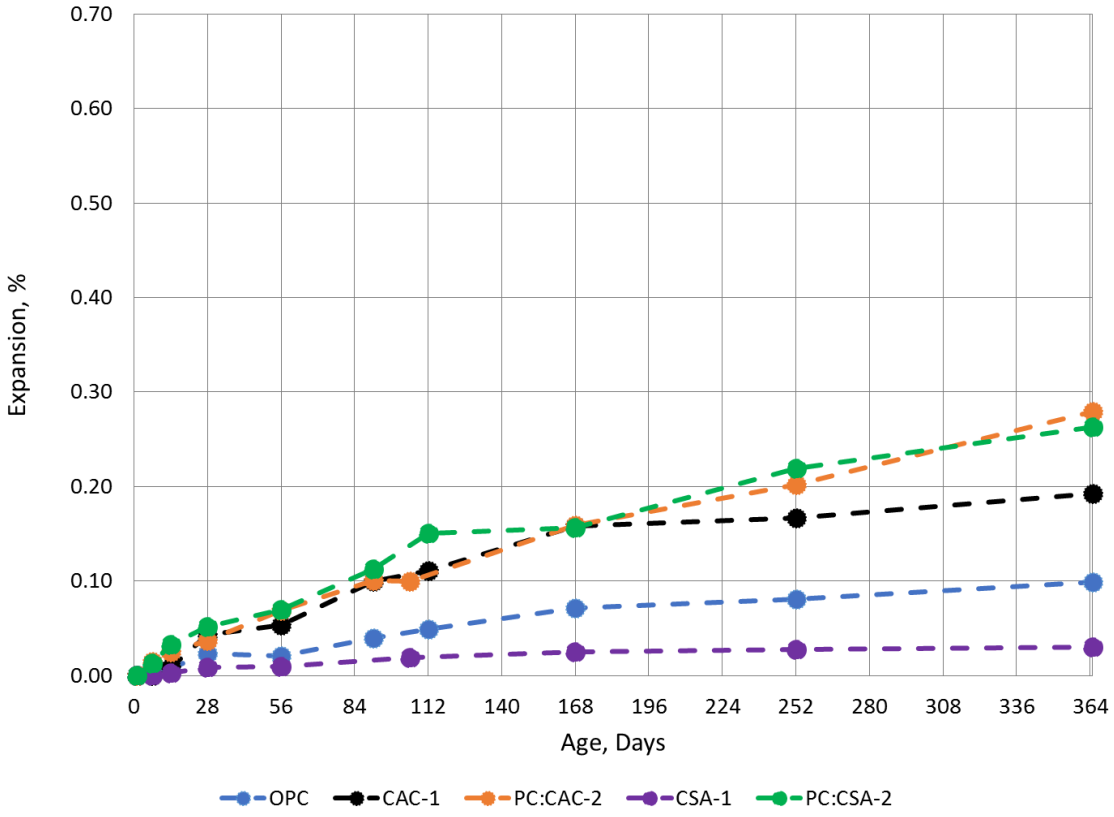

Figure 3.6: Expansion of Paste Exposed to 0.89% Na_2SO_4 at 28 Days

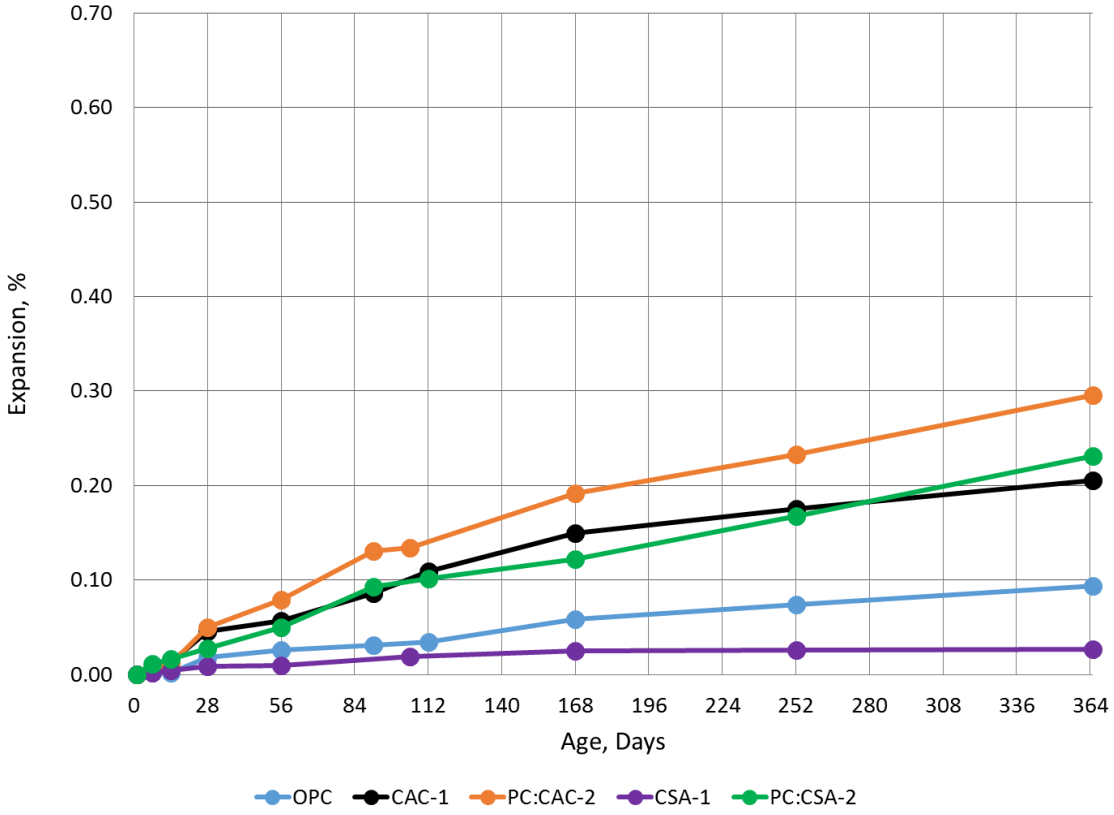

Figure 3.7: Expansion of Paste Exposed to 5.0% Na_2SO_4 at 28 Days

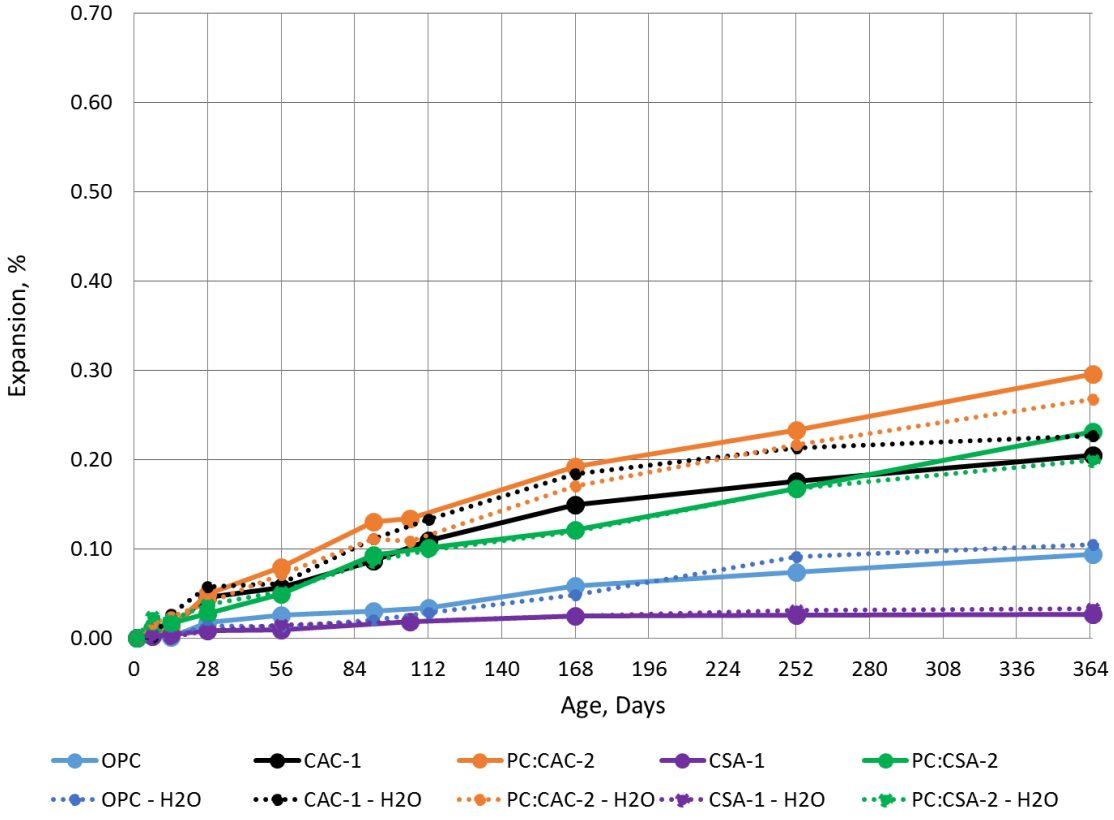

Figure 3.8: Comparison of Paste Exposed to 5% Na_2SO_4 and Water at 28 Days

3.6.1.2 Expansion of Mortar Bars in Sodium Sulfate Solution

Mortar bars were cast for all five binders and placed in 5% Na_2SO_4 solution. Expansion measurements were obtained at intervals as described in ASTM C 1012. Figure 3.9 shows the expansion values for the first set of mortar bar testing. Significant amounts of expansion and cracking were noted in both blended systems, PC:CAC-2 and PC:CSA-2. After two months the PC:CSA-2 mortar bars were completely deteriorated and no longer measureable. At three months, the PC:CAC-2 mixture reached an expansion level of 1.37% and was also completely deteriorated. It was assumed that consolidation issues led to the accelerated deterioration of the PC:CAC-2 mixture; therefore, a subsequent set of mortar bars was cast. The second set of mortar bars, also shown in Figure 3.9, showed slightly

better performance, but significant expansion (1.20%) was noted and the bars were no longer measurable after 6 months. The CAC-1 and CSA-1 mixtures were below the expansion limit of 0.10% after 9 months. The control mixture, OPC, started to expand at 5 months and had exceeded the expansion limit by 6 months.

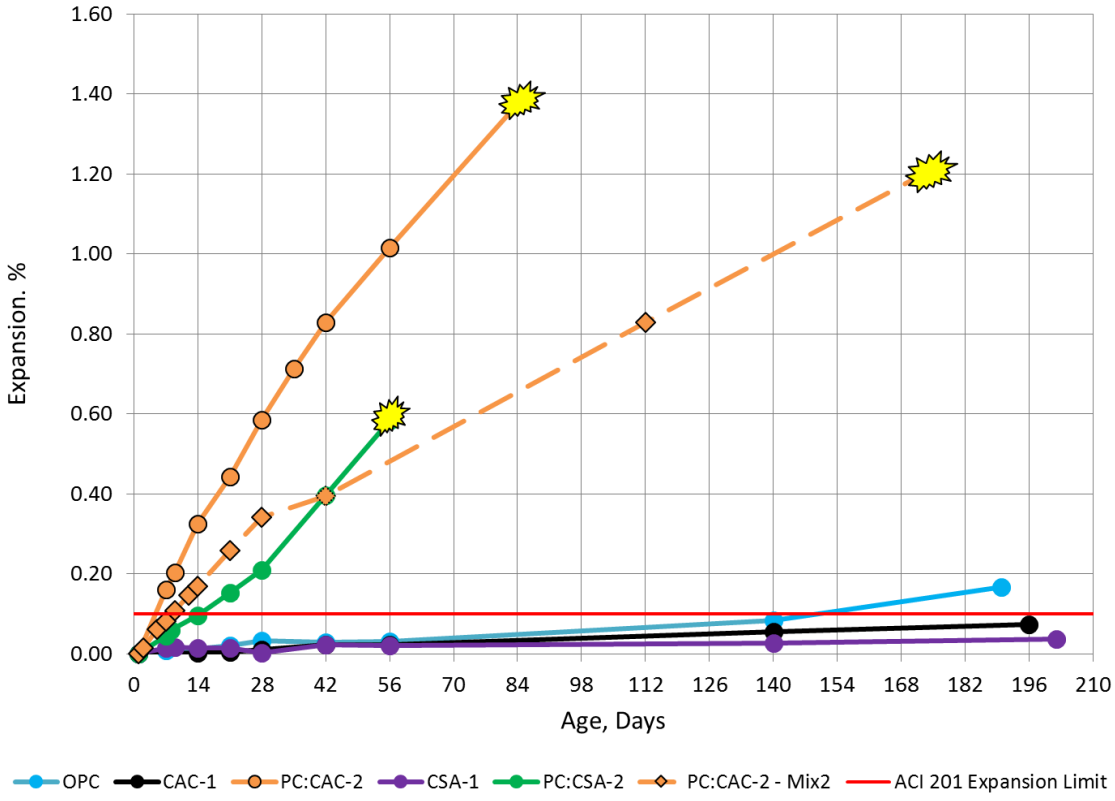

Figure 3.9: Expansion Results for First Round of Mortar Bars for ASTM C 1012

The extremely rapid expansion and deterioration noted in the PC:CAC-2 and PC:CSA-2 mixtures prompted the casting of additional sets of mortar bars for each binder. Additional sets of mortar bars were cast to investigate the influence of moist-curing duration (1 day versus 28 days) and solution concentration (0.89% and 5.0% Na_2SO_4). Mortar bars were also placed in water as a control. Figure 3.10 shows the expansion results for mortar bars that were cured at ambient temperature for 24 hours after casting. Once

demolded, the bars were placed in the different solutions. The PC:CSA-2 mixture exposed to 5.0% Na_2SO_4 solution showed significant expansion within the first weeks and surpassed the expansion limit at 14 days. By four months, these mortar bars were significantly cracked and some bars were broken completely. At nine months, none of the PC:CSA-2 mortar bars in 5.0% Na_2SO_4 were measurable due to significant cracking and breakage. Contrary to the results from the first round of mortar testing, the PC:CAC-2 mixture exposed to 5.0% Na_2SO_4 seems to perform significantly better. However, the mixture still surpassed the expansion limit of 0.10% at three months. Both mixtures placed in the 0.89% Na2SO4 solution also surpassed the expansion limit quite early. The PC:CAC-2 mixture reached 0.12% expansion at 56 days, and the PC:CSA-2 mixture reached 0.13% expansion also at 56 days. It is also important to note that the mortar bars for both mixtures stored in water also surpassed the expansion limit around 6 months.

It is known that systems of CAC or CSA with high additions of calcium sulfate can experience unstable expansion in the presence of water. The blended systems used in this study were specifically designed to prevent such unstable expansion; however, gradual and steady expansion in the presence of water seems to be unavoidable for the mortar bars placed in water after curing for one day. The low water to cement ratio, 0.35, used in this study can be a contributing factor to the expansion seen in water. We know that these systems rely of the formation of ettringite for strength gain, and a 0.35 water to cement ratio is insufficient for complete immediate hydration of these systems. Therefore, in the presence of water, the systems continue to hydrate and gradually produce more ettringite leading to a slow increase in expansion. Also, Bizzozero (2014) states that porosity plays a large role in the expansion of similar systems. It is suggested that ettringite is less confined as water to cement ratios increase and as a result expansion levels should decrease.

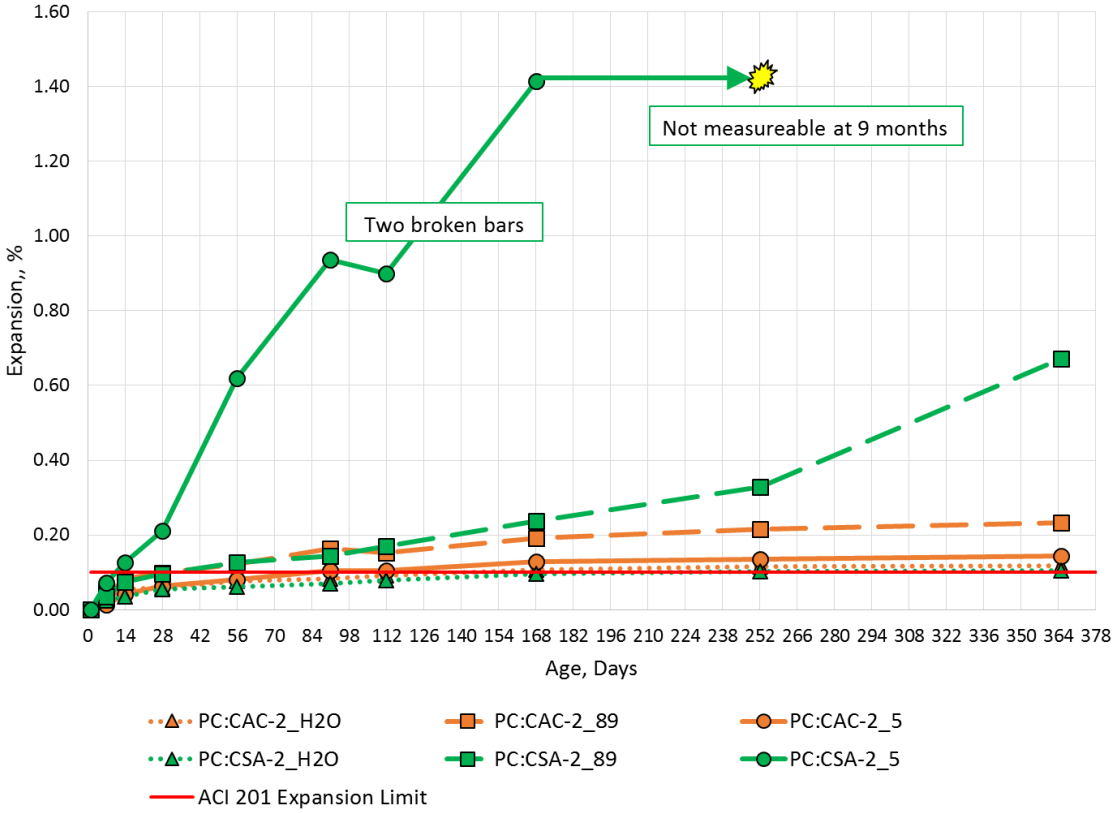

Figure 3.10: Expansion of Mortar Bars after 1 Day Wet Cure

Figure 3.11 shows the expansion results for the sets of mortar bars that were allowed to cure in a fog room at 23 °C (73 °F) for 28 days prior to placement in solution. Again, the PC:CSA-2 mixture in 5.0% Na_2SO_4 solution expanded very rapidly within the first few weeks. After 56 days the mortar bars were completely deteriorated and not measurable as evidenced in Figure 3.12. Similarly, PC:CAC-2 in 5.0% Na_2SO_4 expanded significantly within the first six months to a level of 1.38% and was no longer measureable at nine months. Figure 3.13 shows the difference in deterioration between six and nine months. Both mixtures placed in 0.89% Na_2SO_4 solution expanded at a slower rate than those in 5.0%, as expected. However, they both exceeded the expansion limit within two to three months. The longer curing period seems to exacerbate expansion due to sulfate

attack in all mixtures placed in sodium sulfate solution, regardless of concentration. However, there is a reduction in the amount of expansion seen in the mortar bars placed in water, and they remained below the expansion limit at the most recent measurement interval of nine months. Samples were taken for x-ray diffraction analysis to further explain the varied expansion results observed in these tests. Those results are discussed further in subsequent sections.

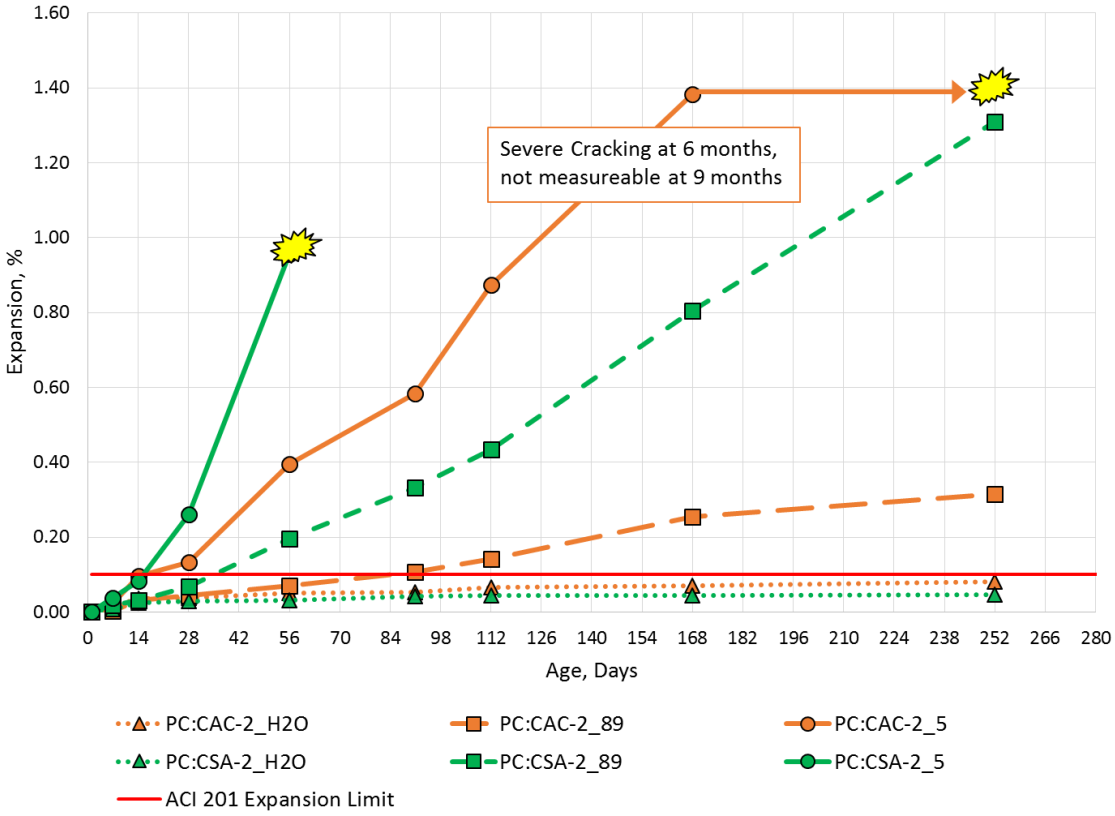

Figure 3.11: Expansion of Mortar Bars after 28 Day Wet Cure

Figure 3.12: Photo of PC:CSA-2 mortar bars after 56 days in 5.0% Na_2SO_4 solution

Figure 3.13: Photos of PC:CAC-2 mortar bars in 5% Na2SO4 at 6 months (top) and 9 months (bottom)

The results of the side study regarding the effects of conversion on the sulfate resistance of CAC proved to be very interesting. Figure 3.14 shows the expansion results for converted and unconverted CAC-1 mortar bars in 5.0% Na_2SO_4 solution. While the expansion values for both mixtures remain below the 0.10% expansion limit, the converted CAC-1 bars were deteriorated and not measurable by 9 months. The expansion value for the converted CAC-1 bars at the last measurement was only 0.06%; however, this value was a significant increase from the previous measurement at 112 days. The conversion of CAC results in an increase in porosity which allows for higher ingress of sulfate ions. This increase in porosity also allows more space for ettringite formation which possibly explains the relatively low level of expansion measured despite obvious evidence of deterioration.

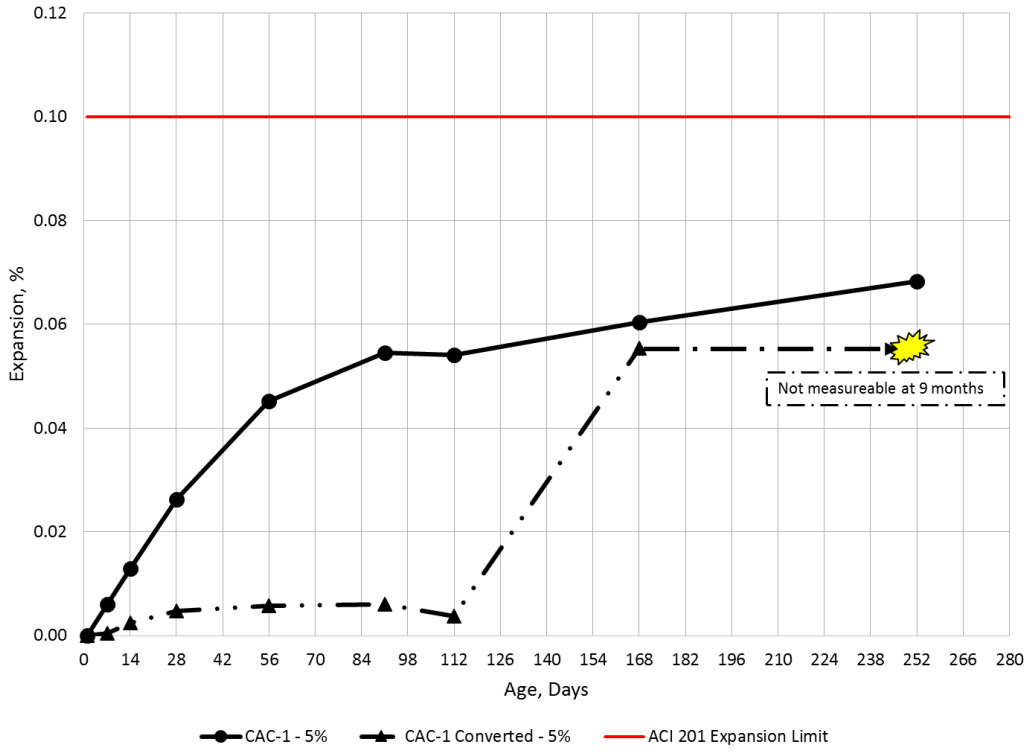

Figure 3.14: Expansion Results for Converted and Unconverted CAC-1 Mortar Bars in 5.0% Na2SO4 Solution

3.6.1.3 Expansion of Concrete Prisms in Sodium Sulfate Solution

ASTM C 1012 has been criticized as not being an appropriate test method for predicting field performance of concrete in sulfate environments. There tends to be a distinct lack of correlation between results obtained from mortar and concrete testing in a laboratory environment as well as between concrete tested in a laboratory setting and concrete exposed to realistic field conditions. Concrete prisms were cast for all five binders previously evaluated with ASTM C 1012. The concrete prisms from each mixture were placed in both an ASTM C 1012 environment which was modified to accommodate the size of the concrete prisms and outdoor within the exposure site. Specimens were placed in both 0.89% and 5.0% Na_2SO_4 solution and expansion measurements were taken monthly for the first three months and periodically thereafter. As expected, little expansion was seen in the OPC mixture until approximately 1 year, which is typical for Type I portland cement (Drimalas, 2011). Expansion results for the OPC mixture are shown in Figure 3.15. The 0.10% expansion limit used for ASTM C 1012 testing is included as a means of relative comparison. The most expansion is seen in the specimens submerged beneath the soil in 5.0% Na_2SO_4 solution in the outdoor exposure site. Little expansion was noted in any of the specimens stored in the 0.89% environments.

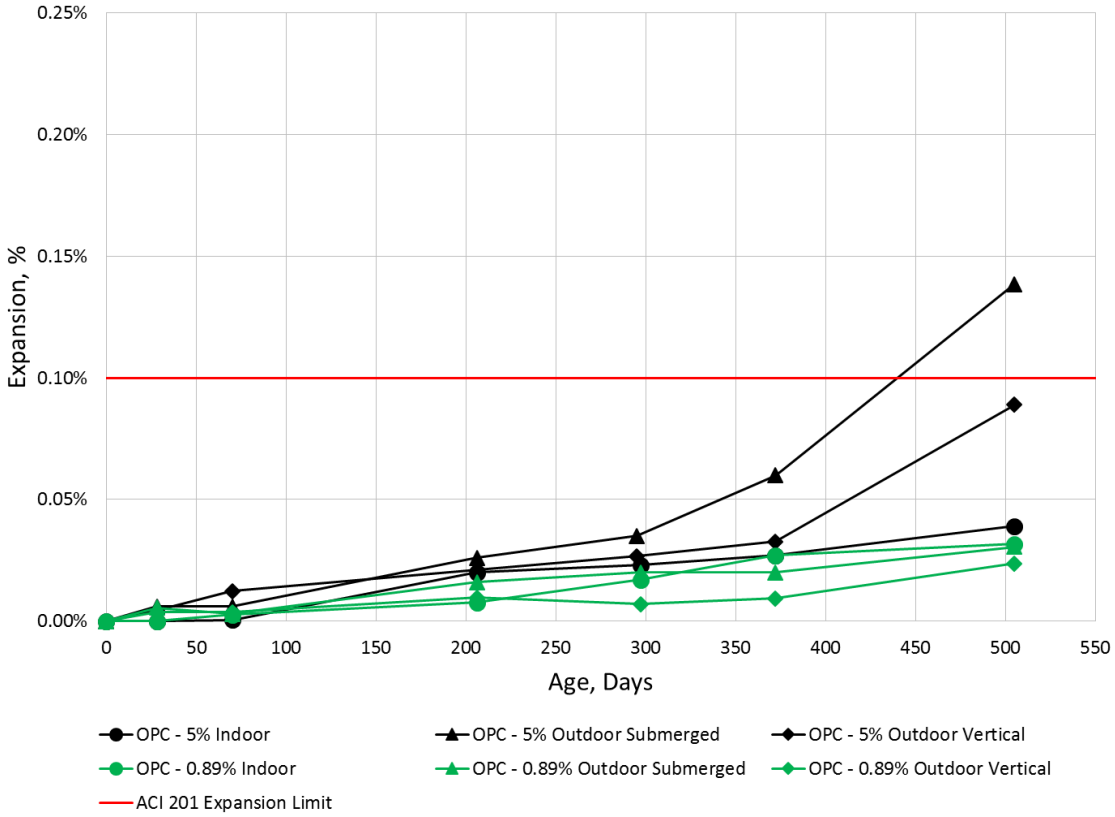

Figure 3.15: Expansion of OPC Concrete Prims in Sodium Sulfate Solution

The CAC-1 mixtures stored in the modified ASTM C 1012 environment started to show signs of expansion after about four months, as shown in Figure 3.16. The expansion for those prisms stored outdoor, regardless of orientation, seemed to level off after roughly a year, whereas the prisms stored indoor in both 0.89% and 5.0% solution continued to expand and surpass 0.10% expansion around 18 months. It is important to note that the expansion limit for most other laboratory test methods involving concrete is only 0.04% as this is typically the level of expansion where concrete begins to crack in field applications. Therefore, the use of 0.1% expansion as a limit for concrete exposed to sulfate rich environments is likely too conservative.

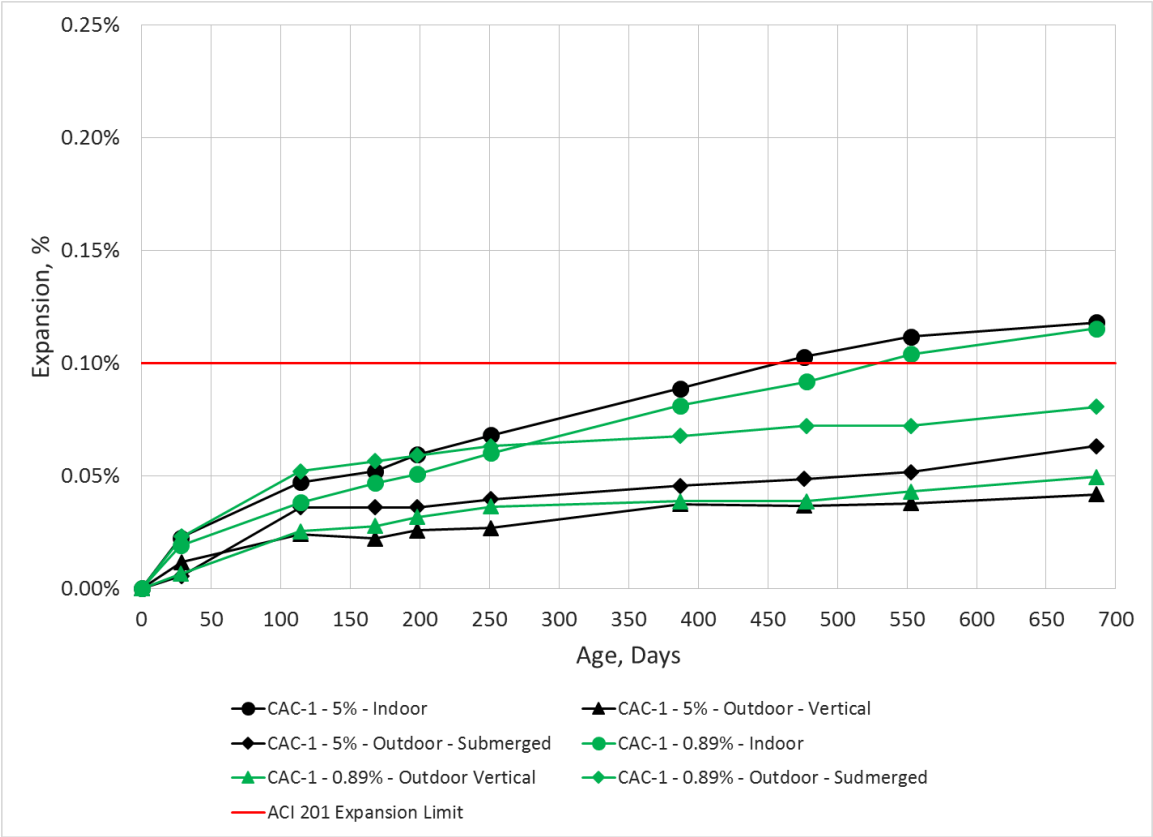

Figure 3.16: Expansion of CAC-1 Concrete Prims in Sodium Sulfate Solution

Very high levels of expansion were seen in the PC:CAC-2 mixtures as shown in Figure 3.17. After two months, the prisms stored indoor in both 0.89% and 5.0% solution have reached expansion levels exceeding 0.04%, the typical cracking point of concrete, and after about four months they both exceed the 0.10% expansion level for mortar stipulated in ASTM C 1012. After about a year, all specimens have reached expansions exceeding 0.04% and all specimens exposed to 5.0% solution have reached expansion levels of 0.10% or above. Significant deterioration was also visible on all samples exposed to the higher concentration. The results obtained from the PC:CAC-2 concrete specimens correlates quite well with that seen in the mortar testing in that this material is highly prone

to sulfate attack and has little capacity for sulfate resistance in the presence of any concentration of sodium sulfate.

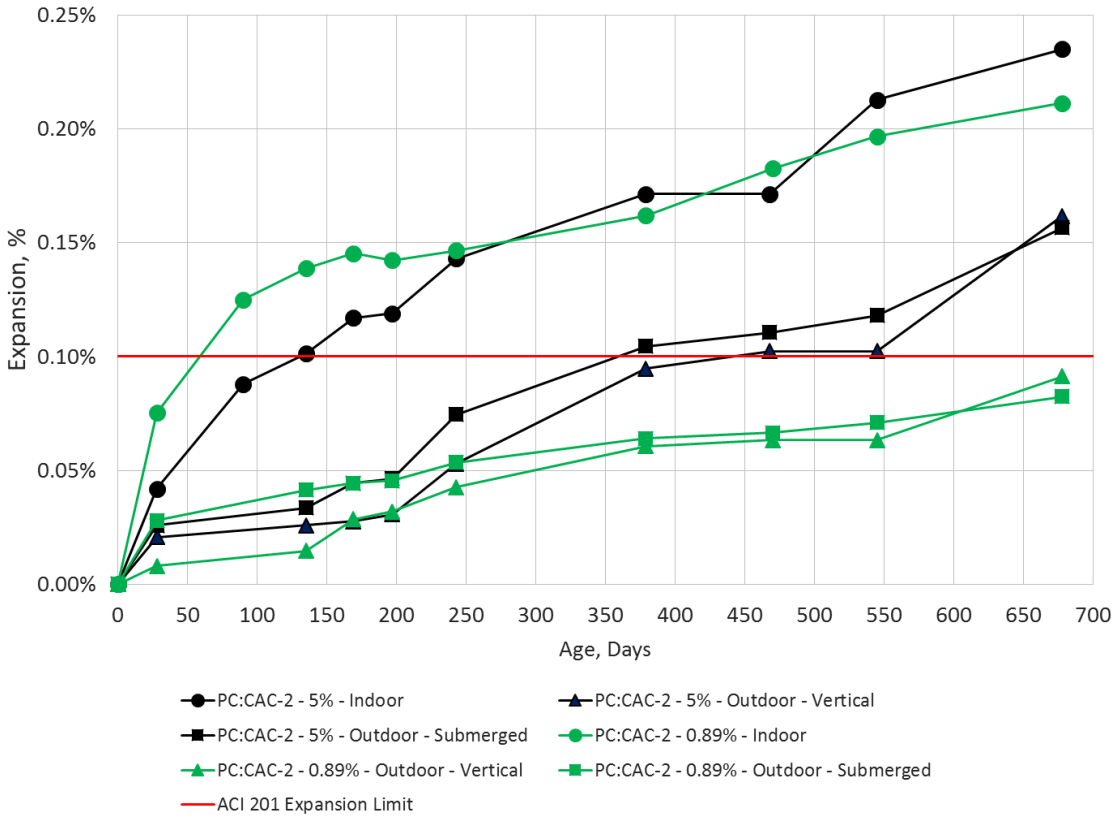

Figure 3.17: Expansion of PC:CAC-2 Concrete Prisms in Sodium Sulfate Solution

The results from the CSA-1 concrete specimens also correlate well with previous mortar bar testing. Little to no expansion was recorded for any storage environment during the first 20 months of monitoring as shown in Figure 3.18. Conversely, the results for the PC:CSA-2 (Figure 3.19) specimens do not seem to correlate with any of the previous mortar testing. Although expansion above 0.04% was measured after nine months for both sets of prisms stored indoor in 0.89% and 5%, high early expansion as seen in previous mortar testing as well as in the PC:CAC-2 concrete prisms did not occur. Deterioration is

evident on those specimens stored outdoor in 5.0% solution and expansion levels are still high enough to support the lack of sulfate resistance for this binder.

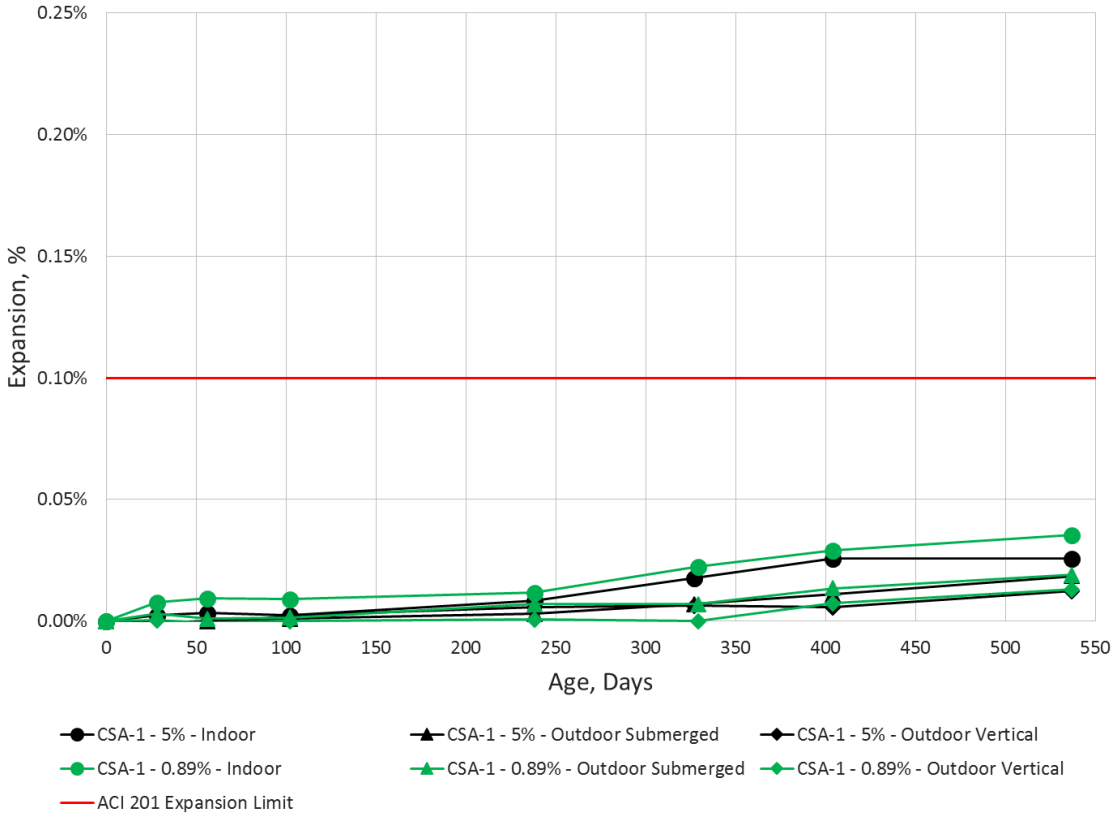

Figure 3.18: Expansion of CSA-1 Concrete Prisms in Sodium Sulfate Solution

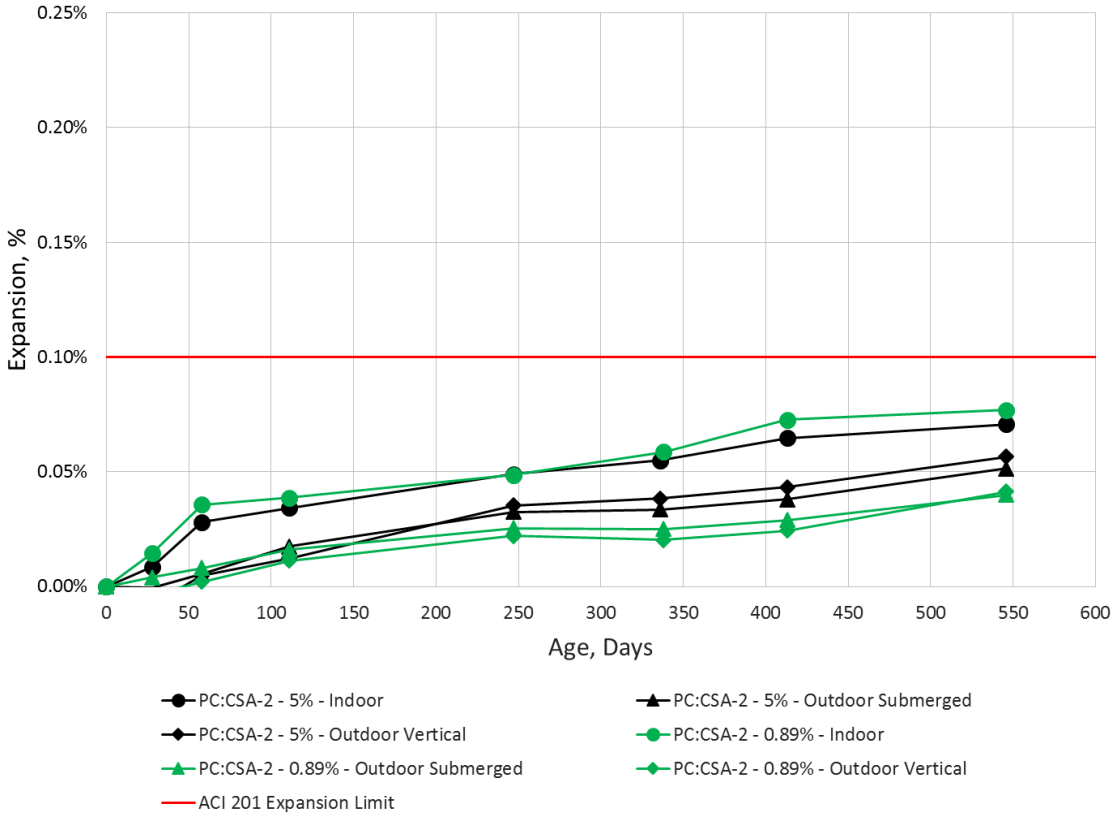

Figure 3.19: Expansion of PC:CSA-2 Concrete Prisms in Sodium Sulfate Solution

3.6.2 X-Ray Diffraction

Qualitative x-ray diffraction analysis was performed on hydrated cement paste and mortar samples to characterize the microstructural development of CAC based binders exposed to sodium sulfate solutions. XRD sampling and analysis was performed on the paste and ASTM C 1012 mortar bar mixtures described earlier in this section. Typically, samples were taken for analysis at 1 day after casting (prior to exposure), 14 and 28 days after exposure. Later samples were also taken when significant levels of expansion were reached. In addition, samples were also taken at 14 and 28 days prior to exposure for mortar bars cured in the fog room for 28 days.

3.6.2.1 XRD of Paste Exposed to Sodium Sulfate Solution

Qualitative XRD was performed on paste specimens exposed to water, 0.89% and 5.0% Na_2SO_4. It was of interest to investigate microstructural changes in these systems over time when exposed to sodium sulfate. The evolution and formation of ettringite was of particular interest. However, very few microstructural changes were observed over the course of a year despite observing significant levels of expansion in some mixtures in previous testing. For example, Figure 3.20 shows several XRD scans for the PC:CSA-2 subjected to a 1 day cure and 28 day prior to immersion in various solution concentrations. Despite varied curing and exposure to different sulfate concentrations very few difference are noted in hydration products formed over time. There are very minor differences in the noted ettringite peaks (E) but these differences are not distinct enough to identify a correlation between ettringite formation, expansion and sulfate concentration. As noted earlier, expansion levels for each binder were very similar regardless of sulfate concentration. The lack of differences between expansion values in different solution concentrations and XRD scans indicates that the use of paste samples to predict sulfate resistance of a binder may not be appropriate. Similar results were seen in all binders evaluated via x-ray diffraction. Contrary to the other binders, little to no expansion was noted in CSA-1 in all scenarios. Previous research (Nuytten, 2014) suggests that CSA-1 is stable in sulfate environments due to an initial composition with a high sulfate to alumina ratio. This high sulfate content prevents the formation of monosulfate at later ages. XRD analysis showed even fewer microstructural differences in this binder between sulfate concentrations as shown in Figure 3.21

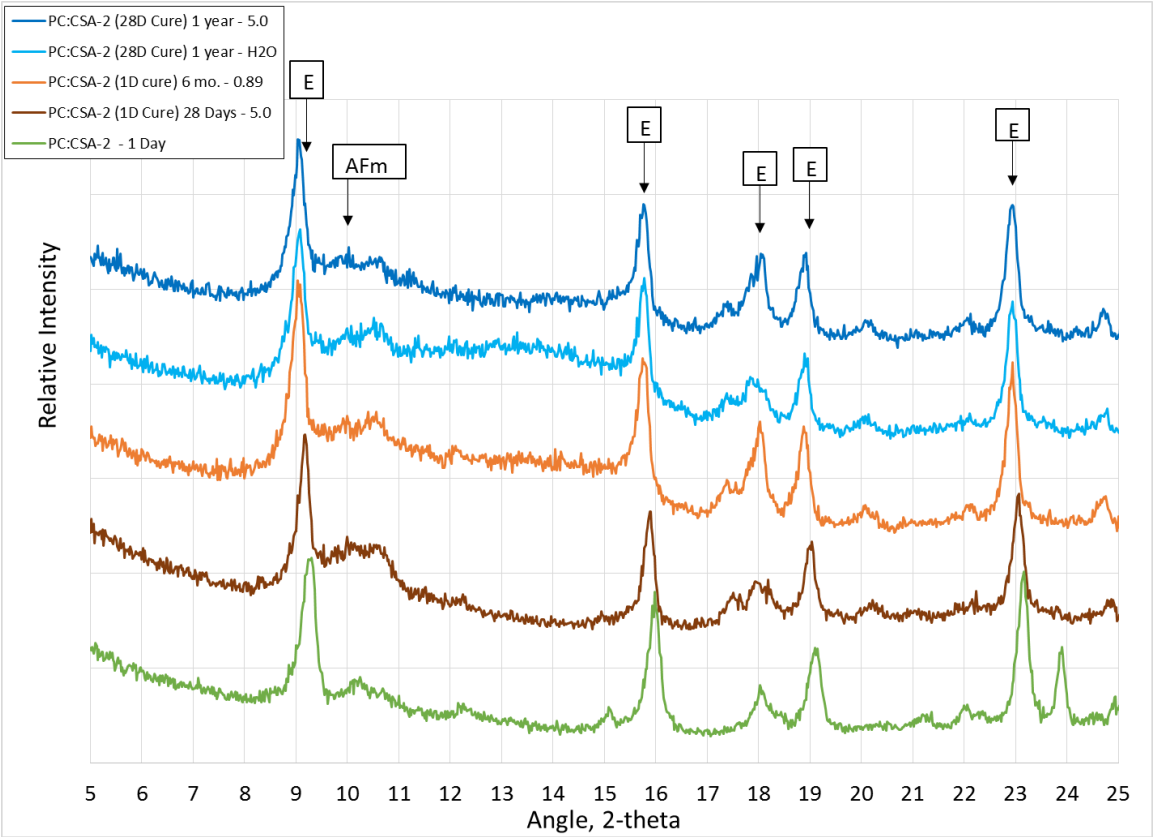

Figure 3.20: XRD scans of PC:CSA-2 pastes subjected to 1 and 28 Day Cure at various Ages and Solution Concentrations where E = ettringite and AFm = monosulfate

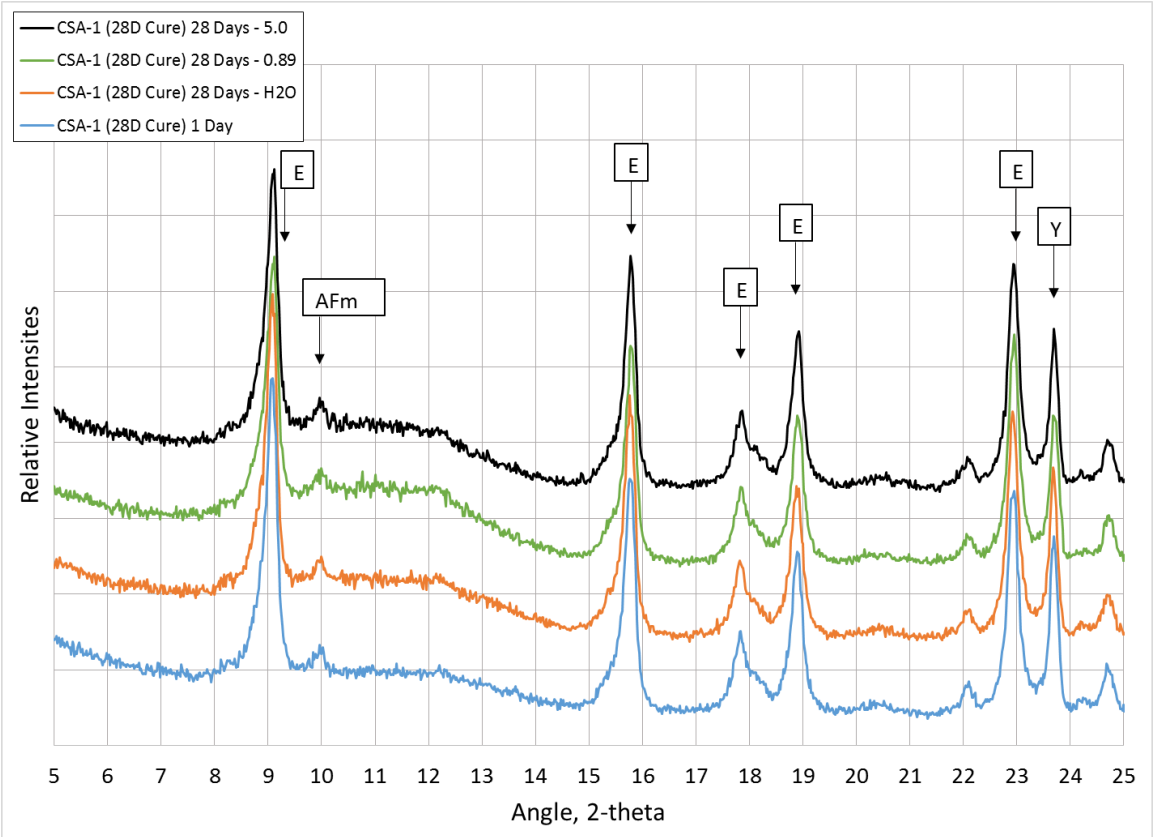

Figure 3.21: XRD Scans of CSA-1 (28 Day Cure) in Several Solution Concentrations where E = ettringite, AFm = monosulfate, and Y = ye'elimite

3.6.2.2 XRD of Mortar Exposed to Sodium Sulfate

In portland cement systems, ettringite is produced in small amounts for the first few hours and formation slowly increases for the first seven days or so. After about a week, the ettringite formed slowly transforms into monosulfate hydrate (AFm). The same transformation of ettringite to monosulfate hydrate occurs in PC:CAC:C$ and PC:CSA systems but at a greater magnitude. As shown in Figure 3.22, the PC:CSA-2 mixture is comprised mainly of ettringite one day after casting. Subsequent immersion in 5.0% Na_2SO_4 led to a slow transformation of ettringite to monosulfate. This monosulfate hydrate is then available to react with the sodium sulfate solution to produce more ettringite as

evidenced by the XRD scan for 252 days highlighted in red. A significant increase in ettringite is noted between 90 and 252 days in the XRD scans which coincides with the high levels of expansion illustrated previously in Figure 3.10.

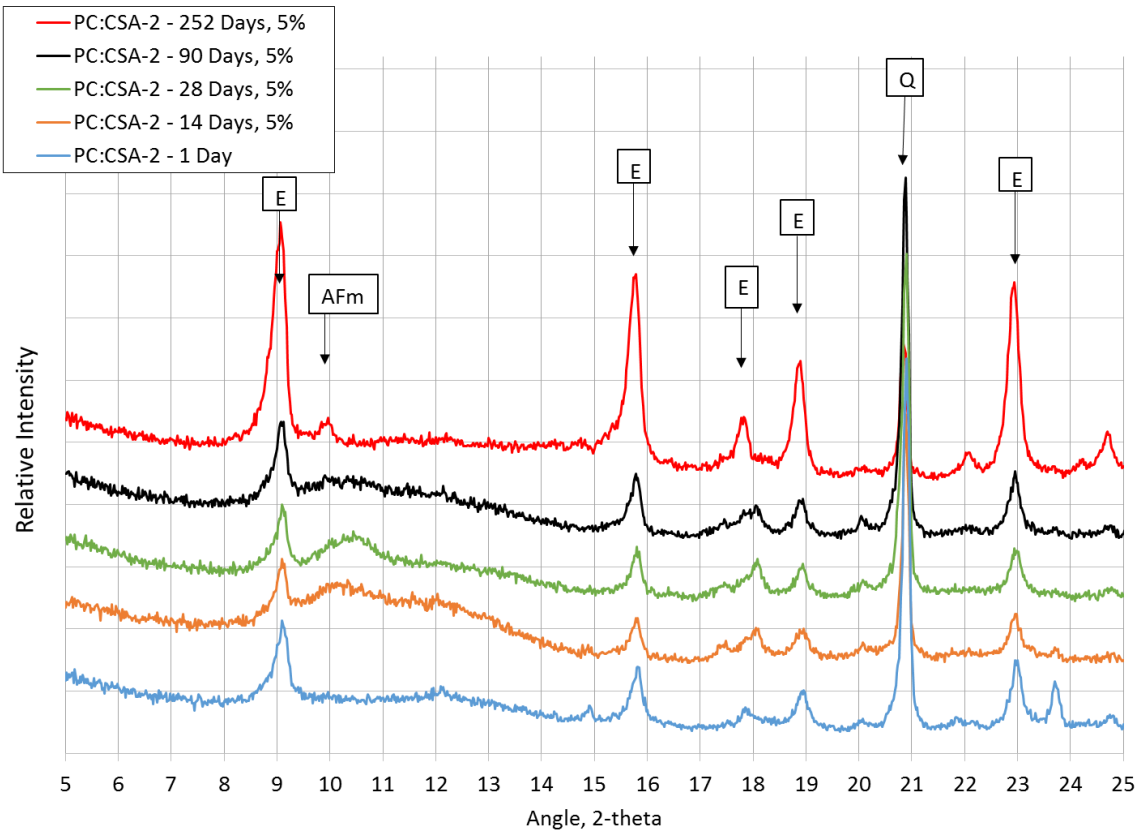

Figure 3.22: XRD Scans of PC:CSA-2 (1 day cure) after exposure to 5.0% Na_2SO_4 where E = ettringite, AFm = monosulfate and Q = quartz

Significantly more rapid expansion and deterioration was noted in the PC:CSA-2 samples that underwent 28 days of curing in the fog room, instead of 1 day, prior to immersion in sulfate solution. XRD sampling was done while the samples were in the fog room and after immersion in sulfate solution to determine the microstructural differences which led to this difference in expansion rates. The 28 day fog room cure allowed for the

transformation of ettringite to monosulfate hydrate to occur without the introduction of external sulfates. As shown in Figure 3.23 this resulted in the production of more monosulfate hydrate than that was seen in the 1 day cure samples. As a result, there was excess monosulfate hydrate available to react with the sodium sulfate solution upon immersion leading to extremely rapid ettringite formation and deterioration.

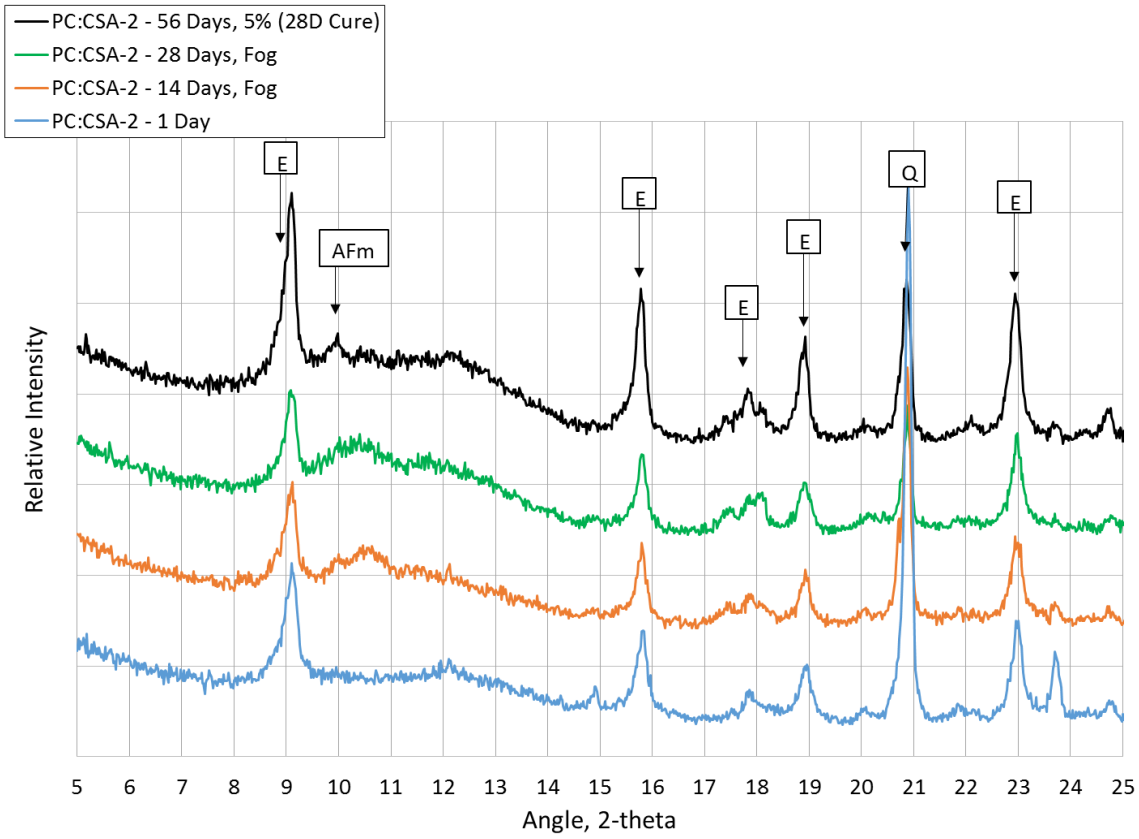

Figure 3.23: XRD Scans of PC:CSA-2 (28 day cure) in fog room and after exposure to 5.0% Na_2SO_4 where E = ettringite, AFm = monosulfate and Q = quartz

Similar trends were noted in the XRD scans for the PC:CAC-2 mixtures. However, there seems to be a slower transformation of ettringite to monosulfate for PC:CAC-2 than PC:CSA-2, resulting in less ettringite formation at later ages as shown in Figure 3.24.

Again, more expansion and deterioration was noted in those PC:CAC-2 samples that underwent a 28 day fog room cure prior to immersion as shown in Figure 3.25. Similar to PC:CSA-2, the extended curing time allowed for the transformation of ettringite to monosulfate prior to immersion. However, it appears that the amount of monosulfate produced was less than that seen in PC:CSA-2, resulting in a slower rate of expansion after immersion in 5.0% sodium sulfate.

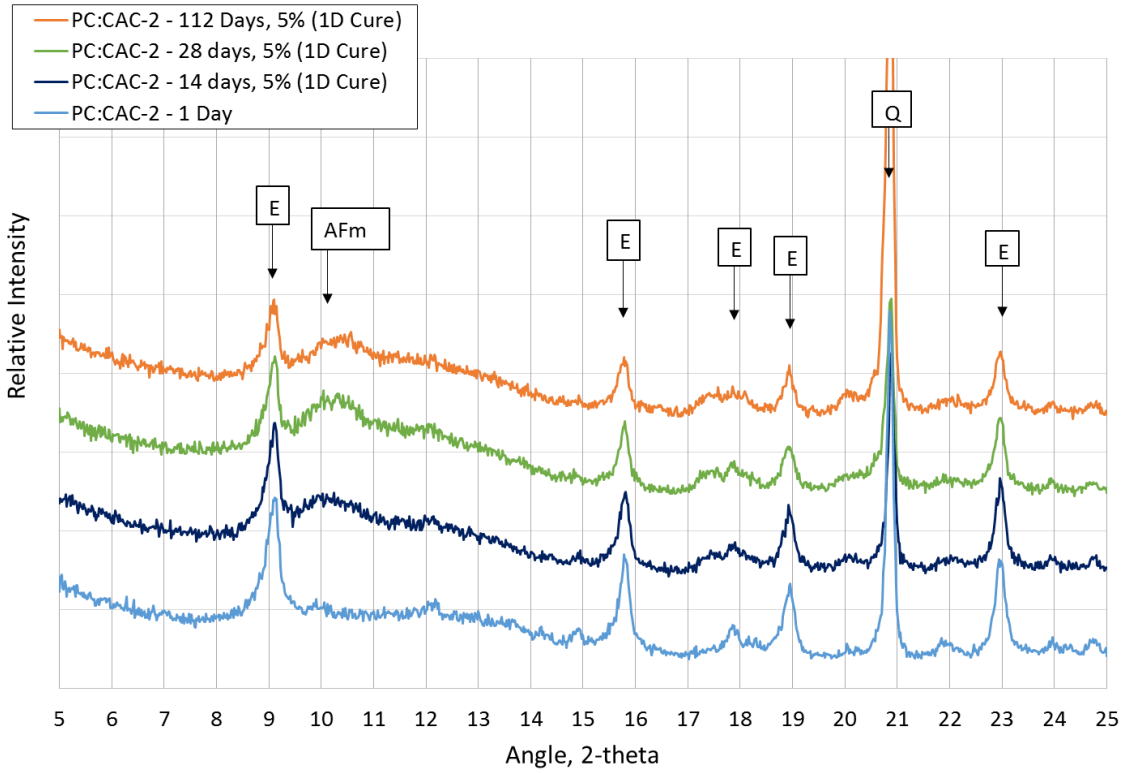

Figure 3.24: XRD Scans of PC:CAC-2 (1 day cure) after exposure to 5.0% Na_2SO_4 where E = ettringite, AFm = monosulfate and Q = quartz

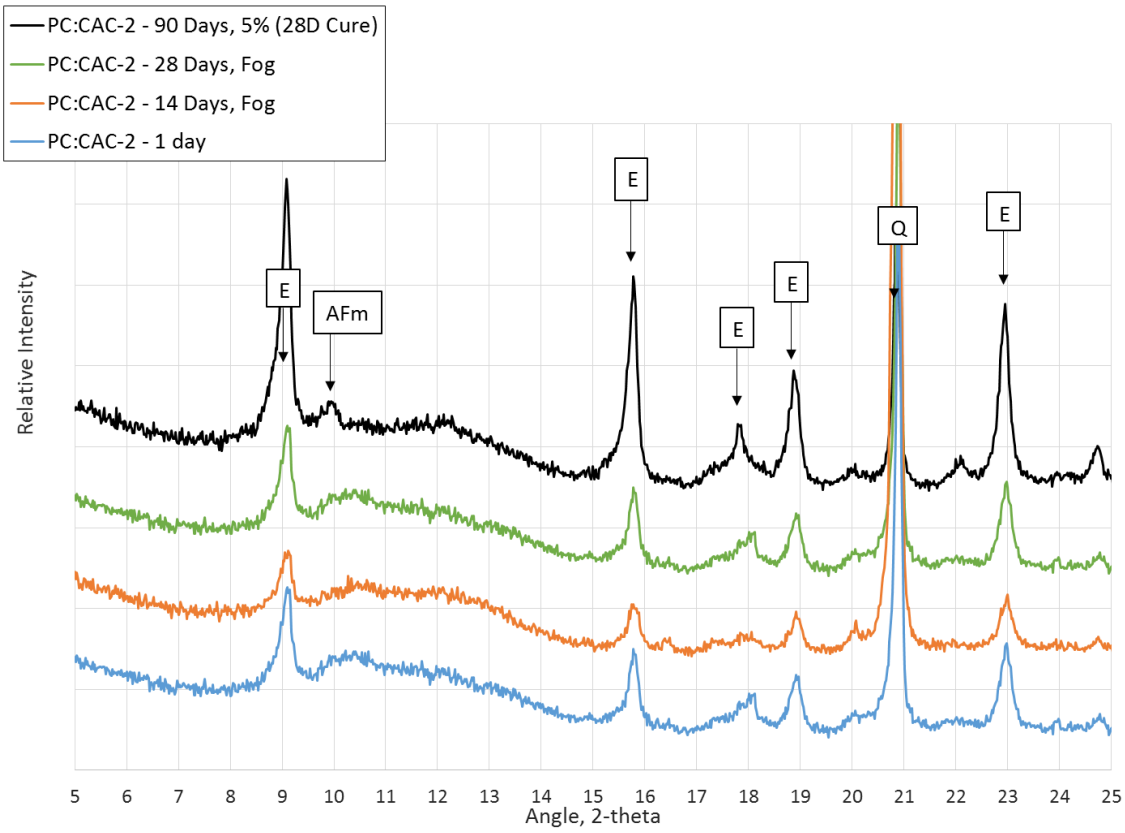

Figure 3.25: XRD Scans of PC:CAC-2 (28 day cure) in fog room and after exposure to 5.0% Na_2SO_4 where E = ettringite, AFm = monosulfate and Q = quartz

After nine months, the converted CAC-1 mortar bars stored in 5.0% Na_2SO_4 were deteriorated and no longer measureable. At this time samples were taken from the both sets of mortar bars for XRD analysis. The XRD scans for these samples are shown in Figure 3.26. The metastable hydrates, C_2AH_8 and CAH_{10}, present in the unconverted sample at 2θ = 8.26 and 12.35 are not present in the converted sample confirming conversion has taken place. There is also evidence of a slight increase in C_3AH_6 and ettringite in the converted sample compared to the unconverted. Despite these minor microstructural differences, there is little evidence to explain the deterioration of the converted sample at such a low level of expansion. Little information exists detailing poor performance of CAC in the

presence of sulfates; however, Dunster and Holton (2001) also reported deterioration of converted CAC concrete at early ages. Unfortunately, they were unable to clearly identify the mechanism of expansion. It is known that conversion of CAC leads to a reduction of strength. It is possible that due to reduced strength the converted mortar bars were unable to withstand the internal pressures from the formation of ettringite.

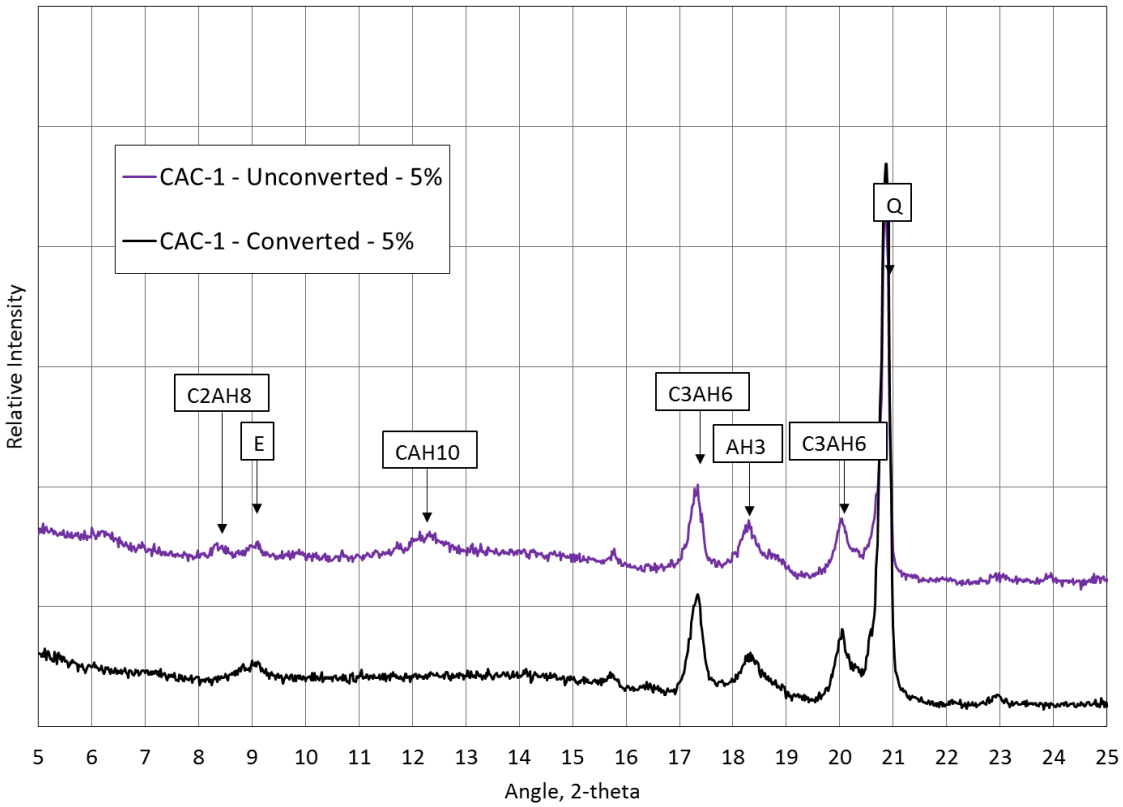

Figure 3.26: XRD scans for converted and unconverted CAC-1 at 9 months

3.7 CONCLUSIONS

The research described in this chapter studied the performance of ettringite-based binders exposed to sulfate environments. Paste, mortar, and concrete specimens were evaluated in varying concentrations of sodium sulfate solution, and the microstructural development of each binder was characterized to help better understand the results. Based on the results of the study the following conclusions can the made.

- The expansion of paste samples in sulfate solution was not found to be a suitable method for characterization of sulfate resistance.
- Ettringite based binders that incorporate portland cement showed little to no sulfate resistance in sodium sulfate solutions of any concentration. This is due to the formation of large amounts of monosulfoaluminate at later ages which is then available to form ettringite in the presence of external sulfates.
- Calcium sulfoaluminate cements with high sulfate to alumina ratios performed exceptionally well in sodium sulfate environments.
- Further research is necessary regarding the sulfate resistance of pure CAC systems. Evidence shows sulfate attack in converted CAC mortar can lead to deterioration at low levels of expansion due to increased porosity and reduced strength.

3.8 REFERENCES

ASTM. (2012). ASTM C 1012 Standard Test Method for Length Change of Hydraulic-Cement Mortars Exposed to Sulfate Solution. West Conshohocken, PA: ASTM International.

ASTM. (2015). ASTM C 114 Standard Test Methods for Chemical Analysis of Hydraulic Cement. West Conshokocken, PA: ASTM International.

ASTM C 150, Standard Specification for Portland Cement. (2015). West Conshokocken, PA: ASTM International.

Bizzozero, J. (2014). Hydration and Dimensional Stability of Calcium Aluminate Based Systems (Dissertation). Lausanne: Ecole Polutechnique Federale de Lausanne.

Capmas, A. & Scrivener, K. (1998). Lea's Chemistry of Cement and Concrete (Fourth Ed. ed.). (P. Hewlett, Ed.) New York: Arnold.

Chabrelie, A. (2010). Mechanisms of Degradation of Concrete by External Sulfate Ions under Laboratroy and FIeld Conditions (Thesis). Lausanne, Switzerland: Ecolo Polytechnique Federale de Lausanne.

Crammond, N. (1990). Long term performance of high alumina cement in sulfate-bearing environments. In M. RJ (Ed.), Calcium Aluminate Cements, (pp. 208-221). London.

Drimalas, T., et al. (2011). Laboratory and Field Evaluations of External Sulfate Attack in Concrete (4089 Report). Austin, TX: Texas Department of Transportation.

Dunster, A. & Holton, I. (2001). A Laboratory Study of the Resistance of CAC Concretes to Chemical Attack by Sulphate and Alkali Carbonate Solutions. Proceedings of the International Conference on Calcium Aluminate Cements (CAC). Edinburgh, Scotland.

Miller, D. and Manson, P. (1933). Technical Bulletin 358. United States Department of Agriculture.

Nuytten, S. (2014). Microstructure and Durability Against Sulfate Attacks of Ettringite Bases Rapid Repair Binders (Thesis). Lausanne, Switzerland: Ecole Polytechnique Federale de Lausanne.

Chapter 4: Delayed Ettringite Formation in Calcium-Aluminate Based Binders for Rapid Repair Applications

4.1 Introduction

The formation of ettringite in portland cement concrete after hardening can lead to high levels of expansion and cracking. This durability issue is known as delayed ettringite formation (DEF) and typically occurs in concrete that has reached a temperature above 70 °C (Taylor, 2001) for a substantial period of time during curing. DEF is also sometimes referred to as internal sulfate attack as the formation of ettringite is attributed to the availability of sulfates within the system rather than external sulfates often found in groundwater or soils.

Under normal conditions ettringite is formed in portland cement systems during the early stages of hydration along with calcium silicate hydrate (C-S-H) and calcium hydroxide (CH) and other hydration products. The formation of this early ettringite does not lead to expansion due to the plastic state of the system at the time. Curing at elevated temperatures can cause the incongruous dissolution of ettringite, releasing alumina and sulfate that gets encapsulated in the rapidly-forming C-S-H. Later, in the concrete's life as it is exposed to moisture and ambient temperatures, ettringite once again becomes the preferred hydration product and will form as the alumina and sulfate migrate from the inner C-S-H and react with monosulfate hydrate. DEF is typically triggered by ASR in field structures as the reduction in pore solution pH caused by ASR help to hasten the reformation of ettringite. This process can take months or years to occur. By this time the system has hardened, and the formation of ettringite can result in high levels of expansion.

The sulfate content of cement has a large influence on the early hydration reactions and hydration products formed. Typically, the allowable sulfate content for portland cements ranges between 3.0 – 4.5%. This amount of sulfate provides adequate working

time for placement of concrete. In fact, calcium sulfate is typically added to portland cement clinker to control setting time. ASTM C150 (ASTM, 2015) places limits on the sulfate content of portland cements as excess sulfate content has been known to lead to excessive expansion.

Portland cement systems rely of the formation of C-S-H and CH for long term strength gain; however, portland cements can be blended with calcium aluminate cement (CAC) and a small amount of calcium sulfate (C$) to create a binder which achieves high early strength through the formation of ettringite. This high early strength can also be achieved by blending portland cement with calcium sulfoaluminate cements (CSA). These types of systems are called ettringite-based binders and can be used in rapid repair applications. These ettringite-based binders rely on the reaction of excess of sulfates to facilitate the formation of large amounts of ettringite to achieve high early strength. It is this excess of sulfates which creates cause for concern regarding the implication of future durability issues such as DEF. DEF in portland cement systems has been studied extensively (Ramlochan, 2003; Drimalas, 2004); however, little information is available on the potential for DEF in ettringite based binders.

The purpose of the study described herein was to evaluate the potential for DEF in several ettringite-based binders. This was achieved through laboratory testing and large scale field exposure of concrete specimens. Expansion and cracking was noted in several tests; therefore, follow up x-ray diffraction analysis was also performed on heat-cured pastes to characterize the microstructural evolution of heat cured ettringite based binders.

4.2 MATERIALS

4.2.1 Binders

Four binders were evaluated under this study: a Type I ordinary portland cement, a calcium aluminate-portland cement blend, a calcium-sulfoaluminate cement, and a calcium sulfoaluminate-portland cement blend. Samples of all binders were sent to a testing laboratory where the chemical compositions of each were determined via ASTM C 114 (ASTM, 2015). Table 4.1 provides the results of an oxide analysis of the binders described below.

Table 4.1 Oxide Composition of Binders

Oxide (%wt)	Binder			
	OPC	**PC:CAC-2**	**CSA-1**	**PC:CSA-2**
SiO2	20.14	15.15	14.46	9.02
Al2O3	5.42	14.98	16.21	23.88
Fe2O3	2.47	2.12	0.94	2.56
CaO	63.63	56.32	50.30	44.03
MgO	1.32	0.97	1.34	0.86
SO3	3.09	8.44	17.09	21.37
Na2O	0.17	0.14	0.21	0.12
K2O	0.95	0.73	0.73	0.35
ZnO	0.01	0.01	0.02	0.01
SrO	0.08	0.07	0.14	0.07
Mn2O3	0.06	0.04	0.03	0.08
P2O5	0.26	0.21	0.09	0.11
TiO2	0.28	0.61	0.58	0.91
Cl	0.00	0.00	0.02	0.00
Cr2O3	0.01	0.02	0.02	0.01
Na2Oe	0.79	0.61	0.69	0.35

4.2.1.1. Portland Cement

A locally-sourced ASTM C 150 Type I portland cement was chosen as the control binder for this study. This cement has been used extensively within this lab as a control binder for various studies; therefore, the long-term performance of this material is well documented and understood making it the clear choice for the control for this study. The total alkali equivalent (Na_2O_{eq}) for this cement is 0.79%.

4.2.1.2 Portland Cement-Calcium Aluminate Cement-Calcium Sulfate Blend

A blended system which combines calcium aluminate cement and calcium sulfate with portland cement was used. This system, designated as PC:CAC-2, is a CAC blend which contained a mixture of calcium-aluminate cement and calcium sulfate (C$) at a ratio of 2.2:1. This blend was then combined with Type I cement at a 30% replacement level (by mass).

4.2.1.3 Calcium Sulfoaluminate Cement and Blended System

A single source of calcium sulfoaluminate cement, refered to as CSA-1, was used in this study and is widely available within the US and abroad. The main phases of this CSA are ye'elimite (C_4A_3\$), belite (ß-C_2S), and calcium sulfate (C$).

The blended CSA system, designated as PC-CSA-2, utilized a combination of CSA in which the main phase was ye'elimite and calcium sulfate. The ratio of these components is not reported by the manufacturer. Similar to PC:CAC-2, PC:CSA-2 was also combined with Type I cement at a 30% replacement level. CSA-1 and CSA-2 are manufactured by different sources and have different in chemical compositions.

4.2.2 Admixtures

For all PC:CAC-2 mixtures powdered citric acid was used as a retarder at a dose of 0.35% by mass of cement in conjunction with a superplasticizer in the form of sulfonated melamine formaldehyde (SMF) at a dose of 0.85% by mass of cement.

All CSA-1 and PC:CSA-2 mixtures utilized a combination of citric acid and SMF to attain the desired workability and three-hour compressive strength of 20 MPa (3,000 psi). The dosage for SMF was 0.1% by mass of the dry materials in the mix for both mixtures, and the citric acid was dosed at 0.2% and 0.35% by mass of cement for CSA-1 and PC:CSA-2, respectively.

4.2.3 Aggregates

The fine aggregate used was a natural, siliceous sand containing quartz (64.0 %) chert (17.1 %), and feldspar (11.5 %) from El Paso, Texas. The coarse aggregate used was a non-reactive dolomitic limestone. The coarse aggregate was sieved using a SIMCO Fractionator sieve machine into three equal parts of the three gradation sizes: 12.5mm (1/2 in), 9.5mm (3/8 in), 4.75mm (1/5 in or No.4) for all mixtures. The absorption capacity of the coarse aggregate was determined to be 3.12%.

4.3 Mixture Proportions and Oxide Analysis

Generally, to achieve good long-term strength and durability with CAC a water/cement ratio below 0.4 and a cement content above 400 kg/m^3 (674 lb/yd^3) are recommended (Capmas & Scrivener, 1998). Therefore, the cement content of the mixtures was 440 kg/m^3 (742 lb/yd^3) for the CAC-1 mixture. The cement content for all other mixtures was 446 kg/m^3 (752 lb/yd^3). This value was chosen over the 440 kg/m^3 used for the CAC-1 mixture to correspond to the colloquial "8 sack" mix design often used by

construction contractors. The water to cement ratio (w/c) was 0.35 by mass for all mixtures. The mixtures labels and binder mixture proportions are listed in Table 4.2.

Table 4.2: Mixture Labels and Proportions

Mixture Label	w/c	Total Binder Content (kg/m^3)	PC Content (kg/m^3)	CAC-2 Content (kg/m^3)	CSA-2 Content (kg/m^3)
OPC	0.35	446.0	446.0		
PC:CAC-2	0.35	446.0	312.2	133.8	
CSA-1	0.35	446.0			
PC:CSA-2	0.35	446.0	312.2		133.8

4.3 EXPERIMENTAL PROCEDURES

Concrete prisms and large scale concrete exposure blocks were cast and heat cured in an attempt to trigger DEF. Follow-up testing was performed on heat cured cement pastes to characterize the microstructural development of ettringite based binders exposed to heat curing. Specimen properties and curing regimens are described in detail in the following sections.

4.3.1 Concrete Prism Testing

A set of three concrete prisms was cast for each binder. The dimensions of the prisms are 7.6 x 7.6 x 29 cm (3 x 3 x 11.25 in). Gauge studs were cast into each end of the prisms to provide an effective length of 25.4 cm (10 in). Fu (1996) developed a heat curing regimen which was intended to mimic the heat curing process utilized by precast concrete manufacturers (Figure 4.1). The "Fu Test" was intended for use with mortar bars. A modified version of the Fu curing cycle was used to heat cure the concrete prisms in this study. However, after the heat curing cycle the Fu method calls for a 24-hour drying period which was omitted from the curing cycle utilized here.

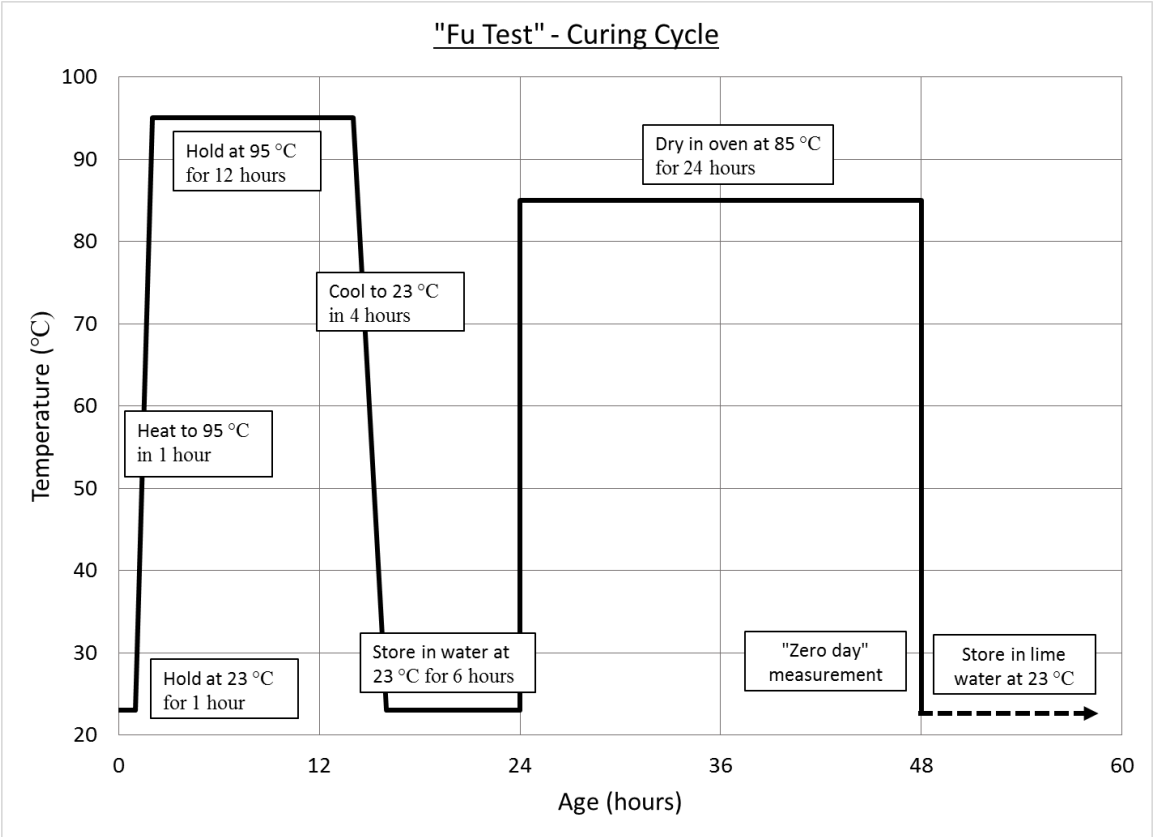

Figure 4.1: Fu Heat Curing Cycle (Folliard et al., 2006)

After casting, the prisms were placed in heat resistant containers, elevated slightly from the bottom with risers. A small amount of water was poured in the bottom of the containers to facilitate a high humidity environment. One hour after casting, the prisms were placed in a 95 °C oven for 12 hours. The oven temperature was then ramped down to ambient temperature over three hours. The prisms were then removed from the oven and within 24 after casting the internal temperature of the prisms returned to ambient temperature. After completion of the heat curing process the prisms were demolded and "zero day" measurements were recorded. The prisms were stored in lime water at 23 °C (73 °F) between measurement intervals. Expansion measurements were taken periodically for over a year. Figure 4.2 illustrates the curing cycle used in this study.

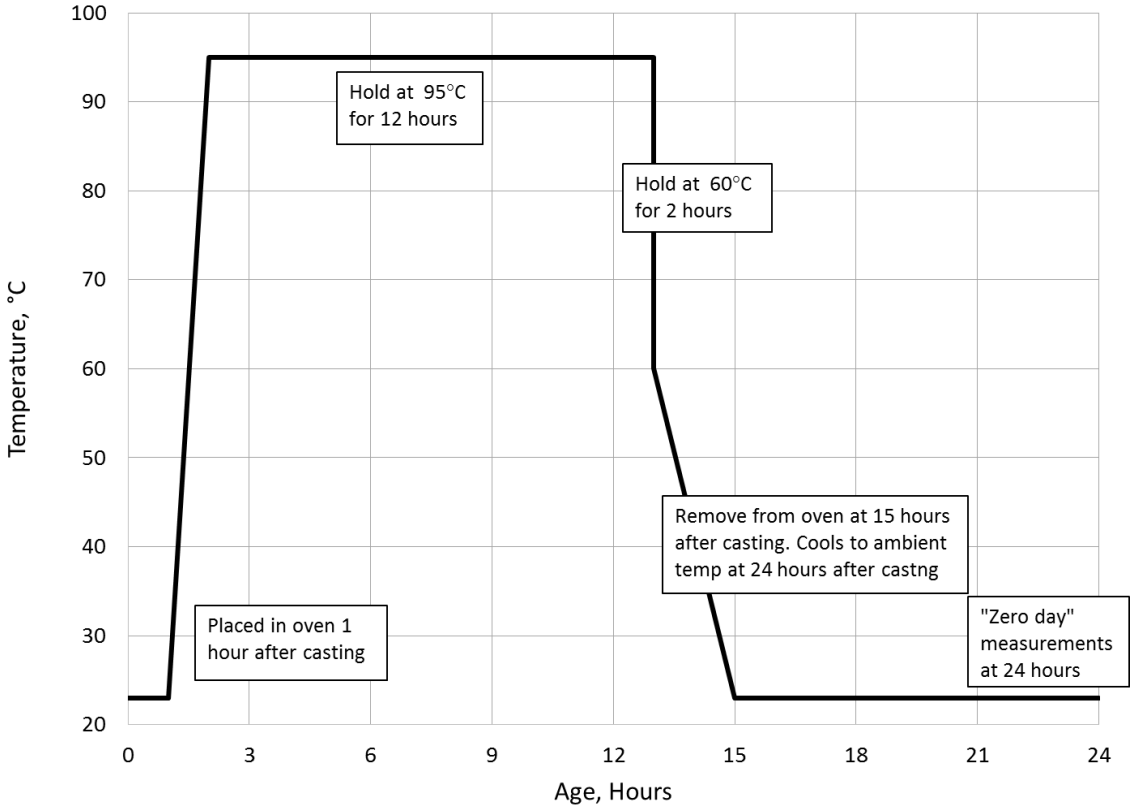

Figure 4.2: Modified Fu Heat Curing Cycle

4.3.2 Exposure Block Testing

4.3.2.1 Exposure Block Casting Procedure

For each concrete mixture, one large-scale exposure block measuring 71 x 38 x 38 cm (28 x 15 x 15 in) was cast. The concrete was cast in the mold in two lifts and consolidation was achieved with a portable vibrating rod after each lift. Each block was instrumented with 12 cast-in-place stainless steel bolts that were later used to measure expansion. Each 9.5 mm (3/8 in) diameter bolt was screwed into wood inserts located within each side of the exposure block mold. After concrete was cast within the mold only the tip of the bolt remained visible on the exterior of the block. Prior to casting, a 1 mm (0.04 in) “demec” hole was machined into the end of each bolt using a drill press with a 1

mm (0.04 in) diameter drill bit. Twelve expansion measurements can be collected using these “demec” points.

4.3.2.2 Curing Procedure

It is known that DEF typically only occurs in concrete that has reached temperatures nominally above 70 ºC (158 ˚F) during curing. In order to initiate DEF in exposure blocks, a high temperature curing process was followed. One exposure block for PC:CAC-2 and another PC:CSA-2 block were cast in a walk-in oven that was held at a constant temperature of 60 ºC (140 ˚F). After finishing, the blocks were covered with damp burlap then wrapped in a thermal blanket. After approximately 18 hours the each block was removed from the oven and allowed to cool at ambient conditions. Each block was instrumented with thermocouple wires at three different depths within the concrete. The time-temperature data obtained from the thermocouple wires were used to confirm that temperatures within the concrete were great enough to instigate DEF; however, after multiple attempts the PC:CAC-2 and PC:CSA-2 blocks did not reach the threshold temperature. Typically, mixing materials are preheated to 60 °C prior to mixing DEF exposure blocks. However, preheating is not possible with rapid setting materials due to lack of sufficient working time. Two PC:CAC-2 blocks and one PC:CSA-2 block were cast before efforts to reach the threshold temperature of 70 °C were aborted. The time-temperature curves for the heat-cured exposure blocks are shown in Figure 4.3. The first PC:CAC-2 block was cured at 38 °C instead of 60 °C due to a malfunction of the oven. This block reached a maximum internal temperature of 54 °C. The other PC:CAC-2 and PC:CSA-2 were cured at the appropriate temperature of 60 °C but only reached 65 °C and 58 °C respectively. After the initial heat cure the exposure blocks were demolded, wrapped in wet burlap and cured at ambient temperatures for 7 days. At this point, initial

measurements were taken and the blocks were placed outside on the outdoor exposure site. Subsequent measurements were taken when outside temperatures are approximately 23 °C (72 °F). Exposure blocks were also cast and subjected to ambient curing for 24 hours for both PC:CAC-2 and PC:CSA-2.

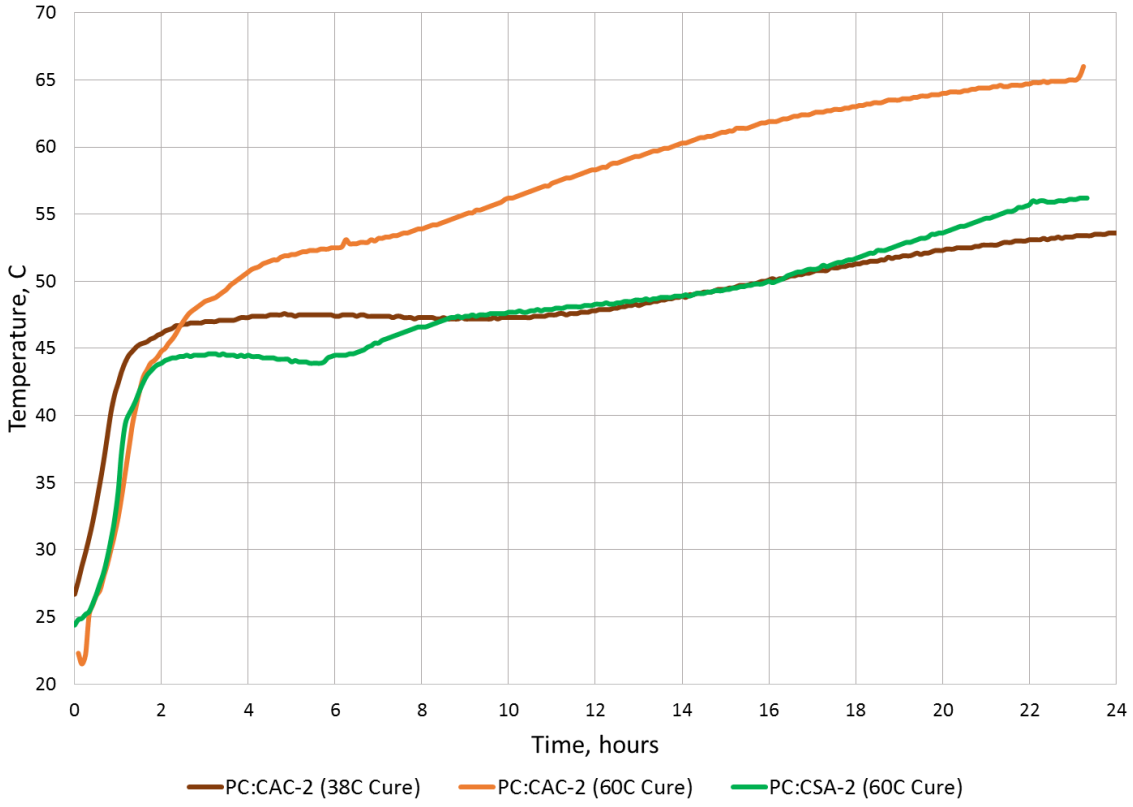

Figure 4.3: Time-Temperature History for Heat Cured Exposure Blocks

4.3.3 Qualitative X-ray Diffraction of Heat Cured Pastes

Qualitative x-ray diffraction analysis was performed on hydrated cement paste to characterize the microstructural development of ettringite based binders subjected to heat curing. XRD sampling and analysis was done on paste samples from the four binders previously evaluated in this study. Pastes samples were mixed according to ASTM C 305 (ASTM, 2013) and then thin samples were cast into 50 mm (2 in.) diameter containers.

Three samples from each binder were cured at 23 °C, 60 °C, and 95 °C. The samples cured at 60 °C were placed in an oven at the specified temperature one hour after casting and remained in the oven for 23 hours. The samples cured at 95 °C were subjected to the modified Fu heat curing method described earlier and illustrated in Figure 4.2. All samples were placed in lime water after curing until a specified test date. XRD analysis was conducted on samples from each curing regime at 1, 7 and 28 days.

The solvent exchange method was used to stop hydration of each sample after removal from lime water. The following steps outline the solvent exchange method used:

1. Remove chunk of paste or mortar from bar, approximately 50 mm (2 in)
2. Cut multiple 3 - 4 mm (0.12 – 0.16 in) slices from chunk
3. Place slices in isopropanol (200-250 mL) for 5 - 7 days
4. Remove from isopropanol, dry in vacuum desiccator 2 days

After completion of the drying cycle, the samples were crushed and passed through a No. 325 sieve and returned to the desiccator until testing. Analysis was conducted with a Siemens D500 diffractometer with a DacoMP controller. The parameters for each scan were: 5-70° 2θ, with a 0.02° 2θ step size and 4 second dwell.

4.4 Results and Discussion

4.4.1 Expansion of Concrete Prisms

Figure 4.4 shows the expansion results for the heat cured concrete prisms. Expansion result for non-heat cured prisms for PC:CAC-2 and PC:CSA-2 prisms are also included for comparison. There are no standard test methods for evaluating DEF in concrete; therefore, the expansion limit from ASTM C 1293, *Standard Test Method of*

Determination of Length Change of Concrete due to Alkali Silica Reaction, was included for relative comparison. This value is relevant due to field data has concluded that 0.04% expansion is the point at which concrete begins to crack (Folliard et al., 2006). At 14 days the expansion for PC:CSA-2 exceeded the typical cracking point of 0.04% and continued to expand to 0.20% at nine months. PC:CSA-2 prisms which were not heat cured also expanded significantly and surpassed the typical cracking point after two months. However, this expansion plateaued soon thereafter and remained under 0.06% after one year. The expansion of the heat cured specimens suggests a high potential for DEF in this system; however, the results of the non-heat cured prisms also suggest that this binder has a greater potential for expansion in water than typical OPC mixtures. The PC:CAC-2 expanded at a much slower rate, but also surpassed the ASTM C 1293 expansion level within nine months. The expansion results for the heat cured specimens for the PC:CAC-2 mixture tracked very closely with those seen in the non-heat cured specimens. Further analysis is necessary to verify that the expansion recorded is due to DEF. After nine months, both the OPC and CSA-1 mixtures were below the level of expansion at which cracking is typically observed. Typically, materials that favor expansion due to DEF experience an S-shaped expansion curve (Drimalas, 2004). Little to no expansion is seen at first followed by a significant increase in expansion and then a plateau. The length of the initial dormant period varies depending on the chemical composition of the binder. Previous research has shown that the OPC binder used in this study has the potential to expand significantly due to DEF; therefore it is likely the onset of expansion for this binder will occur at a later date. The same can also be said for the CSA-1 mixture. Although the expansion at nine months is still below the ASTM C 1293 limit, it may just be too early to determine if expansion due to DEF is possible.

X-ray diffraction analysis of heat cured pastes was conducted in order to gain more insight into the microstructural changes these binders experience due to heat curing. Likely this information will shed light on the expansion results seen here. The results of the XRD analysis are discussed in detail in subsequent sections.

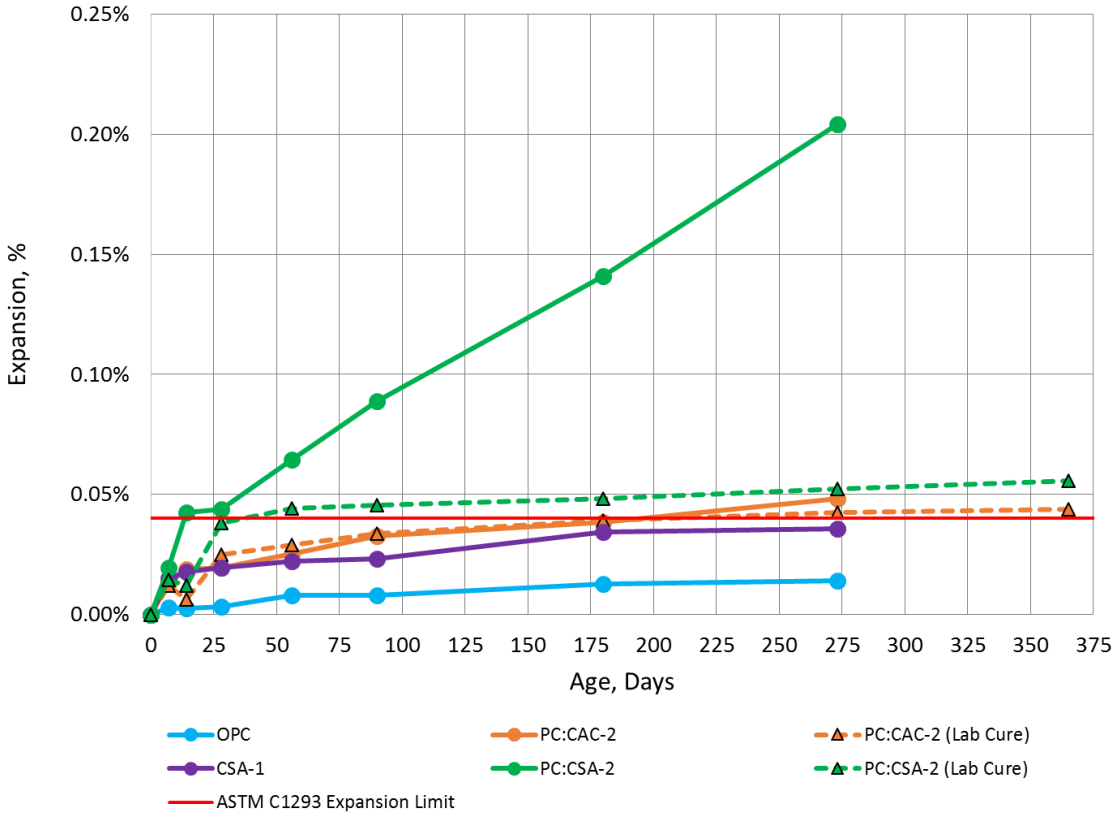

Figure 4.4: Expansion of Heat Cured Concrete Prisms

4.4.2 Expansion of Exposure Blocks

The expansion results for the heat-cured exposure blocks proved to be extremely interesting. The original assumption was that little to no expansion would be seen in the exposure blocks since the internal temperature of the blocks did not meet the threshold temperature of 70 °C. However, expansion and micro-cracking was seen in both PC:CAC-

2 blocks and the PC:CSA-2 block around 18-20 months as illustrated in Figure 4.5. The blocks that underwent ambient curing show no signs of cracking and have much lower expansion levels than their heat-cured counterparts after 2.5 years.

The blending of CAC-2 and CSA-2 with OPC is likely the cause for this expansion. Both CAC-2 and CSA-2 have high SO_3 contents as noted in Table 4.2. The 70 °C threshold typically applies to portland cements with SO_3 contents within the allowable range specified in ASTM C 150. The blends evaluated here rely on high SO_3 contents for higher amounts of ettringite formation. It may be that the threshold temperature would then decrease in the presence of excess SO_3.

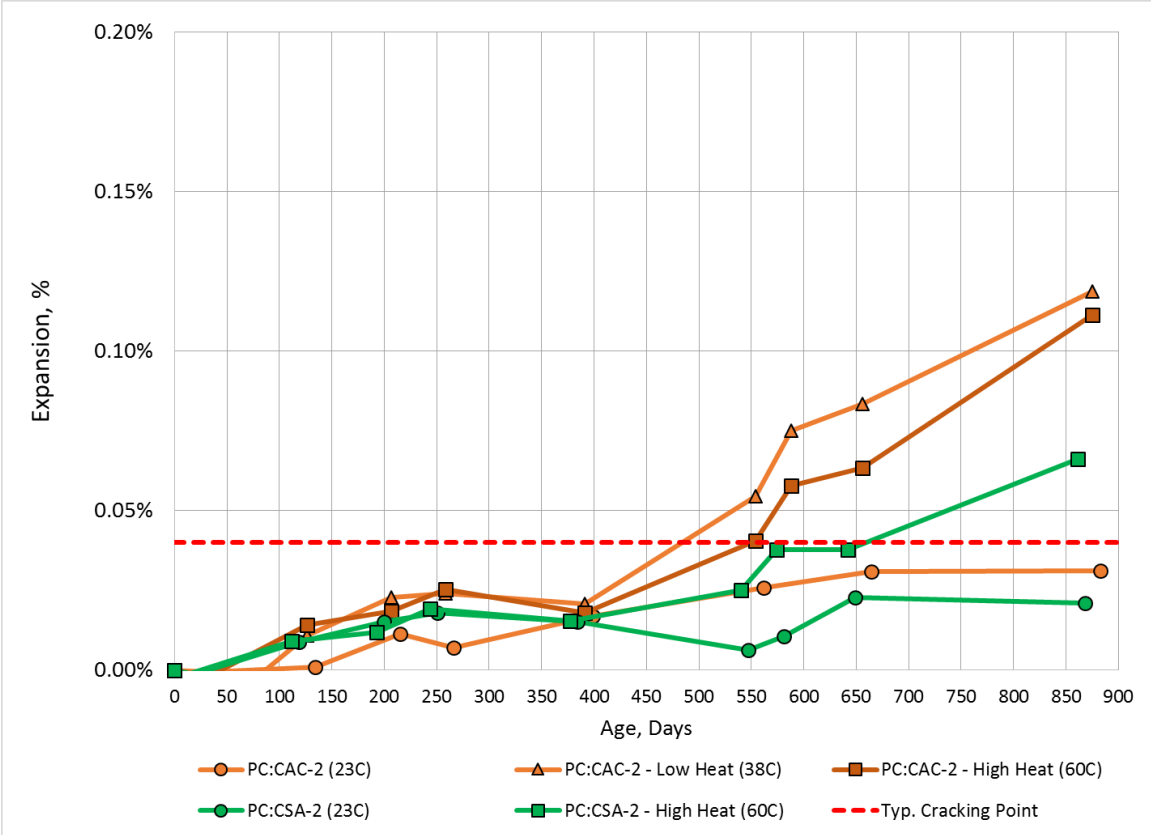

Figure 4.5: Expansion of Heat Cured Concrete Exposure Blocks

4.4.3 Qualitative X-ray Diffraction Analysis of Heat Cured Paste

High levels of expansion were seen in heat cured concrete prisms for PC:CSA-2 and in outdoor field exposure blocks for PC:CSA-2 and PC:CAC-2. The expansion of the exposure blocks was unexpected as it was assumed that little to no expansion would occur since internal temperatures remained below 70 °C during curing. Paste samples were prepared and heat cured at 60 °C and 95 °C and XRD analysis was conducted to characterize the microstructural changes of these binders before and after heat curing.

Figure 4.6 shows XRD scans at 1 and 28 days for OPC cured at 23, 60, and 95 °C. The 23 °C scan at 1 day shows typical ettringite and portlandite formation at 2θ = 9.09° and 2θ = 18.09°, respectively. With increased temperature there is a loss of ettringite formation and increase in portlandite formation. At 28 days there is already an increase in ettringite formation in the 95 °C scan verifying the potential for delayed ettringite formation in the OPC mixture.

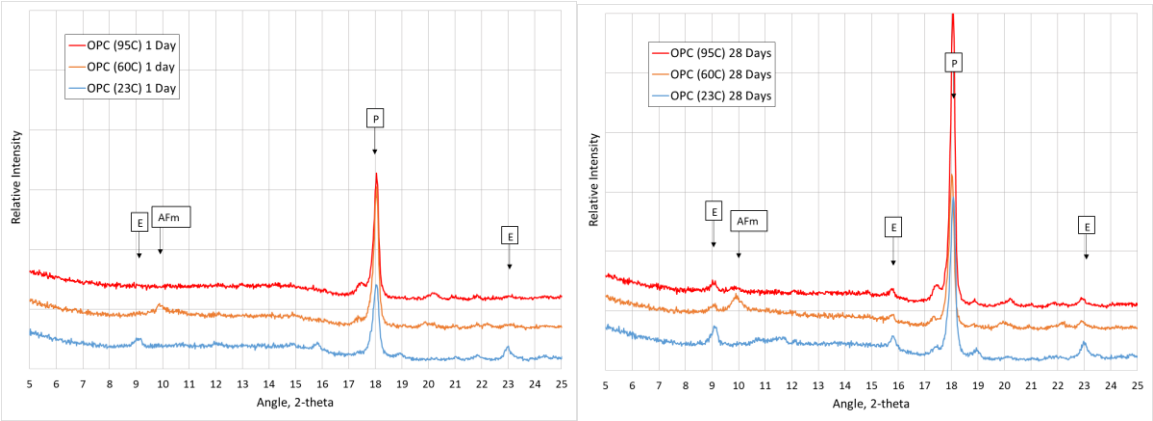

Figure 4.6: XRD Scans at 1 and 28 days for OPC cured at 23 °C, 60 °C, and 95 °C where E = ettringite and AFm = monosulfate and P = portlandite

Figures 4.7 through 4.9 show XRD scans for the ettringite based binders. These scans highlight the magnitude of ettringite formed in these binders and the implication of that to DEF. Figure 4.7 shows XRD scans at 1 and 28 days for PC:CAC-2 cured at 23, 60,

and 95 °C. The 23 °C scan at 1 day shows ettringite at the primary peak at 2θ = 9.09 and at several secondary peaks at 2θ = 15.78, 17.78, and 22.8. By 28 days there is a slight transformation of ettringite to monosulfate, as expected. With increased temperature there is a significant shift from ettringite formation to monosulfate formation at 1 day. By 28 days there is a slight transformation of monosulfate back to ettringite in the 60 °C and 95 °C cured pastes suggesting the potential for DEF.

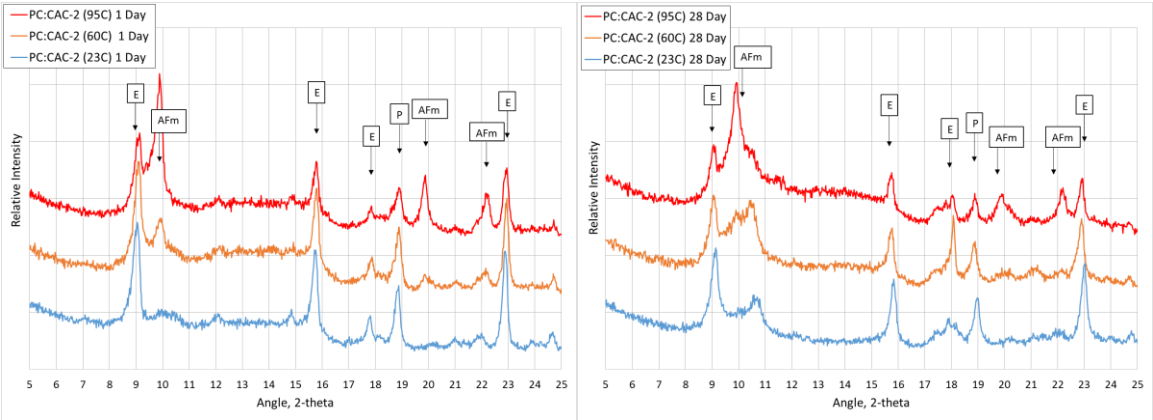

Figure 4.7: XRD Scans at 1 and 28 days for PC:CAC-2 cured at 23 °C, 60 °C, and 95 °C where E = ettringite and AFm = monosulfate and P = portlandite

The influence of heat curing is much more pronounced in PC:CSA-2 as shown in Figure 4.8. Similar to PC:CAC-2 the 23 °C scan at 1 day for PC:CSA-2 shows ettringite at the primary peak at 2θ = 9.09 and at several secondary peaks at 2θ = 15.78, 17.78, and 22.8. Small amounts of portlandite are also noted at 2θ = 18.78. However, with increased temperature, especially at 95 °C, there is more of a significant shift to monosulfate formation instead of ettringite formation. After 28 days, there starts to be an increase in the ettringite formation in the paste cured at 95 °C verifying the potential for delayed ettringite formation in PC:CSA-2. The transformation of ettringite to monosulfate and back again is

more subtle in the 60 °C specimens, but the amount of monosulfate present after heat curing provides the potential for later expansion in the presence of sufficient moisture.

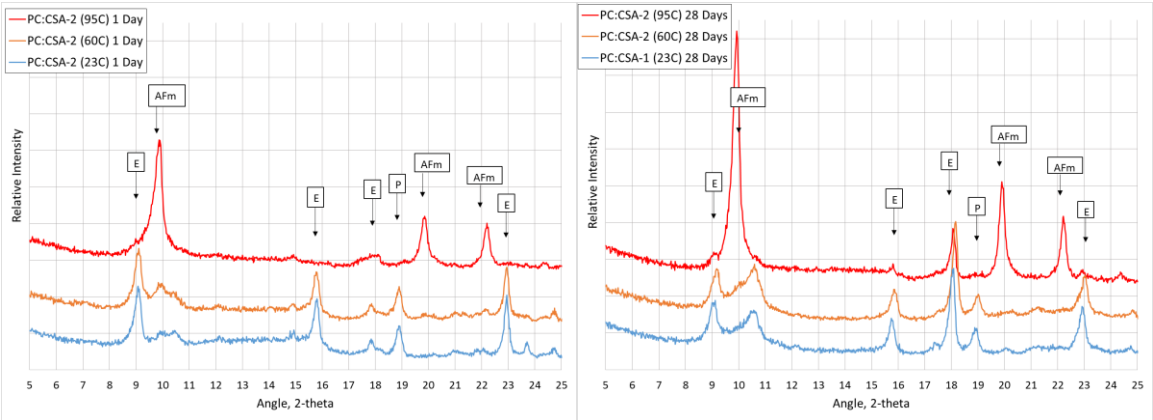

Figure 4.8: XRD Scans at 1 and 28 days for PC:CSA-2 cured at 23 °C, 60 °C, and 95 °C where E = ettringite and AFm = monosulfate and P = portlandite

Contrary to previous results, the XRD scans for CSA-1 remain relatively similar regardless of temperature during curing or time after casting as shown in Figure 4.9. The main hydration products formed in CSA-1 are mostly ettringite along minor amounts of monosulfate. Due to the low water/cement ratio used some unhydrated ye'elimite is also present. The CSA-1 system has an excess of SO_3 as noted in Table 4.1 which results in the presence of ettringite instead of monosulfate after heat treatment. Also, CSA-1 does not incorporate portland cement and therefore does not rely of C-S-H formation for strength gain. Without the development of C-S-H or the decomposition of ettringite there is no potential for DEF in CSA-1.

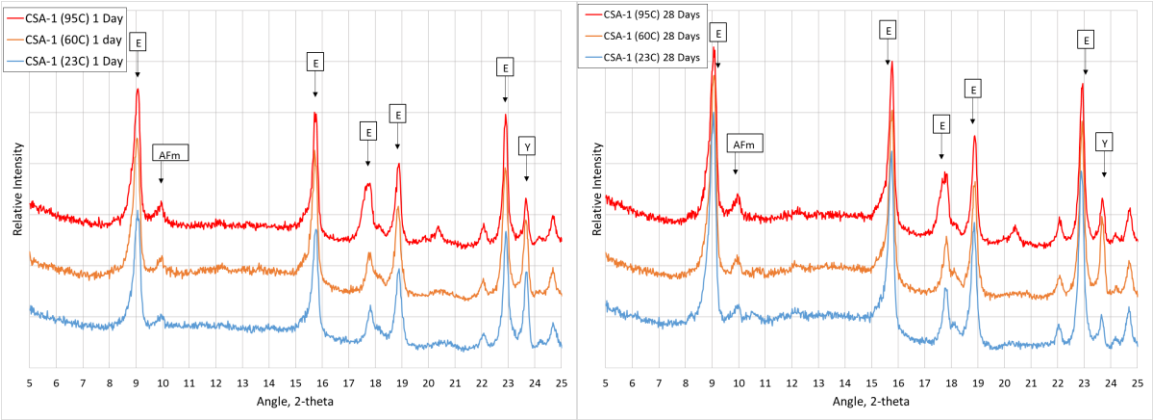

Figure 4.9: XRD Scans at 1 and 28 days for CSA-1 cured at 23 °C, 60 °C, and 95 °C where E = ettringite and AFm = monosulfate and Y = ye'elimite

4.5 CONCLUSIONS

The aim of this study was to evaluate the potential for delayed ettringite formation in "ettringite-based" binders. Such binders are typically composed of blends which incorporate portland cement and calcium aluminate cement with calcium sulfate or portland cement and calcium sulfoaluminate cement. Pure calcium sulfoaluminate cements are also considered ettringite based binders. Unlike portland cement which relies on the formation of C-S-H and CH for long term strength gain, ettringite based binders are able to achieve high early strengths of around 20 MPa (3,000 psi) within three hours through the formation of ettringite.

The results of this study show that there is a significant potential for DEF in ettringite-based binders that incorporate portland cement and are exposed to high early temperatures. These blends create a perfect storm for DEF in that 70% of the mixture is portland cement which contributes to the formation of C-S-H that, when heat cured, is able to encapsulate the large amounts of sulfates available resulting in the formation of monosulfate instead of ettringite. In the presence of moisture, the encapsulated sulfates are released and available to react with the massive amounts of available monosulfate to

produce ettringite and cause expansion. This transformation of ettringite to monosulfate and back is not seen in CSA systems which do not incorporate portland cement. Such systems are so rich in sulfate that the formation of monosulfate is prevented even when subjected to curing at high heat.

4.6 REFERENCES

ASTM. (2005). *ASTM C 114 Standard Test Methods for Chemical Analysis of Hydraulic Cement.* West Conshokocken, PA: ASTM International.

ASTM. (2013). *ASTM C 305 Standard Practice for Mechanical Mixing of Hydraulic Cement Pastes and Mortars of Plastic Consistency.* West Conshohocken, PA: ASTM International.

ASTM. (2015). *ASTM C 150, Standard Specification for Portland Cement.* West Conshokocken, PA: ASTM International.

Capmas, A., and Scrivener, K. (1998). *Lea's Chemistry of Cement and Concrete* (Fourth Ed. ed.). (P. Hewlett, Ed.) New York: Arnold.

Drimalas, T. (2004). *Laboratory Testing and Investigations of Delayed Ettringite Formation (Thesis).* The University of Texas at Austin, Civil Engineering. Austin, TX: The University of Texas at Austin.

Folliard, K., et al. (2006). *Preventing ASR/DEF in New Concrete: Final Report.* Report No. FHWA/TX-06/0-4085-5.

Folliard, K. et. al (2006). *Interim Recommendations for the Use of Lithium to Mitigate or Prevent Alkali-Silica Reaction.* McLean, VA: FHWA.

Fu, Y. (1996). *Delayed ettringite formation in portland cement products.* Ottawa, Ontario: Dissertation, University of Ottawa.

Ramlochan. (2003). *The Effect of Pozzolans and Slag on the Expansion of Mortars and Concrete Cured at Elevated Temperature (Dissertation).* Toronto, Ontario: University of Toronto.

Taylor, H. e. (2001). Delayed ettringite formation. *Cement and Concrete Research, 31*, 683-693.

Chapter 5: Carbonation Resistance of Calcium-Aluminate Based Binders

5.1 INTRODUCTION

Carbonation of concrete occurs when carbon dioxide in the air reacts with hydration products within concrete to produce calcium carbonate and other products. This process itself is not typically harmful to concrete; however, it does result in a drop in the pH of the pore solution of the concrete. Most portland cement (PC) concretes are highly alkaline and have an initial pH between 13.2 and 13.8, which creates a passive, ferrous oxide layer on reinforcing streel. A drop in pH below 11 can lead to corrosion of embedded reinforcing streel which is why carbonation resistance is critical for concrete systems with embedded steel in corrosion prone environments.

Portland cement concretes tend to be highly resistant to carbonation due to the presence of large amounts of portlandite. Research has shown that the use of supplementary cementing materials reduces the carbonation resistance of PC mixtures due to a reduction in portlandite content (Aguayo, 2015). Likewise, ternary ettringite based binders composed of portland cement, calcium aluminate cement (CAC) and calcium sulfate (C$) are also known to carbonate more quickly than pure PC mixtures (Lamberet, 2005; Moffatt, 2016). The carbonation of ettringite based binders is especially troubling as they are often used in repair applications where corrosion is already an issue. Most laboratory studies aimed at evaluating carbonation resistance employ accelerated methods to predict carbonation depths; however, as with most accelerated methods, there exists a large disconnect between the results of the accelerated methods and natural carbonation seen in the field (Thomas, 2000).

With the increased use of ettringite based binders for repair applications it is of the utmost importance to fully, and accurately evaluate the carbonation resistance of these

materials to ensure the quality and long term performance of repairs. The aim of this study was to evaluate the carbonation resistance of several ettringite based binders and other commonly used repair materials exposed to a natural carbonation environment.

5.2 MATERIALS

5.2.1 Binders

Six different binders were selected for evaluation under this study. A Type I portland cement was selected as the control binder. Other binders selected include, a calcium-aluminate cement, a calcium-sulfoaluminate cement, commonly used in commercial applications, blended systems which incorporate CAC or CSA with Type I cement, and a pre-bagged chemically activated concrete mixture.

5.2.1.1. Portland Cement

A locally sourced ASTM C 150 Type I portland cement was chosen as the control binder for this study. This cement has been used extensively within this lab as a control binder for various studies; therefore, the long-term performance of this material is well documented and understood making it the clear choice for the control for this study.

5.2.1.2 Calcium Aluminate Cement and Blended System

A single source of calcium aluminate cement was used in this study and is referred to herein as CAC-1 and represents a binder containing 100 percent CAC. A blended CAC binder, designated as PC:CAC-2, was also evaluated and blend contained a mixture of calcium-aluminate cement and calcium sulfate at a ratio of 2.2:1. This blend was then combined with Type I cement at a 30% replacement level (by total mass).

.

5.2.1.3 Calcium Sulfoaluminate Cement and Blended System

A single source of calcium sulfoaluminate cement, refered to as CSA-1, was used in this study and is widely available within the US and abroad. The main phases of this CSA are ye'elimite ($C_4A_3\$$), belite (ß-C_2S), and calcium sulfate (C$).

The blended CSA system, designated as PC-CSA-2, utilized a combination of CSA in which the main phase was ye'elimite and calcium sulfate. The ratio of these components is unknown for this binder. Similar to PC:CAC-2, PC:CSA-2 was also combined with Type I cement at a 30% replacement level. CSA-1 and CSA-2 are manufactured by different sources and vary in chemical composition.

5.2.1.4 Chemically Activated Fly Ash Mixture

A commercially available pre-packaged concrete mixture, designated AFA, was also evaluated in this study. The binder in this mixture is a chemically activated fly ash blend which contains both Class C and Class F fly ashes. The hydration of this product is controlled by a specific dose of an unreported chemical activator. Coarse aggregate with a maximum size of 9.5 mm (3/8 in) and fine graded sand are also included in each unit of the product. The manufacturer's recommendations prescribe the amount of water necessary to utilize this product.

5.2.2 Admixtures

A superplasticizer and a lithium-based accelerator were used for all CAC-1 mixtures. The superplasticizer and accelerator were dosed at 0.50% and 1.00% by mass of cement, respectively.

For all PC:CAC-2 mixtures powdered citric acid was used as a retarder at a dose of 0.35% by mass of cement in conjunction with a superplasticizer in the form of sulfonated melamine formaldehyde (SMF) at a dose of 0.85% by mass of cement.

All CSA-1 and PC:CSA-2 mixtures utilized a combination of citric acid and SMF to attain the desired workability and three-hour compressive strength of 20 MPa (3,000 psi). The dosage for SMF was 0.1% by mass of the dry materials in the mix for both mixtures, and the citric acid was dosed at 0.2% and 0.35% by mass of cement for CSA-1 and PC:CSA-2, respectively.

5.2.3 Aggregates

The fine aggregate used was a natural, siliceous sand containing quartz (64.0 %) chert (17.1 %), and feldspar (11.5 %) from El Paso, Texas. The coarse aggregate used was a non-reactive dolomitic limestone. The coarse aggregate was sieved using a SIMCO Fractionator sieve machine into three equal parts of the three gradation sizes: 12.5mm (1/2 in), 9.5mm (3/8 in), 4.75mm (1/5 in or No.4) for all mixtures. The absorption capacity of the coarse aggregate was determined to be 3.12%.

5.2.4 Mixture Proportions

Generally, to achieve good long-term strength and durability with CAC a water/cement ratio below 0.4 and a cement content above 400 kg/m^3 (674 lb/yd^3) are recommended (Capmas & Scrivener, 1998). Therefore, the cement content of the mixtures was 440 kg/m^3 (742 lb/yd^3) for the CAC-1 mixture. The cement content for all other mixtures was 446 kg/m^3 (752 lb/yd^3). This value was chosen over the 440 kg/m^3 used for the CAC-1 mixture to correspond to the colloquial "8 sack" mix design often used by construction contractors. The water to cement ratio (w/c) was 0.35 by mass for all mixtures except, of course, the pre-packaged AFA product. The mixtures labels and binder mixture proportions are listed in Table 5.1.

Table 5.1: Mixture Labels and Proportions

Mixture Label	w/c	Total Binder Content (kg/m^3)	PC Content (kg/m^3)	CAC-2 Content (kg/m^3)	CSA-2 Content (kg/m^3)
OPC	0.35	446.0	446.0		
CAC-1	0.35	440.0			
PC:CAC-2	0.35	446.0	312.2	133.8	
CSA-1	0.35	446.0			
PC:CSA-2	0.35	446.0	312.2		133.8
AFA	~0.26	n/a			

5.3 EXPERIMENTAL PROCEDURES

5.3.1 Mixing and Casting

One set of two concrete prisms were cast for each binder. The prisms measure 102 x 102 x 355 mm (4 x 4 x 14 in). After casting, each set was cured in a temperature controlled fog room at 23 °C for 24 hours. The concrete prisms were demolded at 24 hours and placed within the exposure site.

5.3.2 Carbonation Exposure Site

After the specimens were demolded, they were placed on the outdoor carbonation exposure site located at the Concrete Durability Center in Austin, Texas. The outdoor exposure carbonation site provides two exposure environments, sheltered and unsheltered. Stevenson screens, illustrated in Figure 5.1, are wooden structures that shelter the concrete specimens from precipitation and UV exposure while allowing exposure to natural levels of carbon dioxide present in the air. One specimen from each set was placed within the Stevenson screen and the other was placed outdoor in an unsheltered environment. Carbon dioxide levels and relative humidity within the Stevenson screens were recorded daily.

These values fluctuate significantly season to season. The monthly averages for carbon dioxide concentration fluctuated between 385 ppm to 499 ppm during the two year monitoring period (2013-2015). Higher concentrations were noted in the summer months. Likewise, monthly relative humidity and temperature averages fluctuated seasonally between 36-55% RH and 7-30 °C (44-86° F), respectively. Research has shown the optimal relative humidity to facilitate carbonation ranges from 52-75% (Thomas, 2000) (Roy, 1998). This suggests carbonation depths observed in Austin, TX could be less than those seen in other, slightly more humid environments for the same binders.

Figure 5.1: (a) exterior of Stevenson screen; (b) interior of Stevenson screen

5.3.3 Depth of Carbonation

The specimens were stored outside for at least two years. During that time, depth of carbonation measurements were taken at 6 months, 1 year, 18 months, and 2 years. The protocol for measuring depth of carbonation was adapted from the European standard

CEN/TS 12390-10 (2008) *Determination of The Relative Carbonation Resistance of Concrete* (CEN/TS, 2008). At each measurement interval a 50 mm (2 in) thick portion of each specimen was removed using a block cutter. Once the 50 mm (2 in) slice was removed from the specimen, a 5% phenolphthalein solution was sprayed on the (2 in.) freshly broken surface. The use of a block cutter, instead of a saw, was necessary to provide a freshly broken surface capable of fully absorbing the phenolphthalein. The specimen was allowed to sit for 30 minutes prior to recording measurements.

The phenolphthalein solution was used as a pH indicator. Once sprayed on the surface of the concrete specimen those areas with a pH greater than 9.2 turns pink, whereas, areas with a pH lower than 9.2 remain colorless. The depassivation of reinforcing steel occurs when the pH of concrete falls below 11; therefore, it is assumed that the colorless region of the specimen is carbonated to a level which can facilitate corrosion. Five measurements were taken along each side of the specimen. These 20 data points were averaged together to provide an average depth of carbonation for each specimen.

5.4 Results and Discussion

The carbonation depths at 6 months for the specimens exposed to both unsheltered and sheltered natural carbonation are shown in Figure 5.2. As expected the depth of carbonation is greater for all sheltered specimens compared to those in the unsheltered environment. The rate of carbonation is slower for concretes in high humidity environments due to saturation of the pore network (Lamberet, 2005) (Thomas, 2000); therefore, the diffusion of CO_2 is greater in the specimens stored within the Stevenson screen. The OPC mixture showed the least amount of carbonation due to the high amount of portlandite present in the system. At just 6 months the carbonation depth for PC:CSA-2 in the sheltered environment was close to 8 mm (0.31 in) which is more than twice the

carbonation depth for the same binder in the unsheltered environment. This highlights the important influence of exposure conditions on diffusion of CO_2 into concrete.

In CAC systems. the calcium aluminate phase, C_3AH_6, reacts with CO_2 to form calcite and alumina gel as shown in Equation 5.1. Studies have shown that the rate of carbonation for CAC concretes is similar to portland cement concretes of similar quality; however, the initial pH of CAC concretes is typically in the range of 12.2-12.4 (Capmas & Scrivener, 1998) which is significantly lower than that of PC concrete providing less of a buffer to maintain passivation of embedded steel should carbonation occur. The carbonation of ettringite-rich binders generally results in the decomposition of ettringite into denser products such as calcite and gypsum as shown in Equation 5.2 (Lamberet, 2005) which results in an increase in porosity.

$$C_3AH_6 + 3CO_2 \rightarrow 3CaCO_3 + AH_3 + 3H_2O \quad \text{(Eq. 5.1)}$$

$$C_3A.3C\$.H_{32} + 3CO_2 \rightarrow 3CaCO_3 + 3C\$H_2 + AH_3 + 23H_20 \quad \text{(Eq. 5.2)}$$

Due to the high concentration of calcium aluminate and ettringite phases in CAC-1 and PC:CAC-2, respectively, and lack of portlandite present, it follows that the carbonation depths would be significantly greater than that of the OPC mixture. The carbonation depth of CSA-1 is somewhat counter intuitive as one would expect higher carbonation depths for this binder due to the high amounts of ettringite produced. Previous research has shown that CSA-1 typically carbonates to a greater depth than blended ettringite based binders which incorporate PC due to the presence of CH from the portland cement (Moffatt, 2016). The AFA mixture had greater depths of carbonation than all other mixtures, except for the sheltered PC:CSA-2 specimen. This is also due to lack of portlandite within the system.

The depth of carbonation for these specimens was measured every six months for two years. Figure 5.2 shows the results of the depth of carbonation at 6 and 24 months for comparison. Aside from CSA-1, the general trends for depth of carbonation remained constant between binders. Unlike the other binders, which saw gradual and somewhat linear increases in carbonation depth over time, the carbonation depth for CSA-1 almost doubled between 6 and 24 months. This system is a pure calcium sulfoaluminate binder which relies solely on the formation of ettringite for strength gain. As stated earlier the decomposition of ettringite results in the formation of denser products such as calcite and gypsum which results in an increase in porosity. This increased porosity then allows for faster diffusion of CO_2 and faster rate of carbonation at later ages. The other PC based binders have a greater resistance to this at later ages due to the presence of CH and C-S-H. The OPC mixture showed minimal carbonation depth after 24 months. Figure 5.3 shows 24 month samples sprayed with phenolphthalein to illustrate the significant differences between carbonation depth for OPC and other blended and non-portland cement systems.

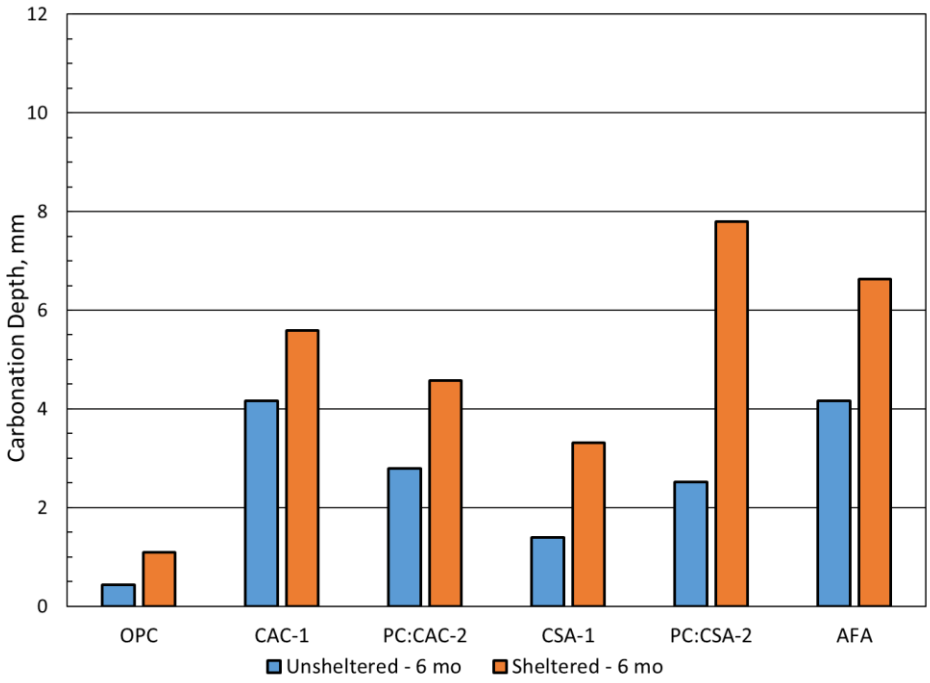

Figure 5.2: Depth of Carbonation for Lab Cured Concrete at 6 Months

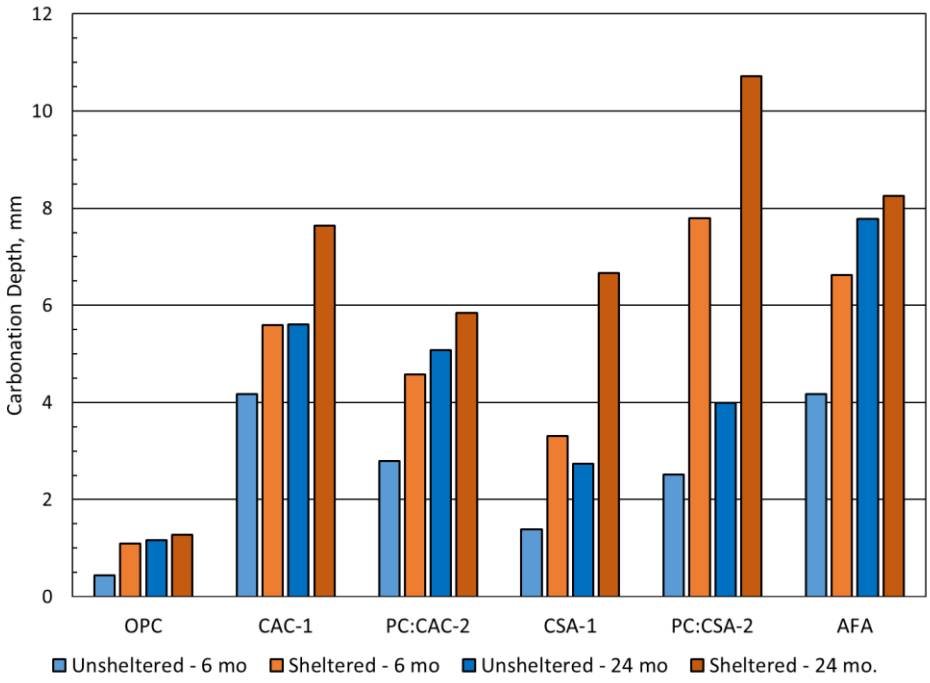

Figure 5.3: Depth of Carbonation Comparison at 6 and 24 Months, Lab Cured Concrete

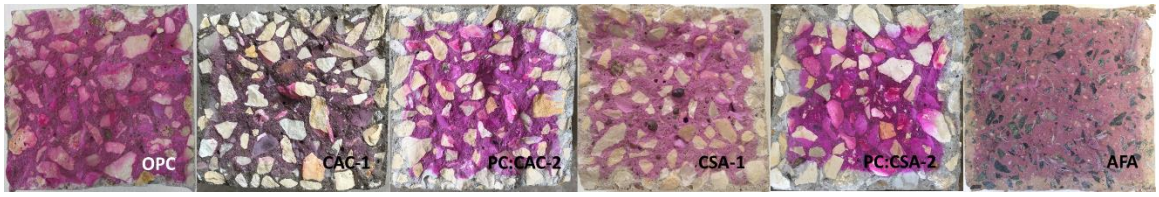

Figure 5.4: Broken sections of 24 month (sheltered) carbonated samples sprayed with phenolphthalein

5.5 CONCLUSIONS

The aim of this study was to evaluate the carbonation resistance of ettringite-rich binders used for repair application through natural outdoor carbonation exposure. Based on the results of the study the following conclusions can be made:

- Portland cement concrete exhibited superior carbonation resistance compared to ettringite-rich binders.
- Contrary to previous literature, CAC concrete carbonated at a faster rate than PC concrete of the same quality.
- Blending PC with CAC and C$ increased the carbonation resistance compared to pure CAC systems.
- Pure CSA systems experienced a rapid increase in carbonation once initiated due to the decomposition of ettringite and resulting increase in porosity.
- Contrary to the results seen when blending CAC with PC, the blending of PC with CSA results in a decrease in carbonation resistance.
- Due to the lack of portlandite, chemically activated fly ash mixtures provide very little carbonation resistance.

5.6 REFERENCES

Aguayo, F. (2015). Natural Carbonation of Concrete in Austin, TX. International Workshop on Durability and Sustainability of Concrete Structures. Bologna, Italy.

Capmas, A., & Scrivener, K. (1998). Lea's Chemistry of Cement and Concrete (Fourth Ed. ed.). (P. Hewlett, Ed.) New York: Arnold.

CEN/TS. (2008). CEN/TS 12390-10 Testing Hardened Concrete - Part 10: Determination of the Relative Carbonation Resistance of Concrete. European Committee for Standardization.

Lamberet, S. (2005). Durability of Ternary Binders Based on Portland Cement, Calcium Aluminate Cement and Calcium Sulfate (Thesis). Lausanne, Switzerland: Ecole Polytechnique Federale de Lausanne.

Moffatt, E. (2016). Durability of Rapid-set (ettringite based) Concrete (Dissertation). Frederickton, New Brunswick: University of New Brunswick.

Roy, S. et al. (1998). Durabiity of Concrete - accelerated carbonation and weahering studies. Building and Environment, 34, 597-606.

Thomas, M. e. (2000). Carbonation of Fly Ash Concrete. ACI Materials Journal Special Publication, 192, 539-556.

Chapter 6: Field Performance of Ettringite Based Repair Materials in a Marine Environment

6.1 INTRODUCTION

The corrosion of reinforcing steel within concrete is one of the leading causes of concrete deterioration, not only for marine environments, but also for highway bridges due to the use of deicing salts. Billions of dollars are spent annually on direct costs for corrosion related maintenance and repair programs in the US, and indirect costs associated with traffic delays are estimated to be even greater (Broomfield, 2007). In an effort to reduce such traffic delays rapid setting repair materials are being utilized more and more frequently. There are a multitude of formulations for rapid setting repair materials; therefore, they are generally defined by their ability to reach high early compressive strengths, typically of 20 MPa (3,000 psi) or greater within three hours. A relatively new subset of rapid repair materials rely of the formation of ettringite for high early strength. These "ettringite based" binders can be composed of calcium sulfoaluminate cements (CSA) or blends of CSA and portland cement (PC). A mixture of calcium aluminate cement (CAC) and calcium sulfate (C$) can also be blended with portland cement to achieve the same results. Though there has been an increase in the use of ettringite based binders for repair applications there is a lack of sufficient information detailing their durability and long term performance.

Concrete in large-scale field exposure is the most effective means of obtaining realistic data regarding material performance as accelerated laboratory test methods often provide inaccurate assessments of long-term performance. Sadly, it is often difficult to find sufficient outdoor space and/or funding for the establishment of outdoor exposure sites. In fact, until recently there were only three large scale marine exposure sites in North America. One of the most notable marine exposure sites was developed by the US Army

Corps in the 1950s on Treat Island, Maine. This site has provided a wealth of information regarding the performance of concrete subjected to very cold waters as well as information regarding the performance of concrete in aggressive freeze/thaw cycle zones. However, less information is available for transportation structures exposed to marine or other similar aggressive environments in warm water climates. Fortunately, The University of Texas was able to establish a new site in Port Aransas, TX in 2014, and with time the site will be able to produce valuable long term performance data for various types of binders and repair materials subjected to marine environments.

Typically, good quality concrete provides adequate protection against corrosion of embedded reinforcing steel. The high alkalinity (i.e. high pH) of portland cement concrete helps create a passive layer on the steel which prevents corrosion. However, there are several factors which can contribute to the destruction of this passive layer. For example, the carbonation of concrete results in a drop in pH due to the consumption of calcium hydroxide (CH) to form calcium carbonate (CO_3). A drop in pH below around 11.5 destroys the passive layer and then, in the presence of moisture, the steel begins to corrode. Carbonation induced corrosion is most common on very old or poorly built structures; however, corrosion due to the ingress of chloride ions is the greater issue for modern highway bridges and other structures (Broomfield, 2007). The diffusion of chlorides into concrete can occur in marine environments or as a result of the use of deicing salts. Once chlorides come into contact with reinforcing steel they begin to breakdown the passive layer; however, unlike carbonation there is no drop in pH of the system. Typically, for portland cement concrete corrosion is initiated once the chloride concentration around the streel reaches approximately 0.05%. The propagation of corrosion within concrete leads to cracking, which allows for a faster rate of chloride penetration, and eventually spalling.

Most of the information available regarding prevention of corrosion in concrete pertains to portland cement systems. The inherent differences between portland cement systems and ettringite based binders highlight the need for additional research to develop adequate measures for preventing corrosion in ettringite based systems. The research presented herein outlines the development of the Texas Marine Exposure Site (TEXMEX) and provides preliminary results on the corrosion resistance of ettringite based binders.

6.2 MATERIALS

6.2.1 Binders

Five different binders were selected for evaluation under this study. An ASTM C 150 (ASTM, 2015) Type I cement was selected as the control binder. Other binders selected include, a calcium-aluminate cement, a calcium-sulfoaluminate cement, commonly used in commercial applications, a blended systems which incorporates calcium aluminate cement and calcium sulfate with Type I cement, and a pre-bagged chemically activated concrete mixture. Samples of all binders were sent to a testing laboratory where the chemical compositions of each were determined via ASTM C 114 (ASTM, 2015). Table 6.1 provides the oxide analysis for the binders described below.

Table 6.1: Oxide Analysis of Binders

Oxide (%wt)	Binder			
	OPC	**CAC-1**	**PC:CAC-2**	**CSA-1**
SiO2	20.14	4.57	15.15	14.46
Al2O3	5.42	41.21	14.98	16.21
Fe2O3	2.47	14.29	2.12	0.94
CaO	63.63	37.49	56.32	50.30
MgO	1.32	0.61	0.97	1.34
SO3	3.09	0.00	8.44	17.09
Na2O	0.17	0.06	0.14	0.21
K2O	0.95	0.21	0.73	0.73
ZnO	0.01	0.01	0.01	0.02
SrO	0.08	0.02	0.07	0.14
Mn2O3	0.06	0.18	0.04	0.03
P2O5	0.26	0.13	0.21	0.09
TiO2	0.28	1.79	0.61	0.58
Cl	0.00	0.00	0.00	0.02
Cr2O3	0.01	0.08	0.02	0.02
Na2Oe	0.79	0.20	0.61	0.69

6.2.1.1 Portland Cement

A locally-sourced ASTM C 150 Type I portland cement was chosen as the control binder for this study. This cement has been used extensively within this lab as a control binder for various studies; therefore, the long term performance of this material is well documented and understood making it the clear choice for the control for this study.

6.2.1.2 Calcium Aluminate Cement and Blended System

A single source of calcium aluminate cement was used in this study and is referred to herein as CAC-1 and represents a binder containing 100 percent CAC. A blended CAC binder, designated as PC:CAC-2, was also evaluated and blend contained a mixture of

calcium-aluminate cement and calcium sulfate at a ratio of 2.2:1. This blend was then combined with Type I cement at a 30% replacement level (by total mass).

6.2.1.3 Calcium Sulfoaluminate Cement

A single source of calcium sulfoaluminate cement, refered to as CSA-1, was used in this study and is widely available within the US and abroad. The main phases of this CSA are ye'elimite ($C_4A_3\$$), belite (ß-C_2S), and calcium sulfate (C$)

6.2.2 Admixtures

A superplasticizer and a lithium-based accelerator were used for all CAC-1 mixtures. The superplasticizer and accelerator were dosed at 0.50% and 1.00% by mass of cement, respectively

For all PC:CAC-2 mixtures powdered citric acid was used as a retarder at a dose of 0.35% by mass of cement in conjunction with a superplasticizer in the form of sulfonated melamine formaldehyde (SMF) at a dose of 0.85% by mass of cement.

All CSA-1 mixtures utilized a combination of citric acid and SMF to attain the desired workability and three-hour compressive strength of 20 MPa (3,000 psi). The dosage for SMF was 0.1% by mass of the dry materials in the mix, and the citric acid was dosed at 0.2% by mass of cement.

6.2.3 Aggregates

A crushed limestone coarse aggregate and manufactured limestone sand were used for all concrete mixtures. These materials are known to be non-reactive in regards to alkali-silica reaction. This distinction is important, especially for field trials, for isolation of the mechanism of deterioration to chloride ingress. A water to cement ratio of 0.35 was used for all concrete mixtures.

6.2.4 Mixture Proportions

Generally, to achieve good long-term strength and durability with CAC a water/cement ratio below 0.4 and a cement content above 400 kg/m^3 (674 lb/yd^3) are recommended (Capmas & Scrivener, 1998). Therefore, the cement content of the mixtures was 440 kg/m^3 (742 lb/yd^3) for the CAC-1 mixture. The cement content for all other mixtures was 446 kg/m^3 (752 lb/yd^3). This value was chosen over the 440 kg/m^3 used for the CAC-1 mixture to correspond to the colloquial "8 sack" mix design often used by construction contractors. The water to cement ratio (w/c) was 0.35 by mass for all mixtures. The mixtures labels and binder mixture proportions are listed in Table 6.2.

It is of note to add that pure CAC systems inevitably experience what is known as "conversion". During the hydration of CAC at ambient temperatures, metastable hydrates (CAH_{10} and C_2AH_8) are formed; however, with time or an increase in temperature these metastable hydrates will convert to C_3AH_6 and AH_3 which are more thermodynamically stable hydrates. Conversion also causes an increase in porosity which can lead to significant strength loss. The increase in porosity associated with conversion is of significant interest in terms of chloride resistance in a marine environment. A CAC-1 exposure block was cast and heat cured at 50 °C (122 °F) for several days to force conversion. This block is referred to as CAC-1C throughout the rest of the paper.

Table 6.2: Mixture Labels and Proportions

Mixture Label	w/c	Total Binder Content (kg/m^3)	PC Content (kg/m^3)	CAC-2 Content (kg/m^3)
OPC	0.35	446.0	446.0	
CAC-1	0.35	440.0		
CAC-1C	0.35	440.0		
PC:CAC-2	0.35	446.0	312.2	133.8
CSA-1	0.35	446.0		
AFA	~0.26	n/a		

6.3 EXPERIMENTAL PROCEDURES

6.3.1 Development of the Texas Marine Exposure Site

In 2013 a comprehensive feasibility study was conducted to identify the specific areas related to marine exposure in need of further research to advance the current practice and use of materials in such environments. As a result of this study The Texas Marine Exposure Site (TEXMEX) was developed and established in 2014. TEXMEX is located along the ship channel which connects Port Aransas, TX to the Gulf of Mexico on property owned by The University of Texas Marine Science Institute. TEXMEX is a real-world proving ground aimed at extending the service life of transportation structures exposed to marine environments or similar aggressive environments, such as those exposed to chloride deicing salts. This site is one of only four marine exposure sites located in North America. Currently, the site focuses on the evaluating corrosion of concrete embedded steel reinforcing, chloride resistance of cementitious materials, and the potential for alkali-silica reactivity and carbonation in concrete exposed to marine environments; however, the site has the potential to also evaluate structural steel, signage, lighting and other infrastructure related components and materials.

The site was established out of a need for more data on marine exposure in warm weather sites. Most data from marine exposure sites has come from very cold sites, such as Treat Island, Maine. The data obtained from this newly established exposure site will help better define the specific exposure conditions along the Texas coastline and provide more information on how other durability mechanisms, such as alkali-silica reaction, delayed ettringite formation, and carbonation are affected by marine exposure.

6.3.2 Marine Exposure Blocks

Two large scale concrete blocks were cast for each concrete mixture. The dimensions of the marine exposure blocks are 305 x 150 x 1145 mm (12 x 6 x 45 in). One block was designed to evaluate reinforcement performance while the other was intended to evaluate resistance to chloride penetration. The reinforced block was instrumented with four reinforcement bars each placed at different depths to provide 12.5, 25, 37.5, and 50 mm (½, 1, 1-1/2, and 2 in) of cover. No. 4 black steel reinforcement was used in all reinforced marine exposure blocks. The ends of each of the reinforcement bars was tapped and threaded to allow a threaded stainless steel rod to be placed into the ends. This serves two purposes: 1) it provides a means for accurately securing the reinforcement bars at the exact cover and 2) it provides a connection between the stainless steel (which is accessible on the outside of the concrete) with the steel being evaluated. This connection helps with non-destructive techniques such as half-cell potential. A stainless steel bar was cast in the center of each block. This bar was hooked after casting and allows for hanging the blocks off the side of the ferry channel wall. Figures 6.1and 6.2 show the layout of the steel within the reinforced exposure blocks.

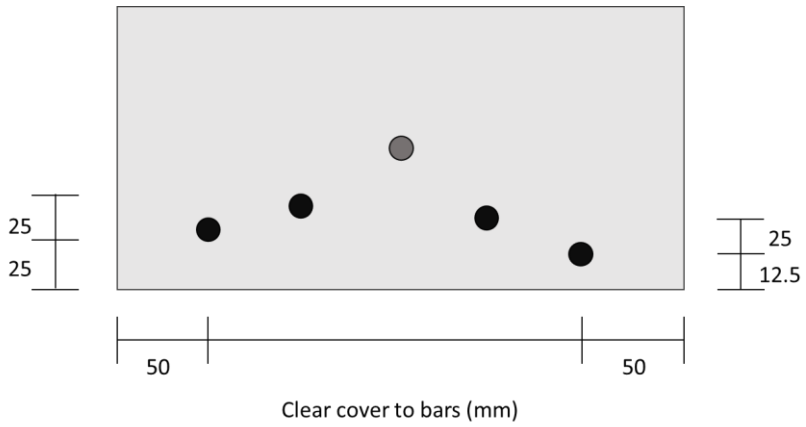

Figure 6.1: Diagram of steel reinforcement locations within reinforced marine blocks

Figure 6.2: Photo of marine exposure block showing locations of reinforcing steel

After casting, the exposure blocks were cured in the laboratory at ambient temperature for approximately 28 days before being placed at the exposure site in Port Aransas, TX. The hooked bar cast into each block was used to attach each exposure block to a chain which is anchored into the top side of the ferry channel wall. This allows for submersion of approximately one-half of each exposure block as illustrated in Figure 6.3. The blocks are placed such that the mid-tide level is situated at or slightly below the mid-

height of the specimen; the zone at or immediately above the high-tide level has been found to be the most aggressive in terms of inducing corrosion of the embedded reinforcement.

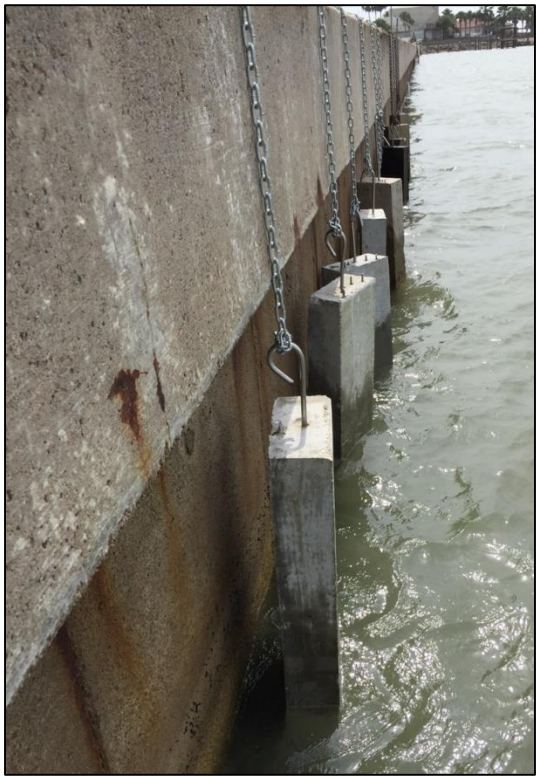

Figure 6.3: Photo showing partially submerged marine exposure blocks

6.3.2 Visual Observations

A visual assessment of the blocks was conducted each time they were removed from the water. The assessment included the identification of crack locations and widths as well as the locations of rust staining.

6.3.3 Evaluation of Corrosion Resistance

The corrosion potential of the embedded steel was evaluated through half-cell potential measurements. Initial measurements were taken when the exposure blocks were delivered to the site. Visual assessments and subsequent half-cell potential measurements

were taken periodically every year. Corrosion potential measurements were obtained per ASTM C 876: *Standard Test Method for Corrosion Potentials of Uncoated Reinforcing Steel in Concrete* (ASTM, 2009). Potential readings taken May 2015 were obtained with a silver-silver chloride (Ag/AgCl) electrode and subsequent measurements were taken relative to a copper-copper sulfate ($Cu/CuSO_4$) reference electrode. The Ag/AgCl measurements were converted to the equivalent $Cu/CuSO_4$ potential as reported here.

6.3.4 Chloride Penetration

Concrete cores were also taken from each unreinforced block to determine depth of chloride penetration after a certain time. Each core was extracted from the mid-section of the block. This is the splash area where corrosion is most likely to occur. The cores were profile ground in 2 mm (0.08 in) increments to a depth of 14 mm (0.55 in). The powder collected from profiling was used to determine chloride content per depth level. The powder from each 2 mm (0.08 in) layer was analyzed using a James Instruments, Inc. CL-2020 chlorimeter according to SHRP Product 2030: Standard Test Method for Chloride Content in Concrete (Islam, 2004). Per the standard, an acetic acid digestion solution was used for extracting chloride ions from the concrete powder. Three grams of powder from each layer was mixed with the digestion and then added to a stabilizing solution of dilute NaCl solution prior to being measured with the CL-202 chlorimeter.

6.4 Results and Discussion

6.4.1 Visual Assessment of Marine Exposure Blocks

The marine exposure blocks were cast in waves (pun intended) and therefore were deployed to the site over a 15 month period. CSA-1 and CAC-1 were deployed first in September 2014 followed by PC:CAC-2 and OPC in May 2015 and CAC-1C and AFA in December 2015. After just seven months, significant rust staining was noted on CAC-1

and CSA-1 at a cover depth of 12.5 mm (0.5 in) and by 14 months hairline cracks were noted at 12.5 mm (0.5 in) and moderate cracks but no signs of rust staining were noted at a cover depths of 25 mm (1 in) (Figures 6.3 and 6.4).

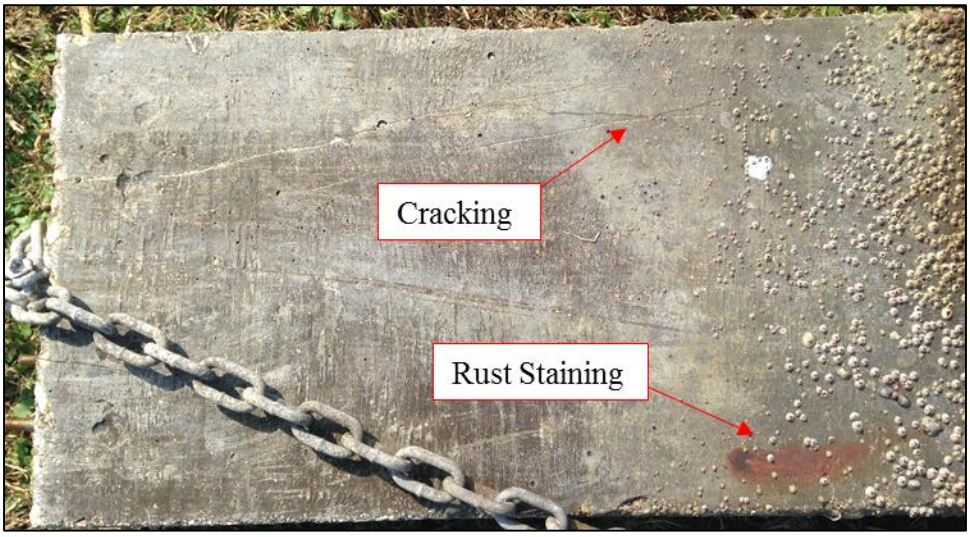

Figure 6.4: CAC-1 Exposure block after 14 months of exposure showing rust staining at 12.5 mm and cracking at 25 mm cover depth

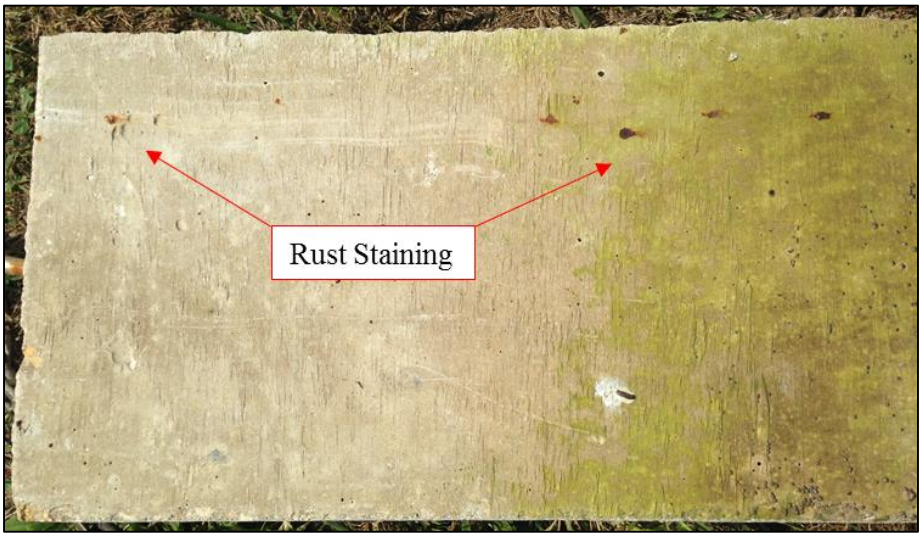

Figure 6.5: CSA-1 Exposure block after 14 months of exposure showing rust staining at 12.5 mm cover depth

Visible signs of corrosion were also noted at cover depths of 12.5 and 25 mm (0.5 and 1 in) on the OPC block and at 12.5mm on the PC:CAC-2 block after seven months (Figures 6.5 and 6.6). Some cracking was also noted at 12.5 mm (0.5 in). Rust staining was noted on the CAC-1C and AFA blocks at a cover depth of 12.5 mm (0.5 in) after just four months. The staining on the AFA block at four months was more abundant than the staining on the other blocks at any age (Figure 6.7).

Figure 6.6: OPC Exposure block after 7 months of exposure showing rust staining at 12.5 mm cover depth

Figure 6.7: PC:CAC-2 Exposure block after 7 months of exposure showing rust staining at 12.5 mm cover depth

Figure 6.8: AFA Exposure block after 4 months of exposure showing significant rust staining at 12.5 mm cover depth

In general, all blocks showed signs visible of corrosion at 12.5 mm (0.5 in) cover depth after four to seven months. Hairline cracking and minor signs of corrosion began to be visible at 25 mm (1 in) in OPC, CAC-1 and CSA-1 after about a year.

6.4.2 Corrosion Potential of Marine Exposure Blocks

A copper-copper sulfate reference electrode was used to determine the latest corrosion potential values for all of the marine exposure blocks. The measured corrosion potential of each binder at various cover depths can be interpreted to determine a relative rate of corrosion as described in ASTM C 876 and listed in Table 6.3. The results from the half-cell potential readings taken during three different visits to the exposure site are listed in Table 6.4. The readings indicate high levels of corrosion activity early on for CAC-1 and CSA-1; however, these specimens show reduced levels of corrosion at later ages. The initial high readings may be the result of preliminary corrosion taking place to form a passivation layer on the steel (Moffatt, 2016). In general, the potential readings for all systems became more negative over time indicating an intermediate rate of corrosion

especially at low depths of cover. Despite evidence provided through visual assessment and half-cell potential readings, is it likely too early to draw significant conclusions regarding corrosion resistance of these binders for reinforcing with sufficient depth of cover (>50 mm (2 in)).

Table 6.3: Corrosion condition/rate based on Corrosion Potential Measurements

$Cu/CuSO_4$ Reference Electrode	
Corrosion Potential (mV)	**Rate of Corrosion**
> -200	Low (<10%) rate of corrosion
-200 to -350	Intermediate (~50%) rate of corrosion
<-350 to -500	High (>90%) rate of corrosion
<-500	Severe rate of corrosion

Table 6.4: Half-Cell Potential Measurements of Marine Exposure Blocks

	Cover Depth (mm)	Half-Cell Potential (mV)					
		OPC	CAC-1	PC:CAC-2	CSA-1		
May-15	12.5	-97.6	-509.7	-163.7	-534.7		
	25.0	-108.3	-493.3	-150.7	-475.7		
	27.5	-111.0	-435.0	-164.7	-417.3		
	50.0	-120.3	-547.0	-159.0	-493.0		
	Months of Exposure	0.0	7.0	0.0	7.0		
	Cover Depth (mm)	Half-Cell Potential (mV)					
		OPC	CAC-1	PC:CAC-2	CSA-1	CAC-1C	AFA
Dec-15	12.5	-438.0	-371.0	-24.0	-359.0	-95.0	-279.0
	25.0	-405.0	-392.0	-54.0	-395.0	-115.0	-173.0
	27.5	-414.0	-374.0	-107.0	-320.0	-78.0	-183.0
	50.0	-210.0	-380.0	-149.0	-320.0	-85.0	-186.0
	Months of Exposure	7.0	14.0	7.0	14.0	0.0	0.0
	Cover Depth (mm)	Half-Cell Potential (mV)					
		OPC	CAC-1	PC:CAC-2	CSA-1	CAC-1C	AFA
Apr-16	12.5	-350.0	-320.0	-210.0	-310.0	-310.0	-400.0
	25.0	-310.0	-320.0	-60.0	-340.0	-300.0	-310.0
	27.5	-390.0	-310.0	-60.0	-250.0	-340.0	-160.0
	50.0	-140.0	-300.0	-30.0	-250.0	-250.0	-100.0
	Months of Exposure	11.0	18.0	11.0	18.0	4.0	4.0

6.4.3 Chloride Penetration

Results from the chloride penetration analyses are illustrated in Figure 6.8. The chloride content values were relatively low considering the visual evidence and half-cell potential readings which support the presence of corrosion within all six of the marine exposure blocks. Aside from the chloride contents measured within the first 2 mm (0.08 in) of the CAC-1 and CAC-1C specimens and the values for depths 2-4 mm (0.08-0.16 in) in the OPC specimen, all other values fall below 0.05% which is generally considered to be the threshold value for corrosion initiation. Despite low chloride concentrations within the systems, the results do correlate with the visual evidence of corrosion. The most significant amounts of rust staining were noted at 12.5 mm (0.5 in) on CAC-1, PC:CAC-2, and AFA which also have the highest chloride concentrations within the first 2 mm (0.08 in). Also, the tide in Port Aransas only varies 0.15 m (0.5 ft) between low and high tides. As a result the splash zone where the cores were extracted is rarely submerged which results in a slow rate of chloride penetration. It is likely that the blocks have not been at the site long enough for significant chloride levels of penetration to take place.

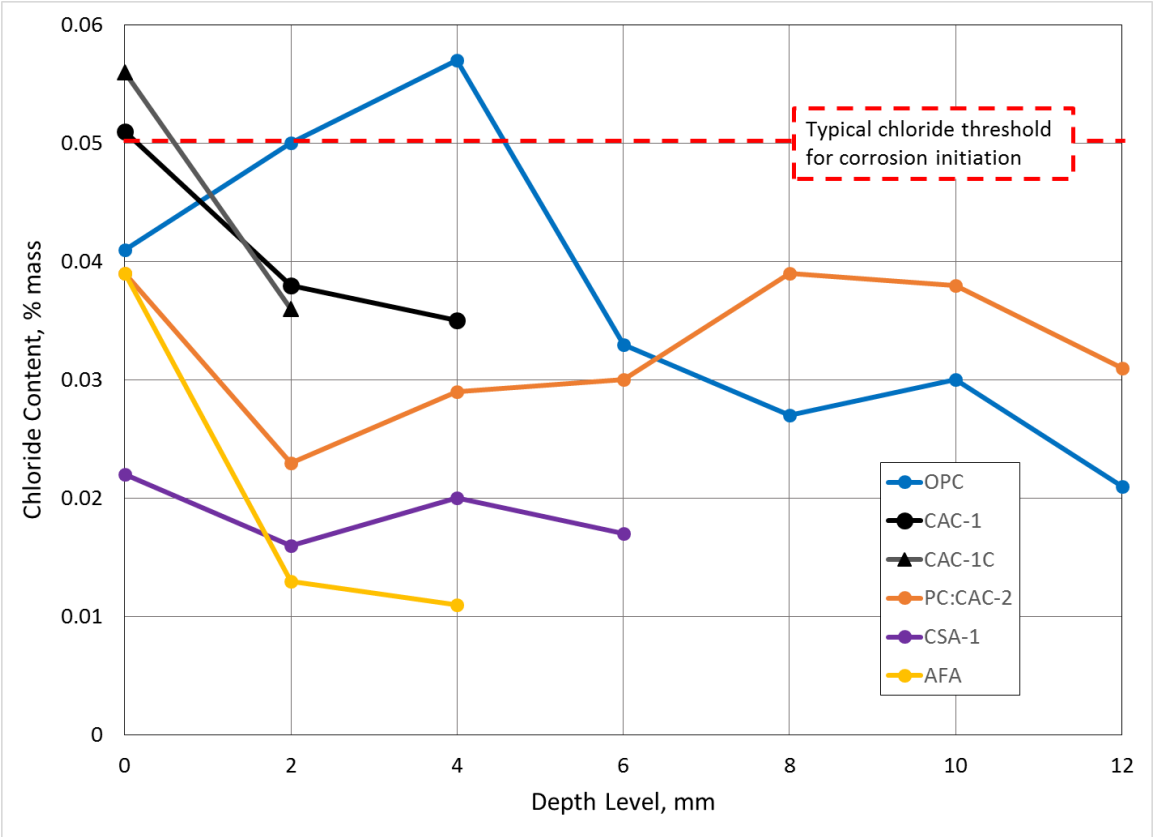

Figure 6.9: Chloride Penetration of Marine Exposure Blocks

6.5 CONCLUSIONS

The information provided herein details the development and preliminary results of the Texas Marine Exposure Site (TEXMEX). The aim of TEXMEX is to provide long term performance data for concrete mixtures and reinforcing in warm water marine environments. Based on the results obtained thus far the following conclusions and suggestions for future work can me made:

- The importance of adequate cover in a marine environment was verified by visual rust staining at 12.5 mm in all samples.
- Further monitoring is necessary to establish chloride thresholds of ettringite based binders in warm water marine environments.

- A site specific standard protocol for visual assessments of marine exposure blocks should be established. This protocol should include instruction on measuring crack length, width and total amount. A method for determining surface area of rust staining would also help in measuring propagation of corrosion.

6.6 REFERENCES

ASTM. (2005). *ASTM C 114 Standard Test Methods for Chemical Analysis of Hydraulic Cement.* West Conshokocken, PA: ASTM International.

ASTM. (2009). *ASTM C 876 Standard Test Method for Corrosion Potentials of Uncoated Reinforcing Steel in Concrete.* West Conshohocken, PA: ASTM International.

ASTM. (2015). *ASTM C 150, Standard Specification for Portland Cement.* West Conshokocken, PA: ASTM International.

Broomfield, J. (2007). *Corrosion of Steel in Concrete: Understanding, Investigation and Repair.* New York: Taylor & Francis.

Capmas,A, & Scrivener, K. (1998). *Lea's Chemistry of Cement and Concrete* (Fourth Ed. ed.). (P. Hewlett, Ed.) New York: Arnold.

Islam, M. (2004). *SHRP Product 2030: Standard Test Method for Chloride Content in Concrete.* Washington, DC: strategic Highway Research Program (SHRP).

Moffatt, E. (2016). *Durability of Rapid-set (ettringite based) Concrete (Dissertation).* Frederickton, New Brunswick: University of New Brunswick.

Chapter 7: Conclusions and Future Research Needs

This chapter summarizes the main findings of the research conducted for this dissertation. Recommendations and suggestions for future research are also discussed.

7.1 SUMMARY

Through the work of the Scientific Network, a wealth of information on CAC based systems has been produced in the last decade. Most previous research has focused on the early-age properties and microstructural development of CAC; however, within the last few years the research documented here and other research conducted at the University of New Brunswick has focused on documenting the durability and long-term performance of CAC based blends. The main objective of the research presented within this dissertation was to evaluate the durability of a newly developed calcium aluminate based binder composed of a mixture of PC, CAC, and C$. The performance of PC:CAC-2, as it has been described previously, was compared to other similar or competitive binders. More specifically the potential for common modes of concrete deterioration such as alkali-silica reaction, external sulfate attack, delayed ettringite formation, carbonation, and corrosion in a marine environment were investigated. The key findings of the work presented herein include:

- The use of CAC:C$ or CSA with portland cement to achieve high early strength can produce significant levels of ASR if used with reactive aggregate and high alkali cement.
- Calcium sulfoaluminate cement is also prone to low levels of ASR when used with reactive aggregate.
- When used as 100% of the binder, calcium aluminate cement does not present a concern regarding ASR.

- Standard ASR lab tests, particulary ASTM C 1293, can be used effectively to evaluate alternative binders and their impact on ASR-induced expansion. The accelerated mortar bar test was also shown to be a useful test, although the high alkalinity of the soak solution may make it difficult to assess alternative binders.
- Ettringite-based binders that incorporate portland cement show little to no sulfate resistance in sodium sulfate solutions of any concentration. This is due to the formation of large amounts of monosulfoaluminate at later ages which is then available to form ettringite in the presence of external sulfates.
- Calcium sulfoaluminate cements with high sulfate to alumina ratios perform exceptionally well in sodium sulfate environments.
- Ettringite-based binders show a definite potential for delayed ettringite formation. This is especially evident in ettringite-based binders which incorporate portland cement.
- Contrary to previous literature, CAC concrete carbonates at a faster rate than PC concrete of the same quality.
- Blending PC with CAC and C$ increases the carbonation resistance compared to pure CAC systems.
- Pure CSA systems experience a rapid increase in carbonation once initiated due to the decomposition of ettringite and resulting increase in porosity.

7.2 FUTURE WORK

Although many questions were answered through this research, the findings also raised new questions and ideas for future research. Some recommendations for future work are as follows:

- It is necessary to investigate the potential for ASR in ettringite-based systems blended with low-alkali portland cement. This will aid manufacturers in developing recommendations for on-site blending.
- Continued monitoring of the ASR exposure blocks will further elucidate the resulted obtained from laboratory tests which indicated the potential for ASR in ettringite-based systems.
- Further research is necessary regarding the sulfate resistance of pure CAC systems. Evidence shows sulfate attack in converted CAC mortar can lead to deterioration at low levels of expansion due to increased porosity and reduced strength.
- Continued monitoring of the marine exposure blocks located at TEXMEX is necessary to obtain more information regarding corrosion resistance of cementitious materials in warm water marine environments.

Appendix

Table A1: Tabulated damage rating index counts for OPC

Binder ID: OPC		Total Counts	Weighting Factors	DRI Value
Age of Sample: 2 years (ASTM C1293)				
Petrographic Features				
Number of Aggregate Particles Considered		62		
Cracks in the Aggregate particle	Closed or (line), **without** reaction products	40	0.25	10
	Opened or in a fine network, **without** reaction products	5	2	10
	Opened or in a fine network, **with** reaction products	13	2	26
Cracks in the Cement Paste	**without** reaction products	1	3	3
	with reaction products	98	3	294
Debonded Aggregate		1	3	3
Reacted Aggregate Particle		4	2	8
Reaction Rim on Aggregate		19	0	0
Voids Filled with Reaction product		115	0	0
Cement Paste Impregnated with Reaction Product		25	0	0
			Subtotal DRI:	354
			DRI Normalized to 100 cm2 Area:	708

Table A2: Tabulated damage rating index counts for CAC-1

Binder ID: CAC-1		Total Counts	Weighting Factors	DRI Value
Age of Sample: 2 years (ASTM C1293)				
Petrographic Features				
Number of Aggregate Particles Considered		74		
Cracks in the Aggregate particle	Closed or (line), **without** reaction products	43	0.25	10.75
	Opened or in a fine network, **without** reaction products	3	2	6
	Opened or in a fine network, **with** reaction products	3	2	6
Cracks in the Cement Paste	**without** reaction products	3	3	9
	with reaction products	4	3	12
Debonded Aggregate		0	3	0
Reacted Aggregate Particle		0	2	0
Reaction Rim on Aggregate		1	0	0
Voids Filled with Reaction product		1	0	0
Cement Paste Impregnated with Reaction Product		2	0	0
			Subtotal DRI:	43.75
			DRI Normalized to 100 cm2 Area:	87.5

Table A3: Tabulated damage rating index counts for PC:CAC-2

Binder ID: PC:CAC-2		Total Counts	Weighting Factors	DRI Value
Age of Sample: 2 years (ASTM C1293)				
Petrographic Features				
Number of Aggregate Particles Considered		69		
Cracks in the Aggregate particle	Closed or (line), **without** reaction products	6	0.25	1.5
	Opened or in a fine network, **without** reaction products	1	2	2
	Opened or in a fine network, **with** reaction products	10	2	20
Cracks in the Cement Paste	**without** reaction products	0	3	0
	with reaction products	46	3	138
Debonded Aggregate		0	3	0
Reacted Aggregate Particle		0	2	0
Reaction Rim on Aggregate		10	0	0
Voids Filled with Reaction product		71	0	0
Cement Paste Impregnated with Reaction Product		10	0	0
			Subtotal DRI:	161.5
			DRI Normalized to 100 cm2 Area:	323

Table A4: Tabulated damage rating index counts for CSA-1

Binder ID: CSA-1		Total Counts	Weighting Factors	DRI Value
Age of Sample: 2 years (ASTM C1293)				
Petrographic Features				
Number of Aggregate Particles Considered		66		
Cracks in the Aggregate particle	Closed or (line), **without** reaction products	29	0.25	7.25
	Opened or in a fine network, **without** reaction products	2	2	4
	Opened or in a fine network, **with** reaction products	24	2	48
Cracks in the Cement Paste	**without** reaction products	0	3	0
	with reaction products	78	3	234
Debonded Aggregate		0	3	0
Reacted Aggregate Particle		0	2	0
Reaction Rim on Aggregate		3	0	0
Voids Filled with Reaction product		63	0	0
Cement Paste Impregnated with Reaction Product		3	0	0
			Subtotal DRI:	293.25
			DRI Normalized to 100 cm2 Area:	586.5

Table A5: Tabulated damage rating index counts for CSA-1

Binder ID: PC:CSA-2		Total Counts	Weighting Factors	DRI Value
Age of Sample: 2 years (ASTM C1293)				
Petrographic Features				
Number of Aggregate Particles Considered		64		
Cracks in the Aggregate particle	Closed or (line), **without** reaction products	6	0.25	1.5
	Opened or in a fine network, **without** reaction products	6	2	12
	Opened or in a fine network, **with** reaction products	42	2	84
Cracks in the Cement Paste	**without** reaction products	0	3	0
	with reaction products	96	3	288
Debonded Aggregate		0	3	0
Reacted Aggregate Particle		1	2	2
Reaction Rim on Aggregate		2	0	0
Voids Filled with Reaction product		68	0	0
Cement Paste Impregnated with Reaction Product		3	0	0
			Subtotal DRI:	387.5
			DRI Normalized to 100 cm2 Area:	775

Table A6: Tabulated damage rating index counts for AFA

Binder ID: AFA		Total Counts	Weighting Factors	DRI Value
Age of Sample: 2 years (ASTM C1293)				
Petrographic Features				
Number of Aggregate Particles Considered		113		
Cracks in the Aggregate particle	Closed or (line), **without** reaction products	0	0.25	0
	Opened or in a fine network, **without** reaction products	11	2	22
	Opened or in a fine network, **with** reaction products	6	2	12
Cracks in the Cement Paste	**without** reaction products	0	3	0
	with reaction products	1	3	3
Debonded Aggregate		0	3	0
Reacted Aggregate Particle		2	2	4
Reaction Rim on Aggregate		0	0	0
Voids Filled with Reaction product		0	0	0
Cement Paste Impregnated with Reaction Product		0	0	0
			Subtotal DRI:	41
			DRI Normalized to 100 cm2 Area:	82

References

Adams, M. (2015). Factors Influencing Conversion and Volume Stability in Calcium Aluminate Cement Systems (Dissertation). Corvalis, OR: Oregon State University.

Aguayo, F. (2015). Natural Carbonation of Concrete in Austin, TX. International Workshop on Durability and Sustainability of Concrete Structures. Bologna, Italy.

ASTM. (2008). ASTM C 1293, Standard Test Method for Determination of Length Change of Concrete Due to Alkali-Silica Reaction. West Conshokocken, PA: ASTM International.

ASTM. (2012). ASTM C 1012 Standard Test Method for Length Change of Hydraulic-Cement Mortars Exposed to Sulfate Solution. West Conshohocken, PA: ASTM International.

ASTM. (2013). ASTM C 305 Standard Practice for Mechanical Mixing of Hydraulic Cement Pastes and Mortars of Plastic Consistency. West Conshohocken, PA: ASTM International.

ASTM. (2014). ASTM C 1260 Standard Test Method for Potential Alkali Reactivity of Aggregates (Mortar-Bar Method). West Conshokocken, PA: ASTM International.

ASTM. (2015). ASTM C 114 Standard Test Methods for Chemical Analysis of Hydraulic Cement. West Conshokocken, PA: ASTM International.

ASTM. (2015). ASTM C 150, Standard Specification for Portland Cement. West Conshokocken, PA: ASTM International.

ASTM. (2016). ASTM C 33, Standard Specification for Concrete Aggregates. West Conshokocken, PA: ASTM International.

Bentivegna, A. (2012). Multi-Scale Characterization, Implementation, and Monitoring of Calcium Aluminte Cement Based Systems (Dissertation). Austin, TX: The University of Texas at Austin.

Berube, M. et al. (2002). Measurement of the Alkali Content of Concrete Using Hot-Water Extraction . Cement, Concrete, and Aggregates, 24(1), pp. 28-36.

Bizzozero, J. (2014). Hydration and Dimensional Stability of Calcium Aluminate Based Systems (Dissertation). Lausanne: Ecole Polutechnique Federale de Lausanne.

Bizzozero, J., et al. (2014). Expansion mechanisms in calcium aluminate and sulfoaluminate systems with calcium sulfate. Cement and Concrete Research, 56, 190-202.

Bleszynski, R. T. (1998). Microstructural Studies of Alkali-Silica Reaction in Fly Ash Concrete Immersed in Alkaline Solutions. Advanced Cement Based Materials, 7, 66-78.

Broomfield, J. (2007). Corrosion of Steel in Concrete: Understanding, Investigation and Repair. New York: Taylor & Francis.

Capmas, A., & Scrivener, K. (1998). Lea's Chemistry of Cement and Concrete (Fourth Ed. ed.). (P. Hewlett, Ed.) New York: Arnold.

CEN/TS. (2008). CEN/TS 12390-10 Testing Hardened Concrete - Part 10: Determination of the Relative Carbonation Resistance of Concrete. European Committee for Standardization.

Chabrelie, A. (2010). Mechanisms of Degradation of Concrete by External Sulfate Ions under Laboratroy and FIeld Conditions (Thesis). Lausanne, Switzerland: Ecolo Polytechnique Federale de Lausanne.

Crammond, N. (1990). Long term performance of high alumina cement in sulfate-bearing environments. In M. RJ (Ed.), Calcium Aluminate Cements, (pp. 208-221). London.

Drimalas, T. (2004). Laboratory Testing and Investigations of Delayed Ettringite Formation (Thesis). The University of Texas at Austin, Civil Engineering. Austin, TX: The University of Texas at Austin.

Drimalas, T, et al. (2011). Laboratory and Field Evaluations of External Sulfate Attack in Concrete (4089 Report). Austin, TX: Texas Department of Transportation.

Dunster, A. & Holton, I.. (2001). A Laboratory Study of the Resistance of CAC Concretes to Chemical Attack by Sulphate and Alkali Carbonate Solutions. Proceedings of the International Conference on Calcium Aluminate Cements (CAC). Edinburgh, Scotland.

Folliard, K., et al. (2006). Interim Recommendations for the Use of Lithium to Mitigate or Prevent Alkali-Silica Reaction. McLean, VA: FHWA.

Folliard, K., et al. (2006). Preventing ASR/DEF in New Concrete: Final Report. Report No. FHWA/TX-06/0-4085-5.

Fournier, B., et al. (2015). Description of petrogrpahic features of damage in concrete used in the determination of the Damage Rating Index (DRI). Quebec City, Quebec: Universite Laval, Geology and Geological Department.

Fu, Y. (1996). Delayed ettringite formation in portland cement products. Ottawa, Ontario: Dissertation, University of Ottawa.

Gaboriaud, F., et al. (1999). Aggregation and gel formation in basic silico-calco-alkaline solutions studied: A SAXS, SANS, and ELS study. J. Phys.Chem. B, 103, 5775-5781.

Grattan-Bellew, P., & Danay, A. (1992). Comparison of laboratory and field evaluation of alkali-silica reaction in large dams. Proceedings of the International Conference on Concrete Alkali-Aggregate Reactions in Hydraulic Plants and Dams. Fredericton: Canadian Electrical Association.

Grattan-Bellew, P., & Mitchell, L. (2006). Quantitative petrographic analysis of concrete - The Damage Rating Index (DRI) method, a review. 8th International CANMET-ACI Conference on Recent Advances in Concrete Technology - Marc-Andre Berube Symposium on AAR in Concrete, (pp. 321-334). Montreal (Canada).

Ideker, J. (2008). Early-Age Behaviour of Calcium Aluminate Cement Systems (Dissertation). Austin, TX: The University of Texas at Austin.

Islam, M. (2004). SHRP Product 2030: Standard Test Method for Chloride Content in Concrete. Washington, DC: strategic Highway Research Program (SHRP).

Juenger, M.C.G.,Winnefeld,F., Provis, J.L, & Ideker, J.H. (2011). Advances in alternative cementitious binders. Cement and Concrete Research, 41, 12-32-1243.

Lamberet, S. (2005). Durability of Ternary Binders Based on Portland Cement, Calcium Aluminate Cement and Calcium Sulfate (Thesis). Lausanne, Switzerland: Ecole Polytechnique Federale de Lausanne.

Leemann, A., et al. (2011). Alkali-silica Reaction: the Influence of Calsium on Silica Dissolution and the Formation of Reaction Products. Journal of the American Ceramic Society, 94(4), 1243-1249.

Macias, A., Kindness, A., Glasser, FP. (1996). Corrosion behaviour of steel in high alumina cement mortar cured at 5, 25, and 55C: chemical and physical factors. Journal of Materials Science, 31, 2279-89.

Miller, D., & Manson, P. (1933). Technical Bulletin 358. United States Department of Agriculture.

Moffatt, E. (2016). Durability of Rapid-set (ettringite based) Concrete (Dissertation). Frederickton, New Brunswick: University of New Brunswick.

Nuytten, S. (2014). Microstructure and Durability Against Sulfate Attacks of Ettringite Bases Rapid Repair Binders (Thesis). Lausanne, Switzerland: Ecole Polytechnique Federale de Lausanne.

Rajabipour, F., et al. (2015). Alkali-silica reaction: Current Understanding of the reaction mechanisms and the knowledge gaps. Cement and Concrete Research, 76, 130-146.

Ramlochan. (2003). The Effect of Pozzolans and Slag on the Expansion of Mortars and Concrete Cured at Elevated Temperature (Dissertation). Toronto, Ontario: University of Toronto.

Roy, S,. et al. (1998). Durabiity of Concrete - accelerated carbonation and weahering studies. Building and Environment, 34, 597-606.

Scrivener, K. (2001). Historical and Present Day Applications of Calcium Aluminate Cements. Proceedings of the International Conference on Calcium Aluminate Cements (CAC). Edinburgh, Scotland.

Stanton, T. (1940). Expansion of Concrete Through Reaction Between Cement and Aggregate. 66 (10), p. 1781 - 1811.

Stark, D. (1991). The Moisture Condition of Field Concrete Exhibiting Alkali-Silica Reactivity. ACI Special Publication, 126, 973-988.

Taylor, H., et al. (2001). Delayed ettringite formation. Cement and Concrete Research, 31, 683-693.

Thomas, M., et al (2000). Carbonation of Fly Ash Concrete. ACI Materials Journal Special Publication, 192, 539-556.

Tuan, C. (2005). Evaluation of Use of Lithium Nitrate in Controlling Alkali-Silica Reactivity in Existing Concrete Pavement. Journal of the Transportaion Reserach Board, No. 1914, 34-44.

Villenueve, V. F. (2012). Determination of the damage in concrete affected by AST - the Damage Rating Index (DRI). 14th International Conference of alkali aggregate reaction (AAR) in concrete. Austin, TX.

Williams, S. (2005). Structures Affected by Premature Concrete Deterioration: Diagnosis and Assessment of Deterioration Mechanisms (Thesis). Austin: Civil Engineering Department, The University of Texas.

Winnefeld, F., Lothenbach, B.. (2010). Hydration of calcium sulfoaluminate cements - experiemental findings and thermodynamic modelling. Cement and Concrete Research, 40, 1239-1247.

Vita

Racheal Dawn Lute was born in Houston, Texas, but soon moved and was raised in Taylor, Texas. She is the daughter of Richard James Lute and Lori Cacioppo Lute. After finishing her primary education at Taylor High School she entered The University of Texas at Austin in 2002. She was awarded a Bachelor of Science in Architectural Engineering in May, 2006. In August 2006, she began her graduate studies in the Civil Engineering Department at The University of Texas at Austin. After completion of her master's degree in 2008, she moved to Washington, D.C. where she worked as a consultant on structural repair and restoration projects. In May 2013, she returned to The University of Texas to begin the doctoral research described within this document.

Permanent email: rachealdawn@gmail.com

This dissertation was typed by Racheal Dawn Lute